FATTY ACID METABOLISM AND METABOLIC INFLAMMATION – TWO IMPORTANT PLAYERS IN THE DEVELOPMENT OF INSULIN RESISTANCE

Layout and printing: Off Page, Amsterdam, The Netherlands

Cover: Jaap Karssenberg

FATTY ACID METABOLISM AND METABOLIC INFLAMMATION – TWO IMPORTANT PLAYERS IN THE DEVELOPMENT OF INSULIN RESISTANCE

Proefschrift

ter verkrijging van
de graad van Doctor aan de Universiteit Leiden,
op gezag van Rector Magnificus prof.mr. C.J.J.M. Stolker,
volgens besluit van het College voor Promoties
te verdedigen op donderdag 16 mei 2013
klokke 16.15 uur
door

Irene Olga Cornelia Maria Vroegrijk

geboren te Roosendaal en Nispen
in 1983

PROMOTIECOMMISSIE

Promotores:	Prof. dr. L.M. Havekes Prof. dr. J.A. Romijn Prof. dr. K. Willems van Dijk
Co-promotor:	Dr. P.J. Voshol (University of Cambridge)
Overige leden:	Dr. V. van Harmelen Dr. S.J. Verbeek Prof. dr. J.F.C. Glatz (Universiteit Maastricht)

The work described in this thesis was performed at the department of Endocrinology and Metabolic Diseases at the Leiden University Medical Center, Leiden, The Netherlands.
The research described in this thesis was financially supported by the Netherlands Organization for Scientific Research (NWO 917.76.301), the Dutch Diabetes Research Foundation (2005.01.003) and the seventh framework program of the EU-funded LipidomicNet (202272).

CONTENTS

1 GENERAL INTRODUCTION

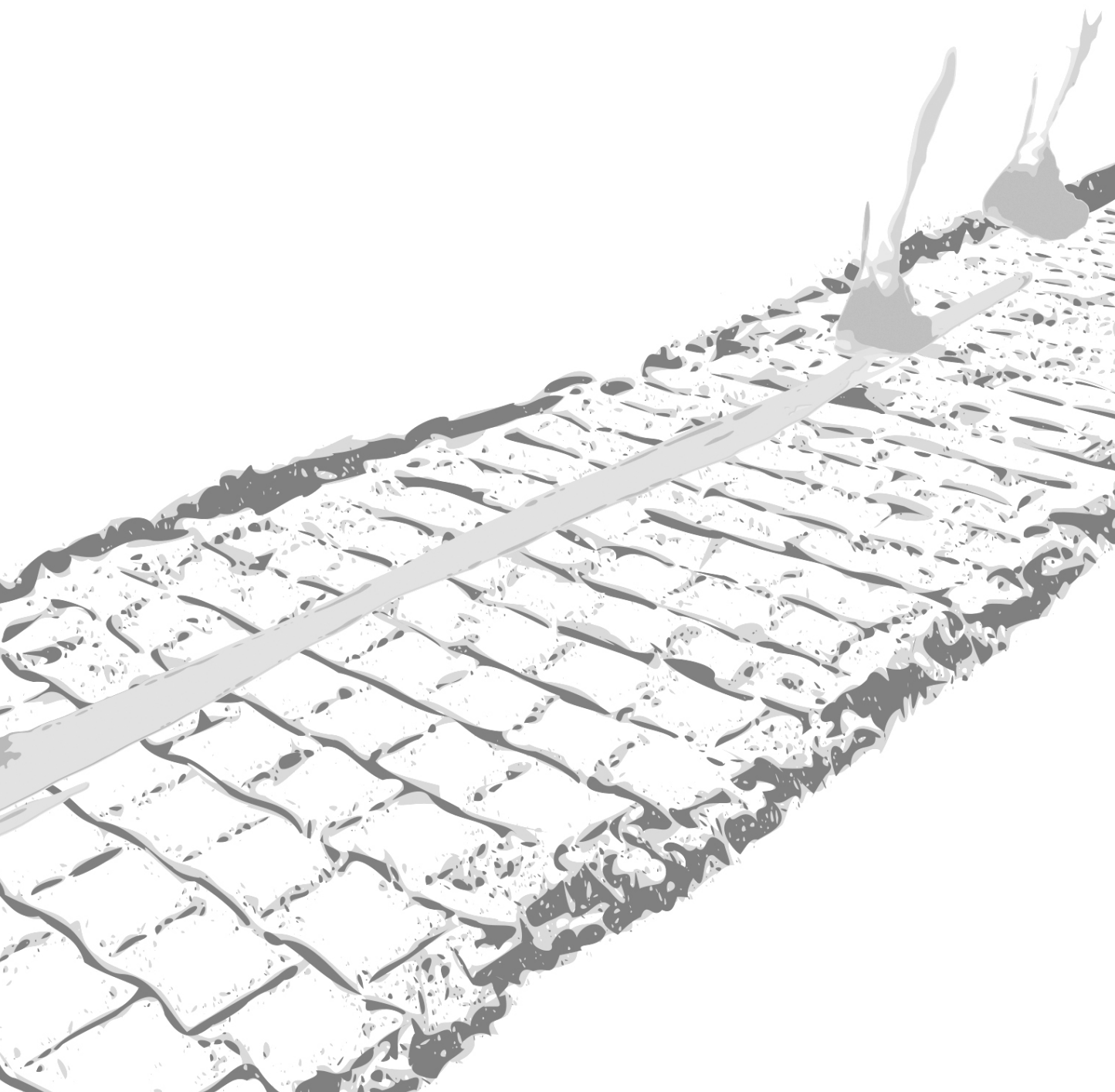

1.1 INTRODUCTION

The metabolic syndrome is defined as a cluster of multiple metabolic abnormalities including obesity, insulin resistance, dyslipidemia and hypertension that co-occur more often than might be expected by chance. Since these abnormalities are all well documented risk factors for cardiovascular disease, the increasing prevalence of the metabolic syndrome in Western societies is a cause for major concern [1]. Diet (e.g. consumption of fruit and vegetables and alcohol), lifestyle factors (e.g. smoking and physical exercise) [2] and genetic makeup [3, 4] influence the susceptibility to develop the metabolic syndrome.

Obesity, in particular visceral obesity, is one of the defining components of the metabolic syndrome. Obesity is a condition in which body fat has accumulated to such an extent that it may impair health. Body Mass Index (BMI), weight in kilograms divided by the square of the height in meters (kg/m^2), is a simple index to classify overweight and obesity in adults. Adults with a BMI ≥ 25 are defined as overweight and adults with a BMI ≥ 30 are classified as obese, according to the guidelines of the World Health Organization (WHO). In 2008 1.5 billion adults were overweight. Of these, over 200 million men and nearly 300 million women were obese [5].

Adipose tissue plays a central role in the development of the metabolic syndrome. Under normal, healthy conditions, adipose tissue stores the excess of nutrients in the form of fat and releases energy under conditions of shortage. Under pathophysiological conditions fat may be disposed in non-adipose tissue (ectopic fat deposition), which will contribute to the pathogenesis of the metabolic syndrome. Excessive adipose tissue expansion may also lead to the development of pathogenic adipose tissue, characterized by chronic low-grade inflammation, which eventually may affect the systemic inflammatory status [6, 7]. This systemic pro inflammatory status can also contribute to the pathogenesis of the metabolic syndrome by affecting peripheral organs such as the liver, causing hypertriglyceridemia [8] or the vasculature, causing atherosclerosis [9]. In this thesis, I have focused on changes in fatty acid (FA) metabolism and inflammatory status to investigate the effects on obesity, fat deposition, insulin resistance and hypertriglyceridemia, all components of the metabolic syndrome.

Insulin resistance is a condition in which tissues of the body do not respond adequately to the actions of insulin [10]. As a result, insulin induced transport of glucose across the cell membrane into muscle, adipose tissue and heart is impaired [11, 12, 13]. In the liver, insulin inhibits glucose production and insulin resistance compromises the inhibition of glucose production by the liver [14]. This results in fasting and postprandial hyperglycemia. Besides the effects on glucose metabolism, insulin resistance also influences lipid metabolism. Insulin resistance is associated with increased secretion of triglycerides (TG) by the liver [15] and with increased secretion of FA from adipose tissue [16]. Both of these altered conditions can result in hypertriglyceridemia.

In this chapter, FA metabolism is introduced and the role of FA in the pathology of insulin resistance is discussed. Subsequently, metabolic inflammation is introduced, as well as its role in insulin resistance.

1.2 FATTY ACID METABOLISM

Dyslipidemia is an important characteristic of the metabolic syndrome and specifically, elevated plasma TG and decreased high density lipoprotein (HDL) cholesterol [17]. TG, which is composed of glycerol and three FA, and cholesterol are common lipids in our diet and are essential for life because they provide energy and are needed for proper cellular functioning. Lipids are hydrophobic molecules that are insoluble in an aqueous environment such as blood. Therefore, after absorption in the intestine, TG and cholesterol are packed into water-soluble particles called lipoproteins. These lipoproteins have a hydrophobic inner core, containing TG and cholesteryl esters (CE), that is covered by a shell of hydrophilic phospholipids (PL), unesterified cholesterol and proteins, termed apolipoproteins. Lipoproteins are divided into 5 classes, according to their origin and density: chylomicrons, very low density lipoproteins (VLDL), intermediate density lipoproteins (IDL), low density lipoproteins (LDL) and high density lipoproteins (HDL). The metabolism of these lipoproteins and the subsequent distribution and cellular processing of TG derived FA is described in the following sections and a schematic overview is depicted in Figure 1. In addition, the role of FA in the pathogenesis of insulin resistance will be discussed.

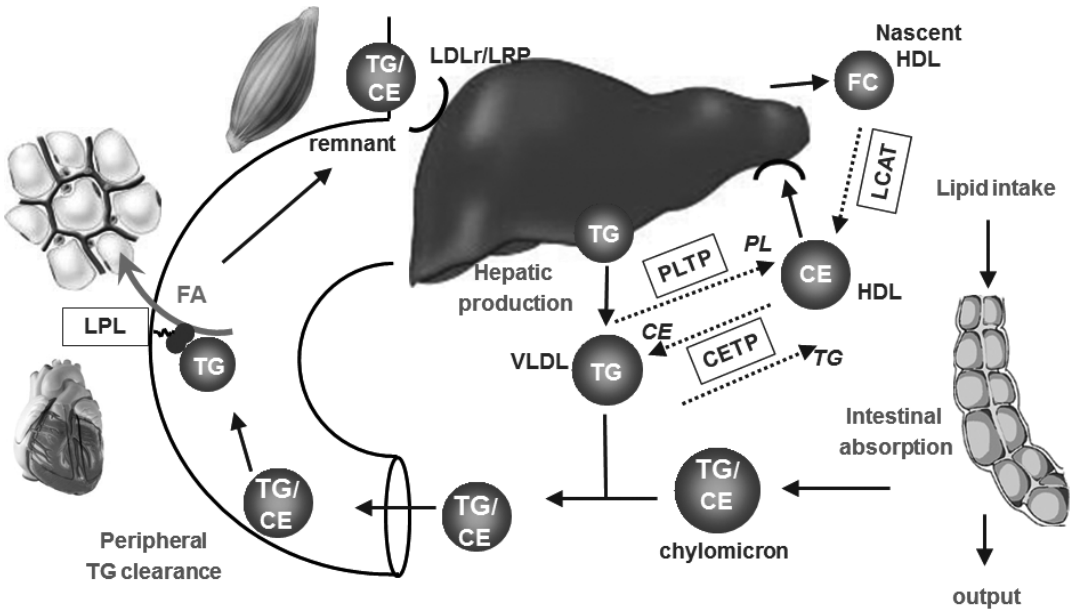

Figure 1. Schematic overview of lipoprotein metabolism. See text for explanation. CE, cholesteryl ester; CETP, cholesteryl ester transfer protein; FC, free cholesterol; FA, fatty acids; LCAT, lechitin:cholesterol acyltransferase; LDLr, LDL receptor; LPL, lipoprotein lipase; LRP, LDLr related protein; PL, phospholipid; PLTP, phospholipid transfer protein; TG, triglycerides.

Formation of lipoproteins

In the intestine, dietary lipids are emulsified by bile acids and subsequently lipolysed by pancreatic lipase to glycerol and FA [18]. FA are absorbed by the epithelial cells of the small intestinal villi, named enterocytes. Inside the enterocytes FA are re-esterified to TG and chylomicrons are formed: very large particles that consist mainly of TG, but also of cholesterol, phospholipids and apoproteins (apoAI, apoAIV, apoB48, apoCI, apoCII, apoCIII and apoE) [19]. Chylomicrons are secreted into the lymph, from which they are transported to the blood circulation.

In the fasting state, the liver is the main site of cholesterol and TG secretion. The liver secrets lipids in the form of VLDL particles. VLDL particles are formed within the endoplasmatic reticulum (ER) of hepatocytes where microsomal triglyceride transfer protein (MTP) transfers lipids onto apoB, thereby forming a pre-VLDL particle. This pre-VLDL particle undergoes a second step of lipidation in the Golgi system and is subsequently secreted as mature TG-rich particle [20]. The lipids that are used for loading onto apoB originate from lipoprotein remnants, adipose tissue or can be synthesized de novo by the liver itself [21]. When the VLDL particles have entered the bloodstream, they become enriched with apoCI, apoCII, apoCIII and apoE [22].

HDL is needed for the removal of excess cholesterol from peripheral tissues back to the liver. Nascent HDL is produced by the liver and intestine from apoAI and PL. This HDL particle can take up cholesterol from various tissues via ATP-binding cassette transporter A1 (ABCA1) [23]. Cholesterol is subsequently esterified by lecithin:cholesterol acyltransferase (LCAT) into CE that are stored in the core of HDL. Due to cholesterol accumulation, the HDL particle expands and matures into spherical HDL [24]. HDL-derived cholesterol can be taken up by the liver and secreted in the bile, thus maintaining cholesterol homeostasis [25]. HDL can exchange lipids with other lipoproteins via interaction with phospholipid transfer protein (PLTP), which facilitates the transport of PL from chylomicrons and VLDL to HDL [26] and cholesteryl ester transfer protein (CETP), which can exchange CE from HDL with TG from apoB-containing lipoproteins [27]. When CE is transferred from HDL to apoB containing lipoproteins, a more atherogenic profile is created with low levels of HDL cholesterol and high levels of LDL cholesterol [28].

Lipolysis of lipoproteins

Lipoprotein lipase (LPL) is the main enzyme responsible for lipolysis of chylomicron and VLDL TG into glycerol and FA. LPL hydrolyses the ester bonds of mono-, di-, and triglycerides. After TG depletion, the resulting chylomicron remnants are taken up by the liver mainly via apoE specific recognition sites such as the LDL receptor (LDLr) and the LDLr related protein (LRP)[29, 30]. IDL and LDL particles, formed after lipolysis of VLDL particles, can also be cleared by the LDLr via apoE. In addition, LDL particles can be taken up by extra-hepatic tissues that need the cholesterol from LDL for proper cellular functioning and steroid hormone synthesis [22].

LPL is expressed in almost all tissues, though most abundantly in tissues that utilize FA for energy (e.g. heart and skeletal muscle) or storage (adipose tissue) [22]. LPL is not expressed

in adult livers. LPL is formed in parenchymal cells and translocated to the luminal surface of endothelial cells to which it becomes anchored to interact with TG-rich lipoproteins [31]. Regulation of LPL is tissue-specific and dependent on nutritional status. Adipose tissue LPL activity is high in the postprandial state, since in this state FA are primarily used for storage. In contrast, during fasting when FA are needed as an energy source, heart and muscle LPL activity is high [32]. The activity of LPL is also influenced by apolipoproteins. They can either stimulate LPL activity (e.g. apoCII and apoAV) [33] [34], or inhibit the activity (e.g. apoCIII and apoCI) [35] [36], thereby influencing plasma TG and FA levels.

Mouse models with tissue specific deletion or over expression of LPL have indicated an important role for LPL in the metabolic syndrome. For instance, LPL over expression in muscle has been associated with increased TG storage in the muscle [37] [38, 39], reduced high fat diet (HFD)-induced obesity [37] and may affect insulin sensitivity [38], [39]. Deletion of LPL in adipose tissue reduced bodyweight in a genetically obese mouse model [40]. Modifiers of LPL action play a role in the development of the metabolic syndrome as well. For example, mice that lack the LPL inhibitor apoCIII are more obese and develop more severe insulin resistance after HFD feeding [41], whereas genetically obese mice that over express the LPL inhibitor apoCI are less obese and less insulin resistant than control genetically obese mice [42]. Overexpression of apoAV, a stimulator of LPL, however did not affect obesity or insulin resistance development in mice subjected to a HFD [43].

Cellular uptake of fatty acids

Uptake, transport and storage of TG-derived FA into tissues are highly regulated since unbound FA are cytotoxic. FA have been shown to passively transfer across cell membranes, however several fatty acid binding proteins exist to facilitate the cellular entry of FA. CD36, also called FA translocase, is such an important fatty acid binding protein that facilitates FA uptake. CD36 is an 88 kDa integral membrane protein and is expressed in many tissues, including adipose tissue, heart, skeletal muscle and intestine [44], but also in endothelial cells, platelets and macrophages [45]. In liver, CD36 is not a main fatty acid transporter [44]. In addition to its role in facilitating FA transport, CD36 can also function as class B scavenger receptor [46].

As scavenger receptor, CD36 plays a central role in development of different metabolic abnormalities associated with the metabolic syndrome such as hypertriglyceridemia, atherosclerosis, inflammation and insulin resistance [47]. CD36-deficient mice are protected against HFD-induced obesity [48, 49 and this thesis]. However, studies investigating the effects of variants in the CD36 gene on obesity in humans have yielded conflicting results. Choquet et al. found no effect of CD36 single nucleotide polymorphisms (SNPs) on onset of obesity [50], whereas Heni et al. found other SNPs that were associated with waist circumference and BMI [51]. Whether CD36-deficiency protects against insulin resistance is controversial. CD36-deficient mice are insulin resistant in the liver, but remain insulin sensitive in muscle [52]. In a specific CD36-deficient Japanese population insulin sensitivity was decreased [53, 54], although another study did not find an effect on insulin sensitivity in similar CD36-deficient subjects [55]. In addition some SNPs in the CD36 gene are associated with increased insulin resistance [56, 57] , although another is not [58].

Intracellular processing of fatty acids

Inside the cell, diacylglycerol acyltransferases (DGATs) catalyze the re-esterification of FA that are not utilized for energy, so that they can be stored as TG intracellular [59]. In the fed state, adipose tissue is the main site for TG storage. In the adipose tissue there is a continuous cycle of lipolysis and re-esterifcation of FA that is regulated by several enzymes. Adipose triglyceride lipase (ATGL) catalyzes the first step in TG lipolysis: the breakdown of TG into diacylglycerol (DG) and FA. Hormone sensitive lipase (HSL) catalyzes the breakdown of DG into monoacylglycerol (MG) and FA. In the fed state, HSL activity is inhibited by insulin resulting in intracellular net uptake of FA and accumulation of TG in adipose tissue. During fasting or enhanced energy demand hormones such as glucagon stimulate HSL activity, which results in the release of FA into the circulation. The released FA can be taken up by other tissues and used as energy source [60]. Interestingly, decreased ATGL and HSL mRNA and protein levels have been reported in obese individuals with insulin resistance [61 62].

Role of fatty acids in the pathology of insulin resistance

The increased prevalence of the metabolic syndrome in our society is driven by an increasing disbalance between energy intake and energy expenditure. The expanded adipose tissue mass that is characteristic of obesity is thought to play an important role in the pathology of the metabolic syndrome. Adipose tissue continuously takes up and secretes FA in a so called futile cycle as discussed in the previous paragraph. Under normal, healthy conditions, the net balance of absorption and secretion is tightly regulated. The absolute amount of the adipose tissue determines the contribution to the futile cycle. With increasing adipose tissue mass, the contribution of the futile cycle to basal plasma FA levels will increase and it has been hypothesized that this increase in cytotoxic FA is one of the causes driving the metabolic syndrome.

The lipid overload at the onset of HFD-induced obesity has been related to the onset of insulin resistance. In mice and humans, intravenous lipid infusions cause insulin resistance [63-65]. Excess lipids may be delivered to non-adipose tissues (ectopic fat deposition) that are not suited for fat storage (i.e. skeletal muscle and the liver), thereby increasing the formation of specific fatty acid metabolites such as fatty acyl CoA, diacylglycerol, and ceramides that may directly impair insulin signaling. Normally, insulin stimulates tyrosine phosphorylation of insulin receptor substrate (IRS) proteins that mediate insulin signaling. In insulin resistance, serine residues of IRS are phosphorylated instead, which interferes in insulin receptor signaling [66]. In mice and humans it was found that increased intramyocellular diacylglycerol activates protein kinase C isoforms, which can inhibit insulin signaling by phosphorylating serine residues of IRS-1 [67, 68]. Moreover, increased ceramide levels in plasma and muscle of mice and human also inhibit insulin signaling [69 70, 71]. In addition to ectopic fat deposition, high levels of FA can also lead to metabolic inflammation, another key event that can impair insulin signaling which will be further discussed in the following paragraphs.

1.3 METABOLIC INFLAMMATION

Classically, inflammation is described as the primary response of the body against injury. This classical response is strong, acute and limited. In contrast to this acute inflammatory response, it has been discovered in the past decades that many obese subjects have slightly increased levels of inflammatory markers in plasma, which remain elevated over a longer period of time. This kind of inflammation is referred to as low-grade-, chronic- or metabolic inflammation, since it is hypothesized that this inflammation is triggered by a surplus of nutrients [72].

The immune response consists of 2 branches, the innate response that is relatively non-specific and the adaptive response, which is specific. Leukocytes such as macrophages and mast cells are the main cells of the innate immune system. T- and B-lymphocytes are the main cells of the adaptive immune system. T-lymphocytes have diverse roles. CD4 T-lymphocytes activate other cells of the immune system such as B-lymphocytes and macrophages. CD8 T-lymphocytes are cytotoxic and kill cells that are infected with pathogens. The primary function of B-lymphocytes is to produce antibodies that can bind to pathogens so that they become tagged for destruction. Both the innate and the adaptive arms of the immune response are involved in metabolic inflammation [73-76]. In the following sections adipose tissue inflammation and the role of different immune cells herein is described. A schematic overview is depicted in Figure 2. In addition, the role of metabolic inflammation in the pathology of insulin resistance is discussed.

Adipose tissue inflammation

This section specifically focuses on the role of immune cells that reside in adipose tissue. Nowadays, adipose tissue is no longer regarded as a simple depot for excess calories. Adipose tissue secretes hormones such as leptin and adiponectin, acute-phase proteins, cytokines, chemokines, growth factors and components of the complement system [77]. These peptides all influence insulin sensitivity and inflammation. Normally the liver and the lymphoid organs are the main production sites of inflammatory mediators, but when adipose tissue expands, adipose tissue also becomes an important producer of these inflammatory mediators [78]. Besides secretion of pro inflammatory molecules, obese adipose tissue contains more immune cells such as macrophages [79], T-lymphocytes [80] and activated B-lymphocytes [81]. Finally, hypertrophic adipocytes secrete more FA, which can have a pro inflammatory effect via Toll Like Receptor (TLR) 2 or 4. All these aspects contribute to the pro inflammatory phenotype that is highly prevalent in obese subjects.

Role of macrophages in adipose tissue inflammation

When there is a surplus of nutrients, adipose tissue needs to expand to increase its storage capacity. Adipocyte hyperplasia (increase in adipocyte number) and adipocyte hypertrophy (increase in adipocyte size) can contribute to this process [82]. The process of adipose tissue expansion requires tissue remodeling such as extracellular matrix degradation and new

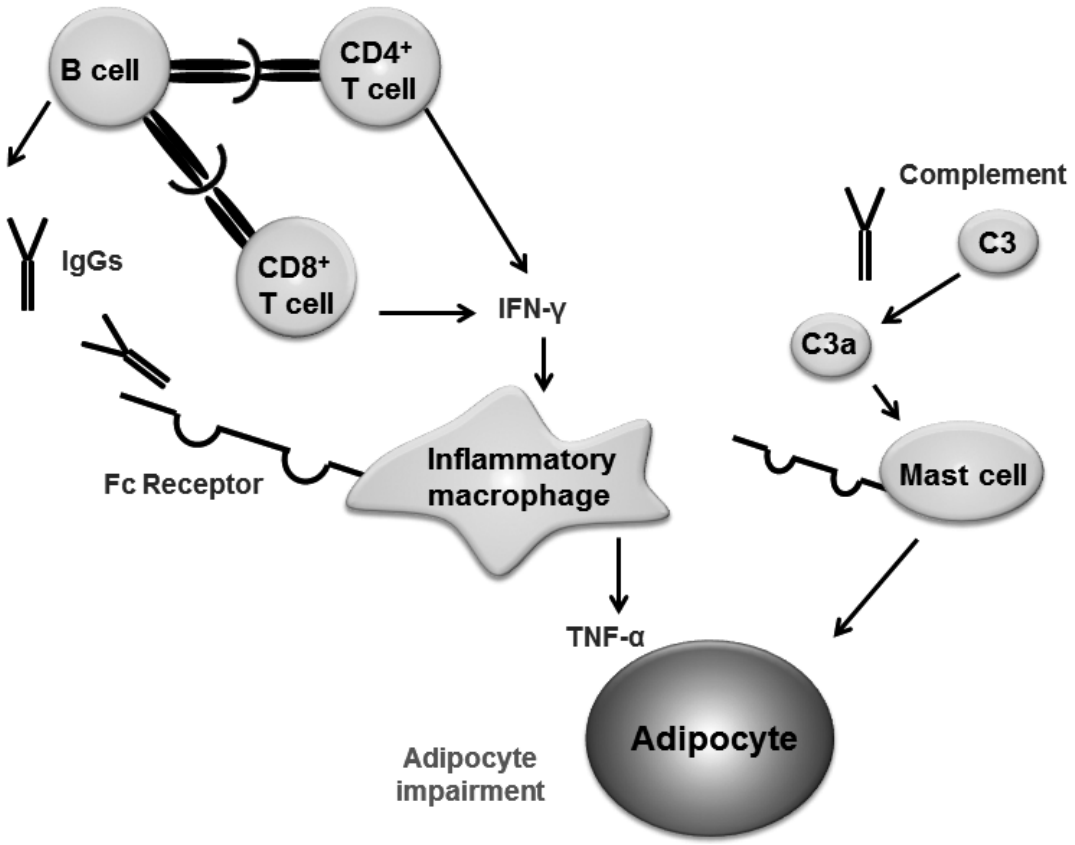

Figure 2. Schematic overview of adipose tissue inflammation. Over nutrition induces an accumulation of B-lymphocytes in adipose tissue. B-lymphocytes are able to interact with T-lymphocytes, which results in the production of IgG autoantibodies. These antibodies may promote complement activation and Fc receptor cross-linking on macrophages and mast cells, which contributes to enhanced adipose tissue inflammation, with subsequent impairment of adipocyte functions (Adapted from Mallat, Nature Medicine 2011).

blood vessel formation, since expansion of adipose tissue is physically limited by nutrient and oxygen supply. Lack of nutrients and oxygen result in hypoxia, adipocyte stress and adipocyte cell death, which are characterized by enhanced chemokine secretion and deregulation of FA fluxes. These processes at the onset of adipose tissue expansion can lead to increased macrophage recruitment within adipose tissue. Indeed, macrophages are increased in obese adipose tissue [73]. These adipose tissue macrophages (ATMs) are not a uniform population of cells, but can exhibit a range of activation states. ATMs that reside in lean adipose tissue are predominately alternatively activated macrophages (M2 macrophages). Alternative activation of macrophages occurs in response to IL-4 and IL-13 and promotes tissue repair and remodeling. Alternative activated macrophages are anti-inflammatory and secrete the anti-inflammatory cytokine IL-10. In contrast, in obese adipose tissue, macrophages are more polarized towards classical activated macrophages (M1 macrophages). Classical activation occurs in response to IFN-γ and results in pro inflammatory macrophages that

secrete e.g. IL-6 and TNF-α [83]. These pro inflammatory cytokines can act on adipocytes to induce insulin resistance (this is further discussed in the section on the role of metabolic inflammation in the pathology of insulin resistance).

Cytokines produced by ATMs can have endocrine cross talk with skeletal muscle and liver; two other organs that have increased macrophage content in obese patients and thus can also develop inflammation-driven insulin resistance [84 85].

Role of T-lymphocytes in adipose tissue inflammation

In addition to macrophages, other immune cells like T-lymphocytes are also increased in obese adipose tissue [86]. Two main populations of T-lymphocytes exist: T-helper lymphocytes, expressing co-receptor CD4 and cytotoxic T-lymphocytes, expressing co-receptor CD8. T-helper lymphocytes are important for the development of an antigen-specific B-lymphocyte response (which will be discussed in the following paragraph). The population of T-helper lymphocytes can roughly be subdivided into pro inflammatory cells (T_H1, T_H17) and anti-inflammatory and regulatory sublineages (T_H2, $Foxp3^+$). In obese subjects the number of T_H1 and $CD8^+$ T-lymphoyctes in adipose tissues is increased, whereas the number of regulatory T-lymphocytes is decreased. Recent studies have suggested that T_H1 lymphocytes and $CD8^+$ T-lymphocytes help recruit macrophages into adipose tissue and stimulate the M1 macrophage inflammatory activation status. It is speculated that these lymphocytes respond to unique antigens that are generated in obese adipose tissue during HFD feeding. Gain- and loss-of-function studies have indicated that these T_H1 and $CD8^+$ T- lymphocytes are associated with increased insulin resistance [76, 87].

Role B-lymphocytes in adipose tissue inflammation

B-lymphocytes are also recruited to adipose tissue shortly after initiation of HFD [86] and activation of B-lymphocytes is increased in patients with type 2 diabetes [81]. B-lymphocytes produce antibodies, also named immunoglobulins (Ig) in response to antigens. These antibodies have a so-called constant part (Fc region) that can bind to C1q, which is the recognition component of the classical complement pathway. Upon binding to C1q, the complement system is activated and processes such as phagocytosis are initiated to clear pathogens [88, 89]. The Fc region can also bind to Fc receptors (FcRs). FcRs can be found on most hematopoietic cells, such as neutrophils, natural killer cells, dendritic cells, mast cells and monocytes/macrophages [90]. Upon binding to FcRs, a range of cellular responses is initiated, such as phagocytosis, antigen-dependent cellular cytotoxicity and secretion of cytokines [91]. FcRs and the complement system thus form a link between the innate and the adaptive immune system. FcRs are multi-subunit receptors, in which the ligand-binding α-chain associates with the signal transducing γ-chain that contains an immunoreceptor tyrosine-based motif (ITAM). In addition to signaling, the γ-chain is also essential for normal surface expression of FcαRI, FcγRI and III and FcεRI.

Recently, it has been shown that B-lymphocytes from HFD-fed mice can activate $CD8^+$ and $CD4^+$ T-lymphocytes [75]. When these T-lymphocytes are activated, they start to produce

pro inflammatory cytokines such as INF-γ that stimulate M1 macrophage polarization, which can eventually lead to insulin resistance. The requirement of T-lymphocytes in this process suggests that the antigen presenting function of B-lymphocytes is important for the development of insulin resistance. In line with this idea, it was found that B-lymphocytes from HFD-fed mice produce IgG antibodies that via their Fc portion elicit a pro inflammatory cytokine response. It is possible that the source of the antigens responsible for the detrimental effect on insulin sensitivity is formed by stressed apoptotic adipocytes, since IgG antibodies concentrate in so called crown-like structures within adipose tissue. Crown-like structures are composed of dead adipocytes surrounded by activated adipose tissue macrophages.

Antibodies produced by B-lymphocytes are thus important for the development of HFD-induced insulin resistance, however the role of antibody effector pathways in this process is not clear yet [75].

The role of metabolic inflammation in the pathology of insulin resistance

Thus, in addition to FA and their metabolites as discussed above, tissue specific and systemic inflammatory signals likely play determinant roles in the pathology of insulin resistance. TNF-α, IL-6 and IL-1β secreted by classical activated macrophages can activate Jun N-terminal kinase (JNK) and inhibitor of κB kinase (IKKB) in adipocytes, myocytes and hepatocytes. Like FA metabolites, these kinases are able to phosphorylate the serine residue of IRS, thereby inhibiting insulin signaling [92 93 94]. Besides acting on IRS, these kinases also activate transcription factor activator protein 1 (AP1) (c-Jun/Fos) and nuclear factor NF-κB, which induces further inflammatory gene expression [95]. Mouse models that lack either JNK1 or IKKB in myeloid cells are protected against obesity-induced insulin resistance [96 84].

Saturated FA may also have a direct pro inflammatory effect. Innate immune cells possess recognition receptors that sense invading pathogens and subsequently start to stimulate pro inflammatory signaling pathways in order to recruit other immune cells. TLRs form such a family of recognition receptors. Recently it has been found that in addition to pathogens, saturated FA can also interact with TLR4 and TLR2 and activate pro inflammatory signaling pathways [64, 97]. Accordingly, TLR4 and TLR2 deficient mice have reduced HFD-induced inflammation, as well as reduced HFD-induced insulin resistance [64, 98, 99]. In addition to TLRs, the inflammasome, a multiprotein complex consisting of a member of the Nod-like receptor family (e.g. NLRP3), and the inflammasome adaptor molecule ASC, can also recognize pathogens. When the inflammasome becomes activated, caspase-1 is recruited and activated which results in activation of the pro inflammatory cytokines IL-1β and IL-18 [100, 101]. Recently, it was discovered that HFD feeding results in activation of caspase-1 in adipose tissue of mice. In these HFD-fed mice increased IL-1β and IL-18 protein levels were observed [102]. In line with these results caspase-1 deficient mice demonstrated reduced HFD-obesity, HFD-induced-insulin resistance and HFD-induced inflammation in adipose tissue [103].

1.4 OUTLINE OF THE THESIS

The research described in this thesis focuses on TG/FA metabolism and inflammation, two key processes that are deranged during the development of the metabolic syndrome. We specifically focus on insulin resistance, an important metabolic abnormality of the metabolic syndrome. In Chapter 2 we studied obesity development, fat deposition, adipocyte development and functioning and insulin sensitivity in a murine model deficient for a major FA transporter, CD36. Mice deficient in CD36 have increased fasting plasma FA, TG and total cholesterol levels and decreased fasting plasma glucose levels on normal chow diet [104], indicating a role for CD36 in lipoprotein, FA and glucose metabolism. Because CD36 facilitates FA uptake and FA uptake is important in adipogenesis, the $CD36^{-/-}$ mice is an appropriate model to study fat deposition, adipocyte development and functioning and its effect on insulin sensitivity. In Chapter 3 and 4 we determined how different pharmacological interventions in inflammation affect lipid metabolism (Chapter 3) or insulin sensitivity (Chapter 4). In Chapter 3 we investigated the mechanism of TG lowering by the non-steroidal anti-inflammatory drug aspirin. Human apolipoprotein CI-expressing mice (*APOC1*) were used as a model for hypertriglyceridemia. *APOC1* mice have increased plasma TG due to diminished clearance of VLDL particles through apoCI-mediated inhibition of LPL. In Chapter 4 we investigated whether an anti-inflammatory compound derived from an extract of *Humulus lupulus L*., META060, had the capacity to improve insulin sensitivity in a HFD fed mouse. In Chapter 5 we investigated a novel mechanism underlying the inflammation that is associated with the metabolic syndrome. We used the FcR γ-$chain^{-/-}$ mice, characterized by diminished activation of IgG and IgE antibody effector pathways, to study the role of functional FcRs in the development of obesity-induced insulin resistance. It has been discovered that HFD-induced IgG play a role in the development of insulin resistance. However, the role of functional FcRs in this process has not been investigated yet. The last chapter provides an overall discussion and conclusion about this PhD project (Chapter 6).

REFERENCES

1. Eckel RH, Grundy SM, Zimmet PZ. The metabolic syndrome. Lancet 2005;365:1415-1428.
2. Yusuf S, Hawken S, Ounpuu S, Dans T, Avezum A, Lanas F, McQueen M, Budaj A, Pais P, Varigos J, Lisheng L. Effect of potentially modifiable risk factors associated with myocardial infarction in 52 countries (the INTERHEART study): case-control study. Lancet 2004;364:937-952.
3. O'Rahilly S, Farooqi IS. Genetics of obesity. Philos Trans R Soc Lond B Biol Sci 2006;361:1095-1105.
4. O'Rahilly S. Human genetics illuminates the paths to metabolic disease. Nature 2009;462:307-314.
5. www.who.int 2012.
6. Aljada A, Mohanty P, Ghanim H, Abdo T, Tripathy D, Chaudhuri A, Dandona P. Increase in intranuclear nuclear factor kappaB and decrease in inhibitor kappaB in mononuclear cells after a mixed meal: evidence for a proinflammatory effect. Am J Clin Nutr 2004;79:682-690.

7. Bruce KD, Byrne CD. The metabolic syndrome: common origins of a multifactorial disorder. Postgrad Med J 2009;85:614-621.
8. Nonogaki K, Fuller GM, Fuentes NL, Moser AH, Staprans I, Grunfeld C, Feingold KR. Interleukin-6 stimulates hepatic triglyceride secretion in rats. Endocrinology 1995;136:2143-2149.
9. Wilson PG, Thompson JC, Webb NR, de Beer FC, King VL, Tannock LR. Serum amyloid A, but not C-reactive protein, stimulates vascular proteoglycan synthesis in a pro-atherogenic manner. Am J Pathol 2008;173:1902-1910.
10. Wallace TM, Matthews DR. The assessment of insulin resistance in man. Diabet Med 2002;19:527-534.
11. Pendergrass M, Bertoldo A, Bonadonna R, Nucci G, Mandarino L, Cobelli C, Defronzo RA. Muscle glucose transport and phosphorylation in type 2 diabetic, obese nondiabetic, and genetically predisposed individuals. Am J Physiol Endocrinol Metab 2007;292:E92-100.
12. Olefsky JM, Garvey WT, Henry RR, Brillon D, Matthaei S, Freidenberg GR. Cellular mechanisms of insulin resistance in non-insulin-dependent (type II) diabetes. Am J Med 1988;85:86-105.
13. Severson DL. Diabetic cardiomyopathy: recent evidence from mouse models of type 1 and type 2 diabetes. Can J Physiol Pharmacol 2004;82:813-823.
14. Gastaldelli A, Baldi S, Pettiti M, Toschi E, Camastra S, Natali A, Landau BR, Ferrannini E. Influence of obesity and type 2 diabetes on gluconeogenesis and glucose output in humans: a quantitative study. Diabetes 2000;49:1367-1373.
15. den BM, Voshol PJ, Kuipers F, Havekes LM, Romijn JA. Hepatic steatosis: a mediator of the metabolic syndrome. Lessons from animal models. Arterioscler Thromb Vasc Biol 2004;24:644-649.
16. SubramanianS,ChaitA.Hypertriglyceridemia secondary to obesity and diabetes. Biochim Biophys Acta 2012;1821:819-825.
17. AbouRjaili G, Shtaynberg N, Wetz R, Costantino T, Abela GS. Current concepts in triglyceride metabolism, pathophysiology, and treatment. Metabolism 2010;59:1210-1220.
18. Mu H, Hoy CE. The digestion of dietary triacylglycerols. Prog Lipid Res 2004;43:105-133.
19. Hussain MM. A proposed model for the assembly of chylomicrons. Atherosclerosis 2000;148:1-15.
20. Fisher EA, Ginsberg HN. Complexity in the secretory pathway: the assembly and secretion of apolipoprotein B-containing lipoproteins. J Biol Chem 2002;277:17377-17380.
21. Barrows BR, Parks EJ. Contributions of different fatty acid sources to very low-density lipoprotein-triacylglycerol in the fasted and fed states. J Clin Endocrinol Metab 2006;91:1446-1452.
22. Ginsberg HN. Lipoprotein physiology. Endocrinol Metab Clin North Am 1998;27:503-519.
23. Zannis VI, Chroni A, Krieger M. Role of apoA-I, ABCA1, LCAT, and SR-BI in the biogenesis of HDL. J Mol Med (Berl) 2006;84:276-294.
24. Jonas A. Lecithin-cholesterol acyltransferase in the metabolism of high-density lipoproteins. Biochim Biophys Acta 1991;1084:205-220.
25. Chiang JY. Regulation of bile acid synthesis: pathways, nuclear receptors, and mechanisms. J Hepatol 2004;40:539-551.
26. Huuskonen J, Olkkonen VM, Jauhiainen M, Ehnholm C. The impact of phospholipid transfer protein (PLTP) on HDL metabolism. Atherosclerosis 2001;155:269-281.
27. Morton RE, Zilversmit DB. Inter-relationship of lipids transferred by the lipid-transfer protein isolated from human lipoprotein-deficient plasma. J Biol Chem 1983;258:11751-11757.
28. Glass CK, Witztum JL. Atherosclerosis. the road ahead. Cell 2001;104:503-516.
29. Mahley RW, Hui DY, Innerarity TL, Beisiegel U. Chylomicron remnant metabolism. Role of hepatic lipoprotein receptors in mediating uptake. Arteriosclerosis 1989;9:I14-I18.
30. Mahley RW, Ji ZS. Remnant lipoprotein metabolism: key pathways involving cell-surface heparan sulfate proteoglycans and apolipoprotein E. J Lipid Res 1999;40:1-16.
31. Preiss-Landl K, Zimmermann R, Hammerle G, Zechner R. Lipoprotein lipase: the regulation of tissue specific expression and its role in lipid and energy metabolism. Curr Opin Lipidol 2002;13:471-481.
32. Wang H, Eckel RH. Lipoprotein lipase: from gene to obesity. Am J Physiol Endocrinol Metab 2009;297:E271-E288.

33. Wang CS. Structure and functional properties of apolipoprotein C-II. Prog Lipid Res 1991;30:253-258.
34. Merkel M, Loeffler B, Kluger M, Fabig N, Geppert G, Pennacchio LA, Laatsch A, Heeren J. Apolipoprotein AV accelerates plasma hydrolysis of triglyceride-rich lipoproteins by interaction with proteoglycan-bound lipoprotein lipase. J Biol Chem 2005;280:21553-21560.
35. Ginsberg HN, Le NA, Goldberg IJ, Gibson JC, Rubinstein A, Wang-Iverson P, Norum R, Brown WV. Apolipoprotein B metabolism in subjects with deficiency of apolipoproteins CIII and AI. Evidence that apolipoprotein CIII inhibits catabolism of triglyceride-rich lipoproteins by lipoprotein lipase in vivo. J Clin Invest 1986;78:1287-1295.
36. Berbee JF, van der Hoogt CC, Sundararaman D, Havekes LM, Rensen PC. Severe hypertriglyceridemia in human APOC1 transgenic mice is caused by apoC-I-induced inhibition of LPL. J Lipid Res 2005;46:297-306.
37. Jensen DR, Schlaepfer IR, Morin CL, Pennington DS, Marcell T, Ammon SM, Gutierrez-Hartmann A, Eckel RH. Prevention of diet-induced obesity in transgenic mice overexpressing skeletal muscle lipoprotein lipase. Am J Physiol 1997;273:R683-R689.
38. Kim JK, Fillmore JJ, Chen Y, Yu C, Moore IK, Pypaert M, Lutz EP, Kako Y, Velez-Carrasco W, Goldberg IJ, Breslow JL, Shulman GI. Tissue-specific overexpression of lipoprotein lipase causes tissue-specific insulin resistance. Proc Natl Acad Sci U S A 2001;98:7522-7527.
39. Voshol PJ, Jong MC, Dahlmans VE, Kratky D, Levak-Frank S, Zechner R, Romijn JA, Havekes LM. In muscle-specific lipoprotein lipase-overexpressing mice, muscle triglyceride content is increased without inhibition of insulin-stimulated whole-body and muscle-specific glucose uptake. Diabetes 2001;50:2585-2590.
40. Weinstock PH, Levak-Frank S, Hudgins LC, Radner H, Friedman JM, Zechner R, Breslow JL. Lipoprotein lipase controls fatty acid entry into adipose tissue, but fat mass is preserved by endogenous synthesis in mice deficient in adipose tissue lipoprotein lipase. Proc Natl Acad Sci U S A 1997;94:10261-10266.
41. Duivenvoorden I, Teusink B, Rensen PC, Romijn JA, Havekes LM, Voshol PJ. Apolipoprotein C3 deficiency results in diet-induced obesity and aggravated insulin resistance in mice. Diabetes 2005;54:664-671.
42. Jong MC, Voshol PJ, Muurling M, Dahlmans VE, Romijn JA, Pijl H, Havekes LM. Protection from obesity and insulin resistance in mice overexpressing human apolipoprotein C1. Diabetes 2001;50:2779-2785.
43. Pamir N, McMillen TS, Li YI, Lai CM, Wong H, LeBoeuf RC. Overexpression of apolipoprotein A5 in mice is not protective against body weight gain and aberrant glucose homeostasis. Metabolism 2009;58:560-567.
44. Abumrad NA, el-Maghrabi MR, Amri EZ, Lopez E, Grimaldi PA. Cloning of a rat adipocyte membrane protein implicated in binding or transport of long-chain fatty acids that is induced during preadipocyte differentiation. Homology with human CD36. J Biol Chem 1993;268:17665-17668.
45. Silverstein RL, Febbraio M. CD36, a scavenger receptor involved in immunity, metabolism, angiogenesis, and behavior. Sci Signal 2009;2:re3.
46. Febbraio M, Hajjar DP, Silverstein RL. CD36: a class B scavenger receptor involved in angiogenesis, atherosclerosis, inflammation, and lipid metabolism. J Clin Invest 2001;108:785-791.
47. Kennedy DJ, Kashyap SR. Pathogenic role of scavenger receptor CD36 in the metabolic syndrome and diabetes. Metab Syndr Relat Disord 2011;9:239-245.
48. Hajri T, Hall AM, Jensen DR, Pietka TA, Drover VA, Tao H, Eckel R, Abumrad NA. CD36-facilitated fatty acid uptake inhibits leptin production and signaling in adipose tissue. Diabetes 2007;56:1872-1880.
49. Koonen DP, Sung MM, Kao CK, Dolinsky VW, Koves TR, Ilkayeva O, Jacobs RL, Vance DE, Light PE, Muoio DM, Febbraio M, Dyck JR. Alterations in skeletal muscle fatty acid handling predisposes middle-aged mice to diet-induced insulin resistance. Diabetes 2010;59:1366-1375.
50. Choquet H, Labrune Y, De GF, Hinney A, Hebebrand J, Scherag A, Lecoeur C, Tauber M, Balkau B, Elliot P, Jarvelin MR, Walley AJ, Besnard P, Froguel P, Meyre D. Lack of association of CD36 SNPs with early onset obesity: a meta-analysis in 9,973 European subjects. Obesity (Silver Spring) 2011;19:833-839.

51. Heni M, Mussig K, Machicao F, Machann J, Schick F, Claussen CD, Stefan N, Fritsche A, Haring HU, Staiger H. Variants in the CD36 gene locus determine whole-body adiposity, but have no independent effect on insulin sensitivity. Obesity (Silver Spring) 2011;19:1004-1009.
52. Goudriaan JR, Dahlmans VE, Teusink B, Ouwens DM, Febbraio M, Maassen JA, Romijn JA, Havekes LM, Voshol PJ. CD36 deficiency increases insulin sensitivity in muscle, but induces insulin resistance in the liver in mice. J Lipid Res 2003;44:2270-2277.
53. Furuhashi M, Ura N, Nakata T, Tanaka T, Shimamoto K. Genotype in human CD36 deficiency and diabetes mellitus. Diabet Med 2004;21:952-953.
54. Kuwasako T, Hirano K, Sakai N, Ishigami M, Hiraoka H, Yakub MJ, Yamauchi-Takihara K, Yamashita S, Matsuzawa Y. Lipoprotein abnormalities in human genetic CD36 deficiency associated with insulin resistance and abnormal fatty acid metabolism. Diabetes Care 2003;26:1647-1648.
55. Yanai H, Chiba H, Morimoto M, Jamieson GA, Matsuno K. Type I CD36 deficiency in humans is not associated with insulin resistance syndrome. Thromb Haemost 2000;83:786.
56. Corpeleijn E, van der Kallen CJ, Kruijshoop M, Magagnin MG, de Bruin TW, Feskens EJ, Saris WH, Blaak EE. Direct association of a promoter polymorphism in the CD36/FAT fatty acid transporter gene with Type 2 diabetes mellitus and insulin resistance. Diabet Med 2006;23:907-911.
57. Lepretre F, Linton KJ, Lacquemant C, Vatin V, Samson C, Dina C, Chikri M, Ali S, Scherer P, Seron K, Vasseur F, Aitman T, Froguel P. Genetic study of the CD36 gene in a French diabetic population. Diabetes Metab 2004;30:459-463.
58. Kajihara S, Hisatomi A, Ogawa Y, Yasutake T, Yoshimura T, Hara T, Mizuta T, Ozaki I, Iwamoto N, Yamamoto K. Association of the Pro90Ser CD36 mutation with elevated free fatty acid concentrations but not with insulin resistance syndrome in Japanese. Clin Chim Acta 2001;314:125-130.
59. Yen CL, Stone SJ, Koliwad S, Harris C, Farese RV, Jr. Thematic review series: glycerolipids. DGAT enzymes and triacylglycerol biosynthesis. J Lipid Res 2008;49:2283-2301.
60. Zechner R, Kienesberger PC, Haemmerle G, Zimmermann R, Lass A. Adipose triglyceride lipase and the lipolytic catabolism of cellular fat stores. J Lipid Res 2009;50:3-21.
61. Jocken JW, Langin D, Smit E, Saris WH, Valle C, Hul GB, Holm C, Arner P, Blaak EE. Adipose triglyceride lipase and hormone-sensitive lipase protein expression is decreased in the obese insulin-resistant state. J Clin Endocrinol Metab 2007;92:2292-2299.
62. Berndt J, Kralisch S, Kloting N, Ruschke K, Kern M, Fasshauer M, Schon MR, Stumvoll M, Bluher M. Adipose triglyceride lipase gene expression in human visceral obesity. Exp Clin Endocrinol Diabetes 2008;116:203-210.
63. Kim JK, Kim YJ, Fillmore JJ, Chen Y, Moore I, Lee J, Yuan M, Li ZW, Karin M, Perret P, Shoelson SE, Shulman GI. Prevention of fat-induced insulin resistance by salicylate. J Clin Invest 2001;108:437-446.
64. Shi H, Kokoeva MV, Inouye K, Tzameli I, Yin H, Flier JS. TLR4 links innate immunity and fatty acid-induced insulin resistance. J Clin Invest 2006;116:3015-3025.
65. Roden M, Price TB, Perseghin G, Petersen KF, Rothman DL, Cline GW, Shulman GI. Mechanism of free fatty acid-induced insulin resistance in humans. J Clin Invest 1996;97:2859-2865.
66. Morino K, Neschen S, Bilz S, Sono S, Tsirigotis D, Reznick RM, Moore I, Nagai Y, Samuel V, Sebastian D, White M, Philbrick W, Shulman GI. Muscle-specific IRS-1 Ser->Ala transgenic mice are protected from fat-induced insulin resistance in skeletal muscle. Diabetes 2008;57:2644-2651.
67. Yu C, Chen Y, Cline GW, Zhang D, Zong H, Wang Y, Bergeron R, Kim JK, Cushman SW, Cooney GJ, Atcheson B, White MF, Kraegen EW, Shulman GI. Mechanism by which fatty acids inhibit insulin activation of insulin receptor substrate-1 (IRS-1)-associated phosphatidylinositol 3-kinase activity in muscle. J Biol Chem 2002;277:50230-50236.
68. Itani SI, Ruderman NB, Schmieder F, Boden G. Lipid-induced insulin resistance in human muscle is associated with changes in diacylglycerol, protein kinase C, and IkappaB-alpha. Diabetes 2002;51:2005-2011.
69. Holland WL, Brozinick JT, Wang LP, Hawkins ED, Sargent KM, Liu Y, Narra K, Hoehn KL, Knotts TA, Siesky A, Nelson DH, Karathanasis SK, Fontenot GK, Birnbaum

MJ, Summers SA. Inhibition of ceramide synthesis ameliorates glucocorticoid-, saturated-fat-, and obesity-induced insulin resistance. Cell Metab 2007;5:167-179.

70. Adams JM, Pratipanawatr T, Berria R, Wang E, Defronzo RA, Sullards MC, Mandarino LJ. Ceramide content is increased in skeletal muscle from obese insulin-resistant humans. Diabetes 2004;53:25-31.
71. Haus JM, Kashyap SR, Kasumov T, Zhang R, Kelly KR, Defronzo RA, Kirwan JP. Plasma ceramides are elevated in obese subjects with type 2 diabetes and correlate with the severity of insulin resistance. Diabetes 2009;58:337-343.
72. Hotamisligil GS. Inflammation and metabolic disorders. Nature 2006;444:860-867.
73. Weisberg SP, McCann D, Desai M, Rosenbaum M, Leibel RL, Ferrante AW, Jr. Obesity is associated with macrophage accumulation in adipose tissue. J Clin Invest 2003;112:1796-1808.
74. Liu J, Divoux A, Sun J, Zhang J, Clement K, Glickman JN, Sukhova GK, Wolters PJ, Du J, Gorgun CZ, Doria A, Libby P, Blumberg RS, Kahn BB, Hotamisligil GS, Shi GP. Genetic deficiency and pharmacological stabilization of mast cells reduce diet-induced obesity and diabetes in mice. Nat Med 2009;15:940-945.
75. Winer DA, Winer S, Shen L, Wadia PP, Yantha J, Paltser G, Tsui H, Wu P, Davidson MG, Alonso MN, Leong HX, Glassford A, Caimol M, Kenkel JA, Tedder TF, McLaughlin T, Miklos DB, Dosch HM, Engleman EG. B cells promote insulin resistance through modulation of T cells and production of pathogenic IgG antibodies. Nat Med 2011;17:610-617.
76. Winer S, Chan Y, Paltser G, Truong D, Tsui H, Bahrami J, Dorfman R, Wang Y, Zielenski J, Mastronardi F, Maezawa Y, Drucker DJ, Engleman E, Winer D, Dosch HM. Normalization of obesity-associated insulin resistance through immunotherapy. Nat Med 2009;15:921-929.
77. Calder PC, Ahluwalia N, Brouns F, Buetler T, Clement K, Cunningham K, Esposito K, Jonsson LS, Kolb H, Lansink M, Marcos A, Margioris A, Matusheski N, Nordmann H, O'Brien J, Pugliese G, Rizkalla S, Schalkwijk C, Tuomilehto J, Warnberg J, Watzl B, Winklhofer-Roob BM. Dietary factors and low-grade inflammation in relation to overweight and obesity. Br J Nutr 2011;106 Suppl 3:S5-78.
78. Skurk T, Alberti-Huber C, Herder C, Hauner H. Relationship between adipocyte size and adipokine expression and secretion. J Clin Endocrinol Metab 2007;92:1023-1033.
79. Xu H, Barnes GT, Yang Q, Tan G, Yang D, Chou CJ, Sole J, Nichols A, Ross JS, Tartaglia LA, Chen H. Chronic inflammation in fat plays a crucial role in the development of obesity-related insulin resistance. J Clin Invest 2003;112:1821-1830.
80. Kintscher U, Hartge M, Hess K, Foryst-Ludwig A, Clemenz M, Wabitsch M, Fischer-Posovszky P, Barth TF, Dragun D, Skurk T, Hauner H, Bluher M, Unger T, Wolf AM, Knippschild U, Hombach V, Marx N. T-lymphocyte infiltration in visceral adipose tissue: a primary event in adipose tissue inflammation and the development of obesity-mediated insulin resistance. Arterioscler Thromb Vasc Biol 2008;28:1304-1310.
81. Jagannathan M, McDonnell M, Liang Y, Hasturk H, Hetzel J, Rubin D, Kantarci A, Van Dyke TE, Ganley-Leal LM, Nikolajczyk BS. Toll-like receptors regulate B cell cytokine production in patients with diabetes. Diabetologia 2010;53:1461-1471.
82. Virtue S, Vidal-Puig A. Adipose tissue expandability, lipotoxicity and the Metabolic Syndrome--an allostatic perspective. Biochim Biophys Acta 2010;1801:338-349.
83. Odegaard JI, Chawla A. Alternative macrophage activation and metabolism. Annu Rev Pathol 2011;6:275-297.
84. Arkan MC, Hevener AL, Greten FR, Maeda S, Li ZW, Long JM, Wynshaw-Boris A, Poli G, Olefsky J, Karin M. IKK-beta links inflammation to obesity-induced insulin resistance. Nat Med 2005;11:191-198.
85. Patsouris D, Li PP, Thapar D, Chapman J, Olefsky JM, Neels JG. Ablation of CD11c-positive cells normalizes insulin sensitivity in obese insulin resistant animals. Cell Metab 2008;8:301-309.
86. Duffaut C, Galitzky J, Lafontan M, Bouloumie A. Unexpected trafficking of immune cells within the adipose tissue during the onset of obesity. Biochem Biophys Res Commun 2009;384:482-485.
87. Nishimura S, Manabe I, Nagasaki M, Eto K, Yamashita H, Ohsugi M, Otsu M, Hara K,

Ueki K, Sugiura S, Yoshimura K, Kadowaki T, Nagai R. CD8+ effector T cells contribute to macrophage recruitment and adipose tissue inflammation in obesity. Nat Med 2009;15:914-920.

88. Walport MJ. Complement. Second of two parts. N Engl J Med 2001;344:1140-1144.
89. Walport MJ. Complement. First of two parts. N Engl J Med 2001;344:1058-1066.
90. Takai T. Roles of Fc receptors in autoimmunity. Nat Rev Immunol 2002;2:580-592.
91. Daeron M. Fc receptor biology. Annu Rev Immunol 1997;15:203-234.
92. Aguirre V, Uchida T, Yenush L, Davis R, White MF. The c-Jun NH(2)-terminal kinase promotes insulin resistance during association with insulin receptor substrate-1 and phosphorylation of Ser(307). J Biol Chem 2000;275:9047-9054.
93. Hirosumi J, Tuncman G, Chang L, Gorgun CZ, Uysal KT, Maeda K, Karin M, Hotamisligil GS. A central role for JNK in obesity and insulin resistance. Nature 2002;420:333-336.
94. Gao Z, Hwang D, Bataille F, Lefevre M, York D, Quon MJ, Ye J. Serine phosphorylation of insulin receptor substrate 1 by inhibitor kappa B kinase complex. J Biol Chem 2002;277:48115-48121.
95. Baud V, Karin M. Signal transduction by tumor necrosis factor and its relatives. Trends Cell Biol 2001;11:372-377.
96. Solinas G, Vilcu C, Neels JG, Bandyopadhyay GK, Luo JL, Naugler W, Grivennikov S, Wynshaw-Boris A, Scadeng M, Olefsky JM, Karin M. JNK1 in hematopoietically derived cells contributes to diet-induced inflammation and insulin resistance without affecting obesity. Cell Metab 2007;6:386-397.
97. Nguyen MT, Favelyukis S, Nguyen AK, Reichart D, Scott PA, Jenn A, Liu-Bryan R, Glass CK, Neels JG, Olefsky JM. A subpopulation of macrophages infiltrates hypertrophic adipose tissue and is activated by free fatty acids via Toll-like receptors 2 and 4 and JNK-dependent pathways. J Biol Chem 2007;282:35279-35292.
98. Ehses JA, Meier DT, Wueest S, Rytka J, Boller S, Wielinga PY, Schraenen A, Lemaire K, Debray S, Van LL, Pospisilik JA, Tschopp O, Schultze SM, Malipiero U, Esterbauer H, Ellingsgaard H, Rutti S, Schuit FC, Lutz TA, Boni-Schnetzler M, Konrad D, Donath MY. Toll-like receptor 2-deficient mice are protected from insulin resistance and beta cell dysfunction induced by a high-fat diet. Diabetologia 2010;53:1795-1806.
99. Tsukumo DM, Carvalho-Filho MA, Carvalheira JB, Prada PO, Hirabara SM, Schenka AA, Araujo EP, Vassallo J, Curi R, Velloso LA, Saad MJ. Loss-of-function mutation in Toll-like receptor 4 prevents diet-induced obesity and insulin resistance. Diabetes 2007;56:1986-1998.
100. Petrilli V, Dostert C, Muruve DA, Tschopp J. The inflammasome: a danger sensing complex triggering innate immunity. Curr Opin Immunol 2007;19:615-622.
101. Franchi L, Eigenbrod T, Munoz-Planillo R, Nunez G. The inflammasome: a caspase-1-activation platform that regulates immune responses and disease pathogenesis. Nat Immunol 2009;10:241-247.
102. Stienstra R, Joosten LA, Koenen T, van TB, van Diepen JA, van den Berg SA, Rensen PC, Voshol PJ, Fantuzzi G, Hijmans A, Kersten S, Muller M, van den Berg WB, van RN, Wabitsch M, Kullberg BJ, van der Meer JW, Kanneganti T, Tack CJ, Netea MG. The inflammasome-mediated caspase-1 activation controls adipocyte differentiation and insulin sensitivity. Cell Metab 2010;12:593-605.
103. Stienstra R, van Diepen JA, Tack CJ, Zaki MH, van de Veerdonk FL, Perera D, Neale GA, Hooiveld GJ, Hijmans A, Vroegrijk I, van den Berg S, Romijn J, Rensen PC, Joosten LA, Netea MG, Kanneganti TD. Inflammasome is a central player in the induction of obesity and insulin resistance. Proc Natl Acad Sci U S A 2011;108:15324-15329.
104. Febbraio M, Abumrad NA, Hajjar DP, Sharma K, Cheng W, Pearce SF, Silverstein RL. A null mutation in murine CD36 reveals an important role in fatty acid and lipoprotein metabolism. J Biol Chem 1999;274:19055-19062.

2 CD36 IS IMPORTANT FOR ADIPOCYTE RECRUITMENT AND AFFECTS LIPOLYSIS

Irene O.C.M. Vroegrijk, Jan Bert van Klinken,
Janna A. van Diepen, Sjoerd A.A. van den Berg,
Maria Febbraio, Laura K.M. Steinbusch, Jan F.C. Glatz,
Louis M. Havekes, Peter J. Voshol, Patrick C.N. Rensen,
Ko Willems van Dijk, Vanessa van Harmelen

Accepted for publication in Obesity

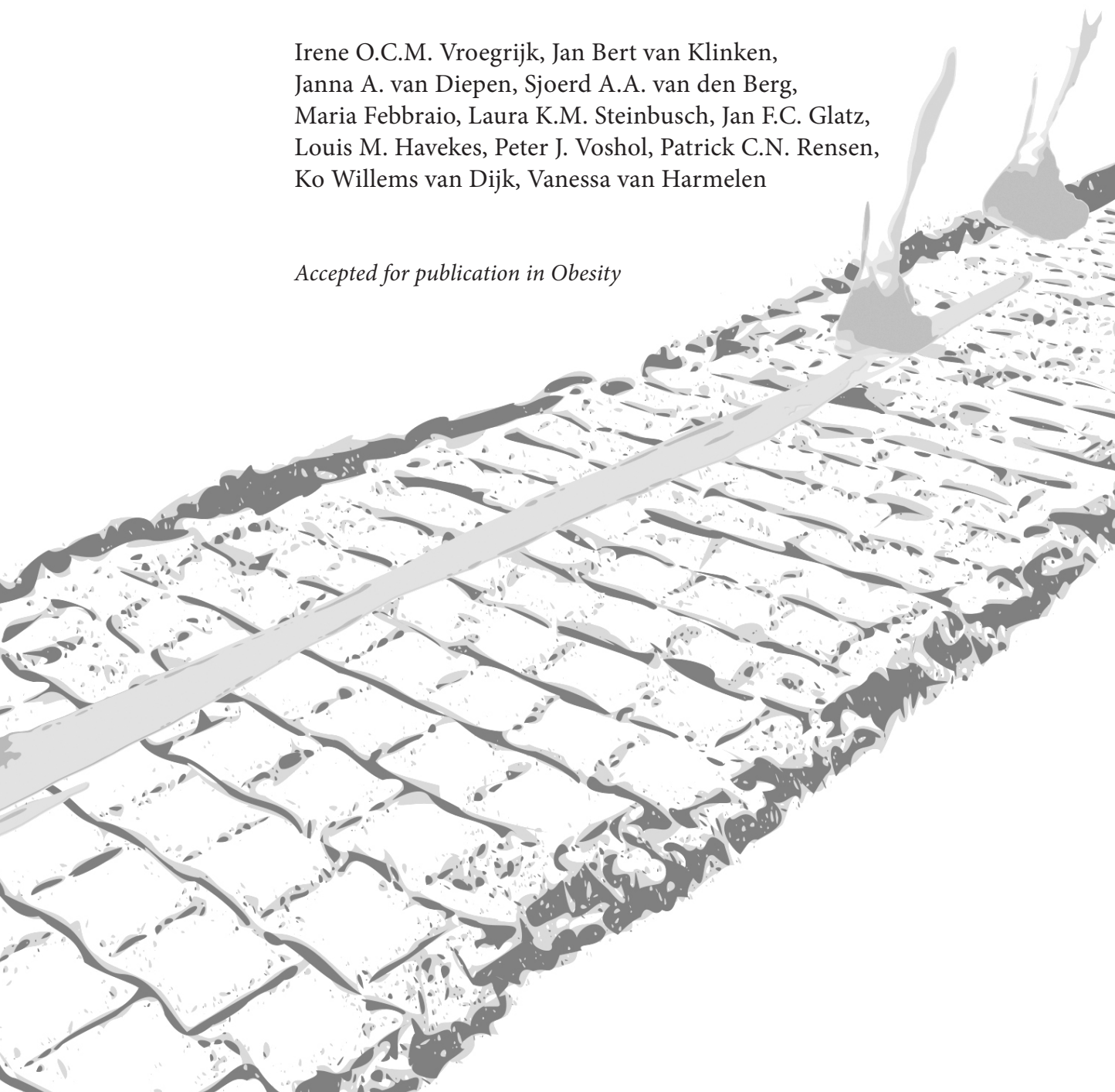

ABSTRACT

Objective: The scavenger receptor CD36 facilitates the cellular uptake of long chain fatty acids. Since CD36-deficiency attenuates the development of high fat diet (HFD)-induced obesity, we set out to characterize the role of CD36-deficiency in preadipocyte recruitment and adipocyte function.

Design and methods: Fat cell size and number were determined in gonadal, visceral and subcutaneous adipose tissue of $CD36^{-/-}$ and WT mice after six weeks on HFD. Basal lipolysis and insulin-inhibited lipolysis were investigated in gonadal adipose tissue.

Results: $CD36^{-/-}$ mice showed a reduction in adipocyte size in all fat pads. Gonadal adipose tissue also showed a lower total number of adipocytes due to a lower number of very small adipocytes (diameter <50 μm). This was accompanied by an increased pool of preadipocytes which suggests that CD36-deficiency reduces the capacity of preadipocytes to become adipocytes. Regarding lipolysis, in adipose tissue from $CD36^{-/-}$ mice cAMP levels were increased and both basal and 8-bromo-cAMP stimulated lipolysis were higher. However, insulin-mediated inhibition of lipolysis was more potent in $CD36^{-/-}$ mice.

Conclusions: These results indicate that during fat depot expansion, CD36-deficiency negatively affects preadipocyte recruitment and that in mature adipocytes, CD36-deficiency is associated with increased basal lipolysis and insulin responsiveness.

2.1 INTRODUCTION

Obesity, and in particular abdominal obesity, is associated with several metabolic abnormalities such as insulin resistance and hypertriglyceridemia, which increase the risk of developing type 2 diabetes and eventually cardiovascular morbidity and mortality [1]. Obesity is caused by a chronic positive energy balance that increases the storage of triglycerides (TG) in adipose tissue. This storage of energy is partly regulated by fatty acid (FA) transporter proteins in adipocytes, which facilitate the cellular entry of lipoprotein derived FA. One of these FA transporters is CD36 [2, 3], a 88 kDa glycoprotein (reviewed in [4]) that primarily facilitates the transport of long chain FA. The role of CD36 in white adipose tissue (WAT) is illustrated by diminished uptake of the FA analogs BMIPP and IPPA in adipose tissue of CD36-deficient ($CD36^{-/-}$) mice fed a chow diet [5]. Other studies have demonstrated that CD36-deficiency protects against obesity induced by a high fat diet (HFD) [6, 7] and development of cardiometabolic problems [8].

Since CD36-deficiency attenuates the development of HFD-induced obesity, we were interested in the role of CD36 in adipocyte development and function. We investigated adipocyte cell size and number in various adipose tissue depots to determine whether CD36-deficiency affects adipocyte hypertrophia (i.e adipocyte growth) and/or hyperplasia (i.e. recruitment of new adipocytes), as both these parameters determine the expansion capacity of adipose tissue. Moreover, we determined the intra cellular lipid accumulation of isolated preadipocytes of $CD36^{-/-}$ versus wild-type (WT) mice in vitro after incubation in adipogenic media. In addition, lipolysis rate of isolated mature adipocytes of CD36-deficient mice versus WT mice was determined, since adipocyte volume is not only determined by uptake of FA which lead to TG storage, but also by the level of FA release during the process of adipocyte lipolysis. Taken together, we aimed to investigate the role of CD36 in adipocyte development and function, since CD36 is involved in development of diet-induced obesity. The current study shows that CD36 affects both adipocyte recruitment and lipolysis.

2.2 MATERIALS AND METHODS

Animals

The generation of $CD36^{-/-}$ mice has been described previously [9]. For this study, $CD36^{-/-}$ mice were crossed back eight times to the C57Bl/6J background. $CD36^{-/-}$ mice were bred at the Leiden University Medical Center, Leiden, The Netherlands. WT control mice (C57Bl/6J background) were purchased from Charles River (Maastricht, The Netherlands). The mice used in experiments were males, housed under standard conditions with free access to water and food. Mice were fed a HFD (45% energy derived from lard fat; D12451, Research Diet Services, Wijk bij Duurstede, The Netherlands) when they were 12 weeks of age to

induce obesity. Body weight was measured regularly. All experiments were approved by the animal ethics committee of Leiden University Medical Center.

Body composition

After 11 weeks of HFD feeding body composition was determined in overnight fasted mice using dual energy X-ray absorptiometry (DEXA) (Norland Stratec Medizintechnik GmbH, Birkenfeld, Germany).

Generation of TG-rich emulsion particles

VLDL-like TG-rich emulsion particles were prepared and characterized as described previously [10]. Lipids (100 mg) at a weight ratio of triolein: egg yolk phosphatidylcholine: lysophosphatidylcholine: cholesteryl oleate: cholesterol of 70: 22.7: 2.3: 3.0: 2.0, supplemented with 100 μCi of glycerol tri[9,10(n)-^{3}H]oleate ([^{3}H]TO) (GE Healthcare, Little Chalfont, UK) were sonicated at 10 μm output using a Soniprep 150 (MSE Scientific Instruments, Crawley, UK). Density gradient ultracentrifugation was used to obtain 80 nm-sized emulsion particles, which were used for subsequent experiments. TG content of the emulsions was measured using a commercially available kit (Roche Molecular Biochemicals, Indianapolis, IN). Emulsions were stored at 4°C under argon and used within 7 days.

In vivo clearance of TG-rich emulsion particles

To study the *in vivo* clearance of the VLDL-like emulsion particles, mice were fed a HFD for 13 weeks. Mice were fasted 4 h (from 8.00 am to 12.00 pm) prior to the start of the experiment and anesthetized by intraperitoneal injection of acepromazine (6.25 mg/kg Neurotranq, Alfasan International BV, Weesp, The Netherlands), midazolam (6.25 mg/kg Dormicum, Roche Diagnostics, Mijdrecht, The Netherlands), and fentanyl (0.31 mg/kg Janssen Pharmaceuticals, Tilburg, The Netherlands). Subsequently, mice were injected (t=0) intravenously with 200 μL of [^{3}H]TO-labeled emulsion particles at a dose of 1 mg of TG per mouse. Blood samples were taken from the tail at 2, 5, 10, 20 and 30 minutes after injection and plasma ^{3}H-activity was counted. Plasma volumes in ml were calculated as 0.04706 x body weight (g) as determined from ^{125}I-BSA clearance studies as described previously [11]. After taking the last blood sample, the liver, heart, spleen, quadriceps, brown adipose tissue and white adipose tissue (*i.e.* gonadal, visceral and subcutaneous) were collected. Organs were dissolved overnight at 60°C in Tissue Solubilizer (Amersham Biosciences, Rosendaal, The Netherlands) and ^{3}H-activity was counted. Uptake of [^{3}H]TO-derived radioactivity by the organs was calculated from the ^{3}H activity in each organ divided by plasma-specific activity of [^{3}H]TG and expressed per mg wet tissue weight. Values were corrected for plasma radioactivity present in the respective tissues [12].

Liver lipids

Lipids were extracted from livers of WT and CD36$^{-/-}$ mice fed a HFD for 11 weeks according to a modified protocol from Bligh and Dyer [13]. Briefly, small liver pieces were homogenized in ice-cold methanol. After centrifugation, lipids were extracted by addition of 1800 μL

chloroform: methanol (3:1 v/v) to 45 µL homogenate. The chloroform phase was dried and dissolved in 2% Triton X-100. Hepatic TG and total cholesterol (TC) concentrations were measured using commercial kits (11488872 and 236691, Roche Molecular Biochemicals, Indianapolis, IN, respectively).

Hepatic phospholipid (PL) concentrations were measured using the commercial available kit phospholipids B (Wako Chemicals GmbH, Neuss, Germany). Liver lipids were expressed per mg protein, which was determined using the BCA protein assay kit (Pierce).

Determination of adipocyte size, adipocyte lipolysis and preadipocyte differentiation capacity

To measure adipocyte size, mice were fed a HFD for 6 weeks and sacrificed. Gonadal, visceral and subcutaneous fat pads were removed and kept in PBS. It was decided to perform the adipocyte morphology and functionality experiments at the week 6 time point to be sure that metabolic adaptions to a HFD were still occurring in the animals and a new set-point had not yet been reached. The tissue was minced and digested in 0.5g/l collagenase in HEPES buffer (pH 7.4) with 20 g/l of dialyzed bovine serum albumin (BSA, fraction V, Sigma, ST Louis, USA) for 1 h at 37°C. The disaggregated adipose tissue was filtered through a nylon mesh with a pore size of 236 µm. For the isolation of mature adipocytes, cells were obtained from the surface of the filtrate and washed several times. Cell size was determined using an imaging processing technique implemented in MATLAB which automatically determines adipocyte sizes of hundreds of adipocytes from microscopic pictures of isolated adipocytes (~1000 cells/fat tissue sample). A manuscript describing the method is under preparation. From the measured cells the adipocyte size distribution, mean adipocyte diameter and adipocyte number per fat pad were determined. Also the volume-weighted mean adipocyte diameter was calculated, which is a measure of the mean adipocyte diameter corrected for the amount of fat that an adipocyte can store [14]. In addition, the anti-lipolytic effect of insulin was determined in the adipocytes by incubating them for 2 h at 37°C in DMEM/F12 with 2% BSA in combination with or without 8-bromoadenosine 3'-5'-cyclic monophosphate (8b-cAMP) (10^{-3}M) (Sigma) and/or insulin (10^{-11}M,10^{-9}M and 10^{-7}M). Glycerol concentrations (index of lipolysis) were determined using a commercially available free glycerol kit (Sigma) with the inclusion of the hydrogen peroxide sensitive fluorescence dye Amplex Ultra Red, as described by Clark et al. [15].

For the isolation of preadipocytes, the infranatant of the adipose tissue filtrate was centrifuged at 200 x g for 10 min at room temperature and treated with erythrocyte lysis buffer. The cells were washed 2 times, re-suspended in DMEM/NUT.MIX.F12 medium and supplemented with 10% fetal calf serum (FCS) and 100 µg/ml penicillin-streptomycin and inoculated into 96-well plates (6 wells/adipose tissue region) at a density of 30 000 cells/ml and kept at 37°C, in 5% CO_2. The cells were expanded until confluency after which adipocyte differentiation was induced using an adipogenic medium containing DMEM/F12 with dexamethasone 0.1µM, 3-isobutyl-1-methylxanthine (IBMX) 25µM, insulin 17 nM, indomethacin 60µM, 10% FCS and 100 µg/ml penicillin-streptomycin. After 4 days medium was changed to maintenance medium containing insulin 17 nM and 10% FCS. After 1 more

day the cells were lipid filled and intra cellular lipid accumulation was determined using a fluorometer after incubating the cells with Nile Red (Sigma-Aldrich, St. Louis, MO).

Adipose tissue cyclic AMP level, RNA isolation and qPCR analysis

Adenosine 3'-5'-cyclic monophosphate (cyclic AMP, cAMP) levels were determined in gonadal fat samples of mice fed a HFD for 6 weeks using the cAMP direct immunoassay kit from Biovision (Biovision, Inc, Milpitas, CA) according to the instructions of the manufacturer. RNA from gonadal fat of mice was isolated using the Nucleospin RNA /Protein kit (Macherey-Nagel, Düren, Germany) according to the instructions of the manufacturer. The quality of each mRNA sample was examined by lab-on-a-chip technology using Experion Stdsens analysis kit (Biorad, Hercules, CA). 600 ng of total RNA was reverse-transcribed with iScript cDNA synthesis kit (Bio-Rad) and obtained cDNA was purified with Nucleospin Extract II kit (Macherey-Nagel). Real-Time PCR was carried out on the IQ5 PCR machine (Biorad) using the Sensimix SYBR Green RT-PCR mix (Quantace, London, UK) and QuantiTect SYBR Green RT-PCR mix (Qiagen). mRNA levels were normalized to mRNA levels of glyceraldehyde-3-phosphate dehydrogenase (Gapdh). Primer sequences are listed in table 1.

Hyperinsulinemic euglycemic clamp analysis

To assess insulin sensitivity mice were fed a HFD for 11 weeks. Hyperinsulinemic euglycemic clamps were performed as described earlier [16]. Briefly, after an overnight fast, animals were anesthetized as described above and an infusion needle was placed in the tail vein. Basal glucose parameters were determined during a 60-min period, by infusion of D-[3-^{3}H]glucose to achieve steady-state levels. A bolus of insulin (3 mU) was given and

Table 1. Primers used for quantitative real-time PCR analysis.

Gene	Forward primer	Reverse primer
F4/80	CTTTGGCTATGGGCTTCCAGTC	GCAAGGAGGACAGAGTTTATCGTG
MRC-1	GAGAGCCAAGCCATGAGAAC	GTCTGCACCCTCCGGTACTA
MCP-1	GCA TCT GCC CTA AGG TCT TCA	TTC ACT GTC ACA CTG GTC ACT CCT A
IL-6	ACCACGGCCTTCCCTACTTC	CTCATTTCCACGATTTCCCAG
IL-10	GACAACATACTGCTAACCGACTC	ATCACTCTTCACCTGCTCCACT
HSL	AGACACCAGCCAACGGATAC	ATCACCCTCGAAGAAGAGCA
ATGL	ACAGTGTCCCCATTCTCAGG	TTGGTTCAGTAGGCCATTCC
CD45	GTTTTCGCTACATGACTGCACA	AGGTTGTCCAACTGACATCTTTC
CD31	CTGCCAGTCCGAAAATGGAAC	CTTCATCCACCGGGGCTATC
GAPDH	TGCACCACCAACTGCTTAGC	GGCATGGACTGTGGTCATGAG

F4/80, marker for macrophages; *MRC-1,* mannose receptor 1; *MCP*-1, monocyte chemotactic protein-1; *IL-6*, interleukin-6; *IL-10*, interleukin-10; *HSL*, hormone sensitive lipase; *ATGL*, adipose triglyceride lipase; *CD45*, marker for leukocytes; *CD31*, marker for endothelial cells; *GAPDH;* glyceraldehyde-3-phosphate dehydrogenase.

a hyperinsulinemic euglycemic clamp was started with a continuous infusion of insulin (5 mU/h) and D-[3-^{3}H]glucose and a variable infusion of 12.5% D-glucose (in PBS) to maintain blood glucose levels at euglycemic levels. Blood samples were taken every 5-10 min from the tip of the tail to monitor plasma glucose levels (AccuCheck). Seventy, eighty and ninety minutes (steady-state) after the start of the clamp, blood samples (70 µl) were taken for determination of plasma glucose and insulin using commercially available kits (Instruchemie and Crystal Chem Inc). Turnover rates of glucose (µmol/min/kg) were calculated during the basal period and in steady-state clamp conditions as the rate of tracer infusion (dpm/min) divided by the plasma-specific activity of ^{3}H-glucose (dpm/µmol). All metabolic parameters were expressed per kilogram of body weight. The hepatic glucose production (EGP) is calculated from the rate of disappearance (Rd) and glucose infusion rate (GIR) by the following equation: Rd = EGP + GIR. The Rd is measured from Steele's equation in steady state using the tracer infusion rate (Vin) and plasma-specific activity (SA) of ^{3}H-glucose (dpm/µmol) by the following formula: Rd = Vin/SA.

Statistical analysis

Data are presented as means ± SD. Statistical differences were calculated using the nonparametric Mann-Whitney test or two-way-ANOVA (SPSS 16, SPSS Inc, Chicago, IL). A P-value < 0.05 was regarded statistically significant.

2.3 RESULTS

CD36-deficiency reduces high fat diet-induced obesity

To induce obesity, male CD36$^{-/-}$ and WT mice were fed a HFD containing 45 energy% fat for 12 weeks, and body weight of the mice was followed during the HFD intervention. CD36$^{-/-}$ mice gained less body weight than WT mice (Fig. 1A). After 11 weeks, body composition was determined by DEXA analysis. As compared to WT mice, lean body mass was similar, but total body fat was 36% lower in CD36$^{-/-}$ mice (5.8 ± 1.6 versus 9.0 ± 3.1 g; P<0.05) (Fig. 1B). In line with this observation, weights of isolated fat pads were lower in CD36$^{-/-}$ mice (gonadal fat -38%; P<0.01, visceral fat -35%; P<0.01, subcutaneous fat -31%; P<0.05) (Fig. 1C). When mice were fed a HFD for 6 weeks, similar differences in phenotype between WT and CD36$^{-/-}$ mice were observed. Fat pad weights of CD36$^{-/-}$ mice were significantly lower after 6 weeks of HFD (gonadal fat -48%; P<0.001, visceral fat -33%; P<0.01, subcutaneous fat -41%; P<0.001), while liver weight was significantly higher (data not shown).

CD36-deficiency decreases uptake of TG-rich particle derived FA by white adipose tissue

To confirm that CD36-deficiency affects the tissue-specific uptake of FA that are derived from TG-rich particles, the plasma clearance and organ distribution of [^{3}H]TO-labeled TG-rich

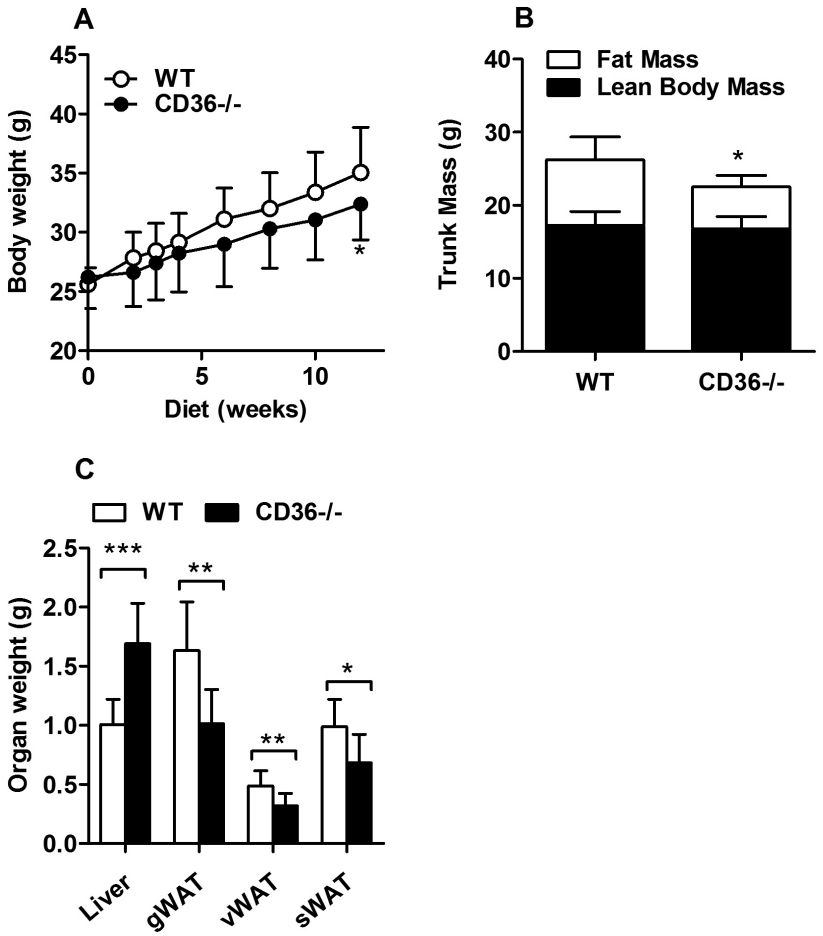

Figure 1. CD36-deficiency reduces HFD-induced obesity. In a first set of mice, wild-type (WT) and CD36-deficient ($CD36^{-/-}$) mice were fed a HFD for 12 weeks. Body weight of WT mice and $CD36^{-/-}$ mice was measured at the indicated time points (A). Values are means ± SD (n= 19-20 per group); **P*<0.05. In a second set of mice, after 11 weeks of HFD and after O/N fast, lean body mass and fat mass were determined by DEXA scan (B). Values are means ± SD (n= 7-11 per group); **P*<0.05. In a third set of mice, after 12 weeks of HFD, tissues were dissected after a 4 h fast and weight of WT tissues and $CD36^{-/-}$ was determined (C). Values are means ± SD (n= 10 per group); **P*<0.05, ***P*<0.01, ****P*<0.001.

VLDL-like emulsion particles was evaluated in HFD-fed $CD36^{-/-}$ mice versus WT mice. CD36-deficiency did not affect the plasma half-life of [^{3}H]TO (t½ = 5.0±1.7 versus 6.0±1.3 min) (Fig. 2A). These results indicate that $CD36^{-/-}$ mice have equal capacity to clear TG-derived FA from plasma. However tissue-distribution of these FA was different for the two mouse strains. CD36-deficiency significantly decreased the uptake of [^{3}H]TO-derived activity in the heart (-38%; P<0.001), gonadal fat (-29%; P<0.01) and visceral fat (-30%; P<0.01), while the uptake of [^{3}H]TO-derived activity in the liver (+42%; P<0.01) and spleen (+49%; P<0.01) was significantly increased in the $CD36^{-/-}$ mice (Fig. 2B). These results imply that CD36-deficiency increases the flux of FA derived from TG-rich particles towards the liver, while decreasing the flux of FA

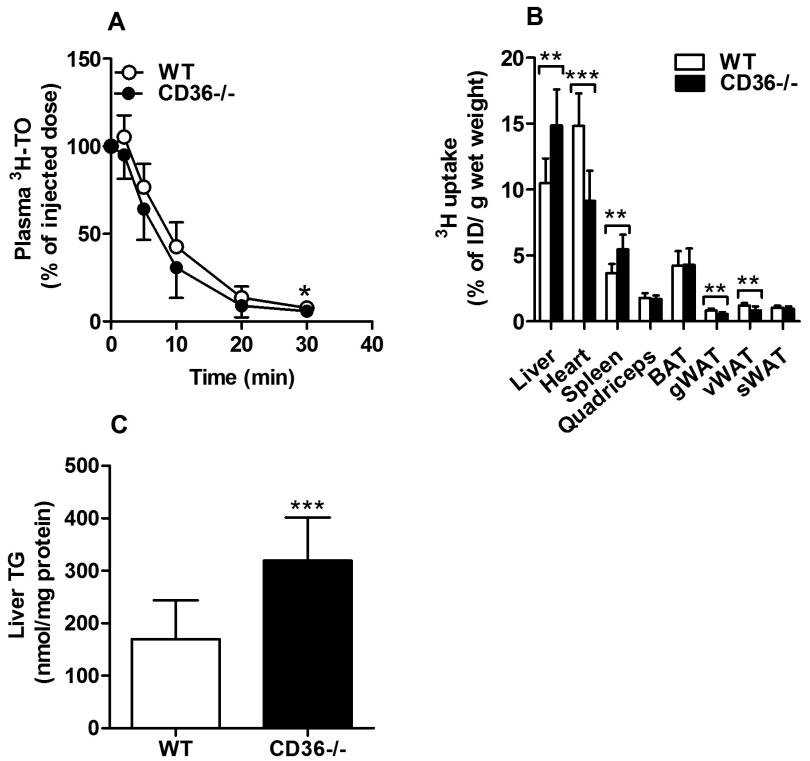

Figure 2. CD36-deficiency decreases uptake of TG-rich particle derived FA by white adipose tissue. Wild-type (WT) and CD36-deficient (CD36$^{-/-}$) mice were fed a HFD for 13 weeks. After a 4 h fast, mice received an intravenous injection of glycerol tri[^{3}H]oleate-labeled VLDL-like emulsion particles (1.0 mg TG). At 2, 5, 10, 20 and 30 minutes after injection, blood samples were taken and ^{3}H activities in plasma were counted and calculated as a percentage of the injected dose (ID) (A). Uptake of radioactivity by various organs of WT and CD36$^{-/-}$ mice was determined and presented as % of injected dose per gram wet weight (B). Values are means ± SD (n= 9); ***P*<0.01, ****P*<0.001. BAT, Brown adipose tissue; WAT, white adipose tissue; g, gonadal; v, visceral; s, subcutaneous. In a second set of mice, after 12 weeks of HFD, liver TG content was determined and expressed per mg protein (C). Values are means ± SD (n= 10-11); ****P*<0.001.

towards the heart and WAT. Indeed, CD36-deficiency increased hepatic lipid content (+88%; P<0.001) (Fig. 2C), without affecting hepatic TC and PL levels (data not shown).

CD36-deficiency decreases adipocyte size in all fat pads and impairs adipocyte recruitment in gWAT

To investigate the effect of reduced FA uptake in adipose tissue on adipocyte morphology; adipocyte size distribution, volume-weighted mean adipocyte diameter and total adipocyte number were determined in isolated adipocytes from gonadal, visceral and subcutaneous fat pads from CD36$^{-/-}$ and WT mice fed a HFD for 6 weeks. In gonadal fat pads of CD36$^{-/-}$ mice less hypertrophic adipocytes (110-170 μM) were observed (Fig. 3A). For visceral and subcutaneous fat, the distribution was also shifted to the left. (Fig. 3B-C). Volume-weighted mean cell diameter was decreased in gonadal (-12%; P<0.001), visceral (-14%; P<0.01)

and subcutaneous fat pads (-18%; P<0.001) of CD36$^{-/-}$ mice, indicating indeed smaller adipocytes (Fig. 3D). In gonadal fat, but not in visceral or subcutaneous fat a decreased number of total adipocytes was observed (-65%; P<0.001) (Fig. 3E).

The number of adipocytes in adipose tissue is dependent upon the recruitment of preadipocytes out of the precursor pool that differentiate into adipocytes. The total number of cells in the stromal vascular fraction (SVF) (which includes the preadipocyte pool) was higher per gram of gonadal fat in CD36$^{-/-}$ mice ($5.0 \times 10^5 \pm 3.3 \times 10^5$ versus $2.3 \times 10^5 \pm 5.3 \times 10^4$ cells; P<0.01), indicating that the preadipocyte pool may be larger in gonadal fat of CD36$^{-/-}$ mice. In contrast, for visceral and subcutaneous fat no differences were observed in number of cells in the SVF (visceral: $1.0 \times 10^6 \pm 7.4 \times 10^5$ versus $8.0 \times 10^5 \pm 2.6 \times 10^5$ and subcutaneous: $4.0 \times 10^5 \pm 3.0 \times 10^5$ versus $2.4 \times 10^5 \pm 8.2 \times 10^4$, respectively) (Fig. 3F).

The SVF is a mixture of cell types where preadipocytes, leukocytes and endothelial cells constitute the major cell populations. mRNA expression of DLK1, a preadipocyte marker, tended to be higher in gonadal fat pads of CD36$^{-/-}$ mice (CD36$^{-/-}$ mice had a 44% higher DLK-1 expression; P=0.09), whereas expression of CD45, a leukocyte marker, was lower in CD36$^{-/-}$ mice (-39%; P<0.01), and CD31, an endothelial cell marker, was similar for CD36$^{-/-}$ and WT mice (Fig. 4A). These data indicate that the increased number of cells in the SVF may be accounted for by an increased number of preadipocytes, but not of leukocytes or endothelial cells. The number of very small adipocytes (diameter <50 μm) on the other hand, was much lower in the gonadal adipose tissue of CD36$^{-/-}$ mice (-65%; P<0.001) (Fig. 4B) which may indicate that less adipocytes are being recruited within gonadal fat pads of CD36$^{-/-}$ mice on a HFD, resulting in a higher pool of preadipocytes that remains in their SVF. This is illustrated in Fig. 3A by the bimodal cell size distribution in the gonadal fat of WT mice as opposed to the single peak in the cell size distribution in CD36$^{-/-}$ mice.

CD36-deficiency does not affect preadipocyte intra cellular lipid accumulation

To further study the underlying mechanisms which may explain the morphology of adipocytes in CD36$^{-/-}$ mice the intra cellular lipid accumulation in these cells was determined. This was assessed using isolated preadipocytes from CD36$^{-/-}$ and WT mice that were differentiated in an adipogenic medium. No differences were observed in intra cellular lipid accumulation between CD36$^{-/-}$ and WT mice for all fat pad regions (Fig. 5).

CD36-deficiency stimulates lipolysis but improves insulin-mediated inhibition of lipolysis

Morphology of adipocytes is not only determined by uptake of FA which leads to TG storage, but also by the level of FA release due to lipolysis. To investigate if CD36 plays a role in lipolysis, basal lipolysis was determined in isolated mature gonadal adipocytes of CD36$^{-/-}$ versus WT mice. Only gonadal adipocytes were studied because only from the gonadal fat pad the yield of adipocytes was enough to perform these experiments. CD36$^{-/-}$ mice had higher glycerol release both expressed per gram adipose tissue (data not shown) and expressed as lipolysis per adipocyte, which was found for both unstimulated

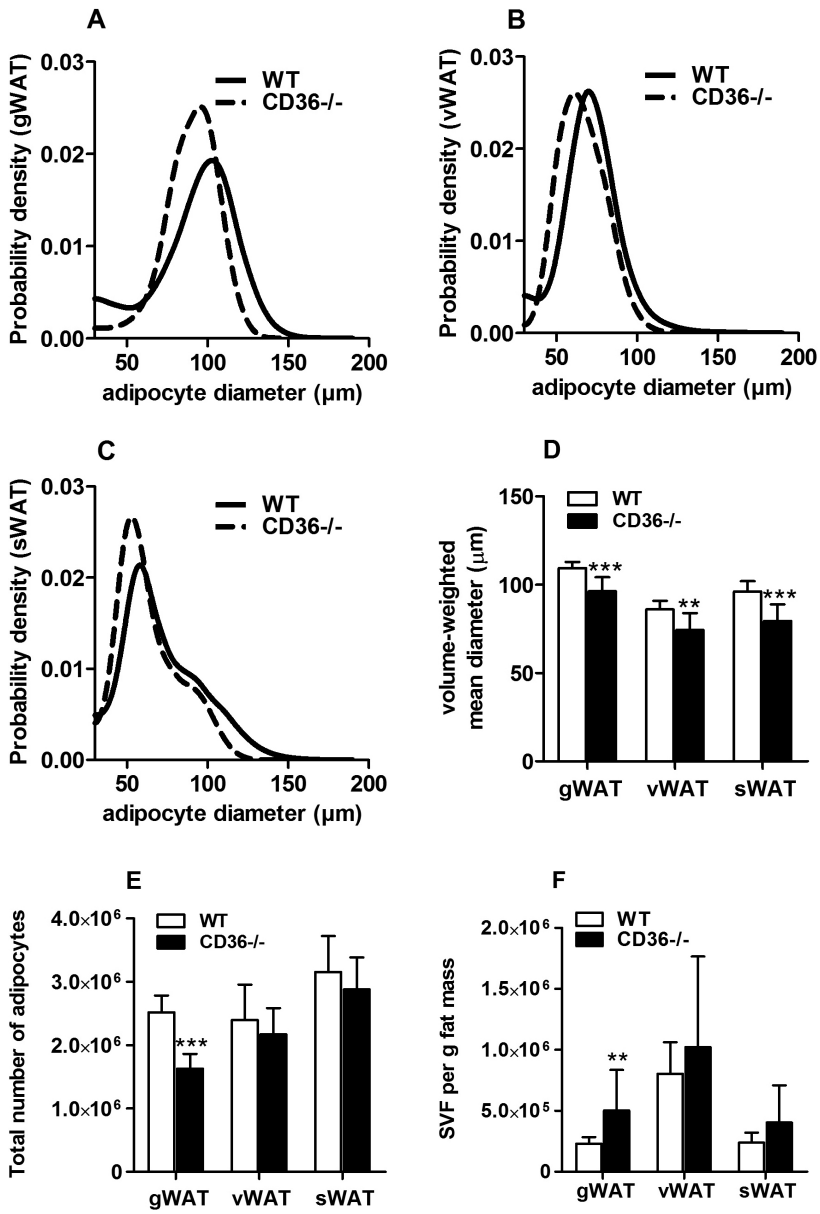

Figure 3. CD36-deficiency decreases adipocyte size. Wild-type (WT) (solid line) and CD36-deficient ($CD36^{-/-}$) (dashed line) mice were fed a HFD for 6 weeks. Gonadal (gWAT), visceral (vWAT) and subcutaneous (sWAT) white adipose tissues were dissected. Adipocytes were isolated and adipocyte size distribution was determined (A-C). Values are means (n=9-10). Volume-weighted mean diameter (D) and total number of adipocytes were calculated (E). Stromal vascular fraction (SVF) was obtained and total number of cells in SVF of gWAT, vWAT and sWAT was determined (F). Values are means ± SD (n=9-10); $^{**}P<0.01$, $^{***}P<0.001$.

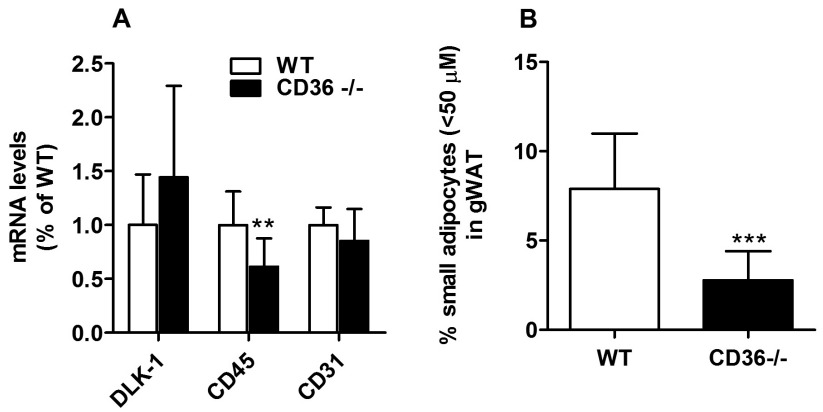

Figure 4. CD36-deficiency impairs adipocyte recruitment in gondal WAT. Wild-type (WT) and CD36-deficient ($CD36^{-/-}$) mice were fed a HFD for 6 weeks. Gonadal white adipose tissue (gWAT) was dissected and mRNA levels of DLK-1, CD45 and CD31 in gWAT were determined (A). Values are means ± SD (n=10); $^{**}P<0.01$. In addition, the % of very small adipocytes (<50μM) in gWAT was calculated (B). Values are means ± SD (n=9-10); $^{***}P<0.001$.

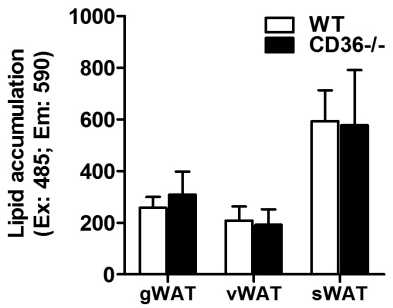

Figure 5. CD36-deficiency does not affect preadipocyte lipid accumulation. Wild-type (WT) and CD36-deficient ($CD36^{-/-}$) mice were fed a HFD for 6 weeks. Gonadal (gWAT), visceral (vWAT) and subcutaneous (sWAT) white adipose tissues were dissected and preadipocytes were isolated and differentiated in adipogenic medium. Lipid accumulation was determined with Nile Red. Values are means ± SD (n=9-10) (6 wells/adipose tissue region per mouse).

and 8-bromo-cAMP (8b-cAMP) stimulated cells (2.1 fold, 2.8 fold respectively; P<0.05) (Fig. 6A). To test whether the increased lipolysis was due to higher levels of the lipolytic enzymes adipose triglyceride lipase (ATGL) and hormone sensitive lipase (HSL), mRNA expression of these enzymes was determined. However, both ATGL and HSL mRNA were lower in gonadal adipose tissue of $CD36^{-/-}$ versus WT mice (-27%; P<0.01 and -48%; P<0.001, respectively) (Fig. 6B). On the other hand, cAMP levels, which are reported to stimulate lipolysis, were increased in gonadal fat samples of $CD36^{-/-}$ mice (+31%; P<0.05) (Fig. 6C). Also the suppression of lipolysis by insulin was investigated in $CD36^{-/-}$ versus WT mice. Inhibition of lipolysis by 3 different insulin concentrations (10^{-11}, 10^{-9}, 10^{-7} M) expressed as % of 8b-cAMP induced lipolysis was tested. An insulin concentration of 10^{-11}M

already maximally suppressed lipolysis, since no further inhibition was found with insulin concentrations of 10^{-9} and 10^{-7} M (2 way ANOVA F=0.37; P=0.7). However inhibition of lipolysis was more potent in CD36$^{-/-}$ mice compared to WT mice (50% versus 29%; 2 way ANOVA F=10.65; P<0.01) (Fig. 6D). To investigate whether the increased adipocyte insulin sensitivity in lipolysis may be related to changes in adipose tissue inflammation, expression of inflammatory markers in gonadal adipose tissue was determined. As mentioned above, expression of CD45 was lower in CD36$^{-/-}$ mice. Moreover, a decreased expression of macrophage marker F4/80 (-29%; P<0.05) and a trend for higher IL-10 expression in gonadal adipose tissue of CD36$^{-/-}$ mice (+53%; P=0.08) (Fig. 6E) was observed.

CD36-deficiency decreases hepatic insulin sensitivity

To investigate the effect of decreased adiposity and increased hepatic lipid content on metabolic abnormalities such as insulin resistance, we performed a hyperinsulinemic euglycemic clamp after an o/n fast. Glucose (5.4 ± 0.7 versus 5.4 ± 0.7 and 5.8 ± 0.6 versus 5.6 ± 0.6 mM) and insulin levels (0.5 ± 0.2 versus 0.4 ± 0.2 and 4.0 ± 0.9 versus 4.5 ± 1.0 ng/mL) were equal for the 2 genotypes under basal as well as under hyperinsulinemic conditions. To maintain euglycemia during the insulin infusion, a similar amount of glucose was needed to be infused in CD36$^{-/-}$ mice compared to WT mice (GIR 25.7 ± 12.9 versus 28.1 ± 5.9 μmol/min/kg) (Fig. 7A). The glucose disposal rates under basal conditions were higher for CD36$^{-/-}$ animals (32.3 ± 8.8 versus 25.1 ± 4.3 μmol/min/kg; P<0.05). During hyperinsulinemic conditions glucose disposal rates were similar for CD36$^{-/-}$ and WT animals (55.2 ± 19.9 versus 43.7 ± 4.6 μmol/min/kg), indicating that there was no difference in peripheral insulin sensitivity between CD36$^{-/-}$ mice compared to WT mice (Fig. 7B). Nevertheless, the CD36$^{-/-}$ mice developed aggravated hepatic insulin resistance compared to WT mice as indicated by the higher hepatic glucose production during the hyperinsulinemia (29.3 ± 11.3 versus 15.5 ± 3.6 μmol/min/kg; P<0.01) (Fig. 7C).

2.4 DISCUSSION

The current study investigated the effects of CD36-deficiency on adipocyte morphology and functionality during HFD to get a better understanding of the role of CD36 in adipocytes.

In accordance with others [6, 7], we found less adiposity in CD36$^{-/-}$ mice, which was due to a reduced uptake of FA in the adipose tissues. A decrease in fat pad mass can be caused by smaller adipocytes and/or by a decreased number of adipocytes. The CD36$^{-/-}$ mice showed less hypertrophy of their gonadal, visceral and subcutaneous adipocytes and the volume-weighted mean cell diameters of all fat pads studied were significantly lower in the CD36$^{-/-}$ mice. Thus the smaller fat pads in the CD36$^{-/-}$ are due to smaller fat cells in their adipose tissues. Moreover, for the gonadal adipose tissue, the CD36$^{-/-}$ mice showed a lower total number of adipocytes. The gonadal (but neither visceral nor subcutaneous) adipose tissue of CD36$^{-/-}$ mice had

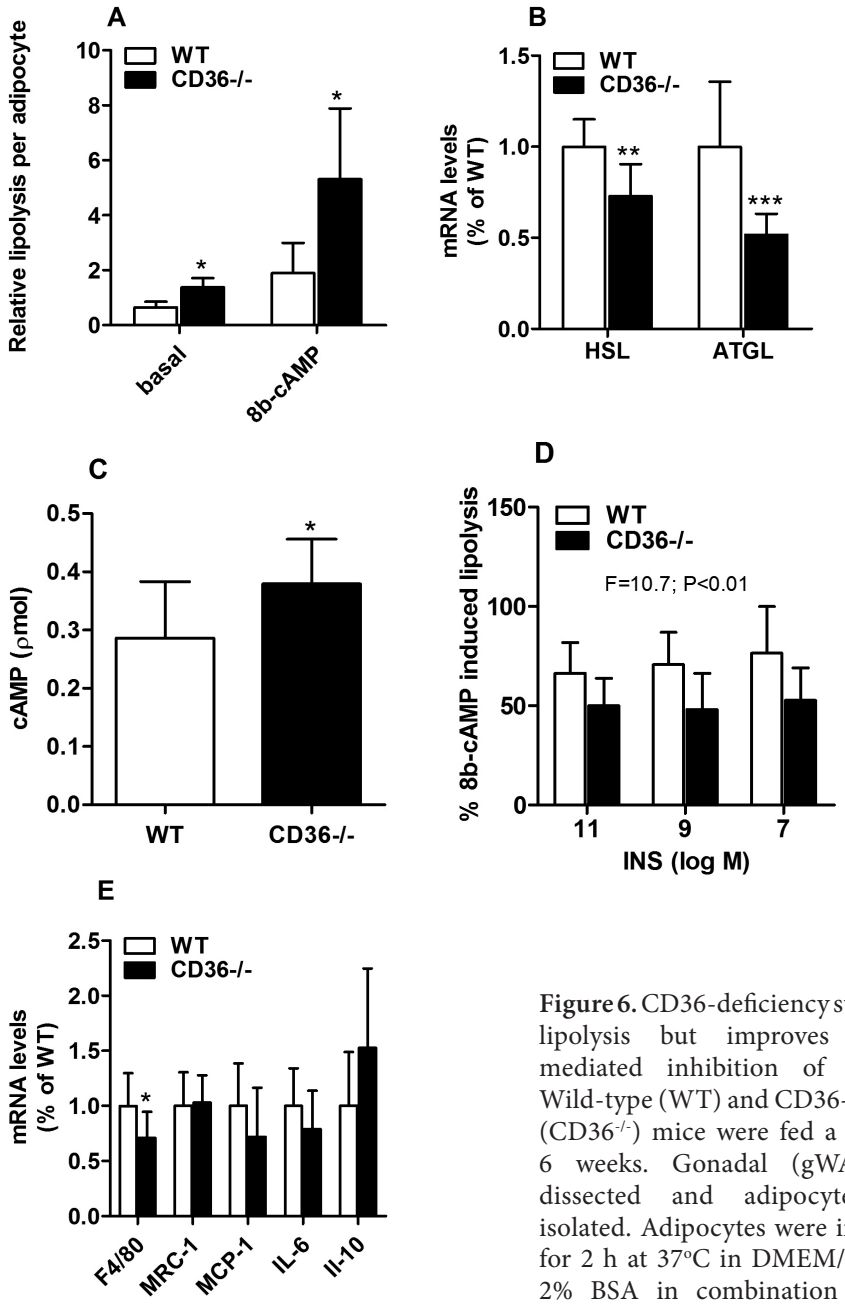

Figure 6. CD36-deficiency stimulates lipolysis but improves insulin-mediated inhibition of lipolysis. Wild-type (WT) and CD36-deficient ($CD36^{-/-}$) mice were fed a HFD for 6 weeks. Gonadal (gWAT) was dissected and adipocytes were isolated. Adipocytes were incubated for 2 h at 37°C in DMEM/F12 with 2% BSA in combination with or without 8-bromo-cAMP (8b-cAMP) (10-3M). Glycerol concentrations (index of lipolysis) were determined using a fluorometric method (A). Values are means ± SD (n=5); **P*<0.05. RNA was isolated from gWAT and mRNA levels of adipose triglyceride lipase (ATGL) and hormone sensitive lipase (HSL) were determined (B). Values are means ± SD (n=10); ***P*<0.01, ****P*<0.001. gWAT cAMP levels were determined using a immunoassay kit (C). Values are means ± SD (n=9-10); **P*<0.05. The anti-lipolytic effect of insulin was determined as % of 8b-cAMP induced lipolysis. Adipocytes were incubated with insulin (10^{-11}M,10^{-9}M and 10^{-7}M) Statistical analysis was done using 2 way ANOVA (D). Values are means ± SD (n=5). mRNA levels of macrophage marker F4/80, mannose receptor C1 (MRC-1), monocyte chemotactic protein-1 (MCP-1), interleukin 6 (IL-6) and interleukin 10 (IL-10) were determined (E). Values are ± SD (n=10); **P*<0.05.

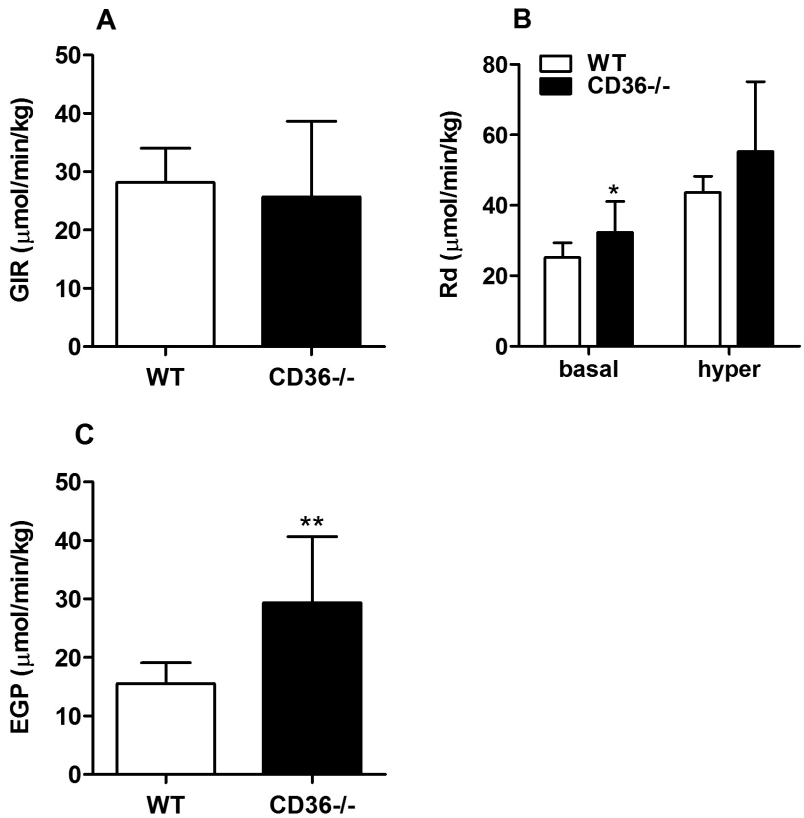

Figure 7. CD36-deficiency decreases hepatic insulin sensitivity. Wild-type (WT) and CD36-deficient ($CD36^{-/-}$ mice) were fed a HFD for 11 weeks. After O/N fast a hyperinsulinemic euglycemic clamp was performed. Glucose infusion rate (GIR) (A), rate of disappearance during basal and hyperinsulinemic period (B) and hepatic glucose production during hyperinsulinemic period (C) were determined. Values are means ± SD (n=7-10 per group); **P*<0.05, ***P*<0.01.

a larger pool of preadipocytes, and a reduced number of very small adipocytes (<50µm). These results suggest that less preadipocytes are being recruited to become adipocytes in the gonadal adipose tissue, resulting in a higher pool of preadipocytes that remains in the SVF. So the $CD36^{-/-}$ mice seem to have a reduced adiposity not only due to a reduced hypertrophy but also due to a reduced hyperplasia of the adipocytes, at least in the gonadal adipose tissue.

The fact that the observed differences in preadipocyte recruitment seemed restricted to the gonadal tissue may be explained by the gonadal adipose tissue being the largest fat pad in the animals and that it has the largest fat cells, as also shown in this paper. We hypothesize that the gonadal adipose tissue was thus exposed to the highest metabolic stress and therefore the need for preadipocyte recruitment was probably the highest in this adipose tissue region. There were no differences in gene expression of CD36 between the subcutaneous and gonadal fat pads of WT mice (data not shown), so differential expression of CD36 cannot explain the observation that the gonadal fat is more affected. Gonadal fat depots are larger in male mice, both in absolute and relative terms. In male mice gonadal fat

depots are larger than subcutaneous fat depots after HFD feeding, whereas in female mice the two fat depots are of almost equal size [17]. The current study investigated only male mice, because male mice are more susceptible to diet-induced obesity and diet-induced insulin resistance than female mice [18]. It remains to be studied whether in female mice changes in adipose tissue due to CD36-deficiency are less restricted to gonadal adipose tissue.

Interestingly, despite the in vivo differences in adipocyte size distributions, isolated preadipocytes showed equal intra cellular lipid accumulation in vitro for CD36$^{-/-}$ mice and WT for all fat depots. Our results are in line with a recent study from Cai et al. that also showed similar differentiation capacity of the SVF of adipose tissue between WT and CD36$^{-/-}$ mice [19]. These in vitro observations may be explained by de novo lipogenesis from carbohydrates present in the culture medium. Collins et al. have shown that de novo lipogenesis in differentiating adipocytes can provide all the FA that are necessary for adipocyte maturation. They showed this using an in vitro model of human preadipocytes which are cultured under serum free conditions without any exogenous fat [20]. We added 10% FCS to our mouse preadipocyte cultures - as these cells cannot survive under serum free conditions- and serum contains FA. Despite the availability of exogenous FA as an energy source in our in vitro experiments, uptake of FA may have been by-passed and glucose was used instead to synthesize FA intracellularly. The fact that the gonadal adipose tissue of CD36$^{-/-}$ mice showed a reduced preadipocyte recruitment in the in vivo experiments may have been due to the high fat diet, which puts a maximum pressure on the expandability of the adipose tissue. The WT mice were able to cope with the FA overload by delivering them to the existing mature adipocytes as well as to the preadipocytes, whereas in the CD36-deficient mice neither mature adipocytes nor preadipocytes could efficiently take up the excess of FA. During preparation of this manuscript, a study was published by Christiaens et al. that showed impaired adipogenesis of 3T3-F442A preadipocytes upon CD36 silencing during preadipocyte differentiation [21]. Whether the discrepancies between the studies are due to differences in cell type and/or CD36 expression level (none in our CD36$^{-/-}$ cells, low in the knock-down 3T3-F442A cell line) remains to be determined.

Gonadal adipocytes of CD36$^{-/-}$ mice showed increased basal and 8b-cAMP induced lipolysis. Published literature suggests that large adipocytes have a higher rate of lipolysis [22]. However, we observed a higher basal- and 8b-cAMP stimulated lipolysis in adipocytes from CD36$^{-/-}$ mice, despite the decreased volume of these adipocytes. The increased lipolysis might be explained by diminished product inhibition of HSL by FA. Since CD36-deficiency impairs FA uptake by adipocytes, less FA might be present intracellularly which may lead to decreased product inhibition of HSL. Recently, it has been shown that long chain FA reduce production of cAMP which results in a decreased phosphorylation of HSL [23]. Moreover, it has been shown that A-FABP null mice have decreased lipolysis, while E-FABP transgenic mice have increased lipolysis [24]. This was explained by FABP being able to bind FA, thereby relieving product inhibition of HSL. We found an unexpected decrease in mRNA levels of ATGL and HSL in adipose tissue of CD36$^{-/-}$ mice compared to expression in WT mice. However cAMP levels were increased in CD36$^{-/-}$ mice, which results in increased phosphorylation of HSL rather than increased expression and thus may explain

the increased lipolysis. Since muscle normally relies on FA, it might also be that in CD36$^{-/-}$ mice there is a continuous signal from muscle to fat to release more FA and/or that there is absence of a stop signal to inhibit adipocyte lipolysis. Our results are in contrast with Zhou et al. who reported similar basal lipolysis and phosphorylation of HSL by WT and CD36$^{-/-}$ adipose tissue. This discrepancy could be due to the fact that Zhou et al. measured rates in incubated tissue versus adipocytes in the present study [25].

Insulin was more potent in inhibiting lipolysis in the CD36-deficient mice, suggesting higher insulin sensitivity of the adipocytes. Hypertrophic subcutaneous adipocytes were associated with increased insulin resistance [26-28]. The fact that CD36$^{-/-}$ mice have less hypertrophic adipocytes could therefore help to explain the more potent inhibition of lipolysis by insulin. Kennedy et al. also observed increased insulin sensitivity in adipocytes from CD36$^{-/-}$ mice. They discovered that adipose tissue of HFD-fed CD36$^{-/-}$ mice is less inflamed, which could explain the increased insulin sensitivity [29]. In accordance with these findings, we measured a decreased expression of the leukocyte marker CD45 as well as the macrophage marker F4/80 and found a trend towards higher expression of the anti-inflammatory cytokine IL-10 in gonadal adipose tissue of the CD36 deficient mice.

The observed reduction in body weight of CD36$^{-/-}$ mice on HFD is in accordance with recent studies by others, although the effect was less pronounced in our study (-6% versus -23% and -51% respectively) [6, 7].The smaller effect on body weight gain could be due to differences in HFD composition. We used a HFD containing 45 energy% of fat, whereas others used a HFD containing 60 energy% of fat [6, 7].

The reduced FA uptake in adipose tissue in CD36 deficient mice was paralleled by a reduced uptake in heart and an increased FA uptake in the liver and spleen. In contrast to the heart and muscle, CD36 is not a major facilitator of FA uptake in the liver, therefore FA uptake was not affected by the loss of CD36. Instead, the impaired uptake of FA in other peripheral organs such as muscle and adipose tissue results in a higher flux of FA to the liver. Our findings are partly in accordance with the study of Coburn et al. which showed that uptake of FA analogs was decreased in muscle and adipose tissue of chow-fed CD36$^{-/-}$ mice. We also found that the decreased FA uptake is solely caused by a lack of the FA transporter CD36 and not due to reduced capacity of lipoprotein lipase (LPL), since we found an even higher post-heparin LPL activity in CD36$^{-/-}$ mice (data not shown), probably due to compensatory mechanisms.

The livers of the CD36-deficient mice contained more TG and were more insulin resistant as indicated by the higher hepatic glucose production under hyperinsulinemic conditions. It is well established that ectopic fat deposition in the liver contributes to development of hepatic insulin resistance [30, 31]. Although the adipocytes of the CD36$^{-/-}$ mice showed increased insulin sensitivity in vitro; in vivo, we did not observe increased peripheral insulin sensitivity. This could be due to the fact that glucose uptake in adipose tissue under hyperinsulinemic conditions is relatively small. Under these conditions, most of the glucose is taken up by heart and muscle [32].

One hypothesis to explain FA trafficking towards other places than adipose tissue, is the so called 'sick adipose tissue' hypothesis [33]. According to this hypothesis unhealthy adipose tissue

consists of hypertrophic cells due to impaired creation of new adipocytes. Ultimately, these hyperthropic adipocytes become dysfunctional which results in increased FA release leading to increased FA availability to nonadipose tissues. Our study shows that CD36-deficiency also leads to 'sick adipose tissue'. However, in this case the adipose tissue has dysfunctional adipocytes which cannot store an overload of FA together with an impaired ability to recruit new adipocytes. As a consequence, the FA are translocated to the liver. Despite the lack of hypertrophic adipocytes, CD36 deficient adipose tissue has an unexpected higher FA release during basal lipolysis which even further increases the availability of FA to the liver. Therefore it appears that CD36 plays an important role in adipose tissue functionality- both by regulating FA uptake and release- and likewise the distribution of fat to adipose and non- adipose tissues.

ACKNOWLEDGEMENTS

The authors would like to thank A.C.M. Pronk and F. el Bouazzaoui for excellent technical assistance. Present address of P.J. Voshol: Metabolic Research Laboratories, Institute of Metabolic Science, University of Cambridge, Cambridge, UK. Present address of L.K.M Steinbusch: Center for Integrative Genomics, Université de Lausanne, Lausanne, Switzerland.

This work was supported by grants from the Netherlands Organization for Scientific Research (NWO Zon-MW; 917.76.301 to P.J.V.), the Netherlands Consortium for Systems Biology (NCSB), the Dutch Diabetes Research Foundation (2005.01.003 to P.J.V.), the seventh framework program of the EU-funded "LipidomicNet" (proposal number 202272) and was performed within the framework of CTMM, the Center for Translational Molecular Medicine (www.ctmm.nl), project PREDICCt (grant 01C-104), and supported by the Netherlands Heart Foundation, Dutch Diabetes Research Foundation and Dutch Kidney Foundation. P.C.N.R. is an Established Investigator of the Netherlands Heart Foundation (2009T038).

REFERENCES

1. Defronzo RA. Insulin resistance, lipotoxicity, type 2 diabetes and atherosclerosis: the missing links. The Claude Bernard Lecture 2009. Diabetologia 2010;53:1270-1287.
2. Abumrad N, Coburn C, Ibrahimi A. Membrane proteins implicated in long-chain fatty acid uptake by mammalian cells: CD36, FATP and FABPm. Biochim Biophys Acta 1999;1441:4-13.
3. Abumrad NA, el-Maghrabi MR, Amri EZ, Lopez E, Grimaldi PA. Cloning of a rat adipocyte membrane protein implicated in binding or transport of long-chain fatty acids that is induced during preadipocyte differentiation. Homology with human CD36. J Biol Chem 1993;268:17665-17668.
4. Silverstein RL, Febbraio M. CD36, a scavenger receptor involved in immunity, metabolism, angiogenesis, and behavior. Sci Signal 2009;2:re3.
5. Coburn CT, Knapp FF, Jr., Febbraio M, Beets AL, Silverstein RL, Abumrad NA. Defective uptake and utilization of long chain fatty acids in muscle and adipose tissues of CD36 knockout mice. J Biol Chem 2000;275:32523-32529.
6. Hajri T, Hall AM, Jensen DR, Pietka TA, Drover VA, Tao H, Eckel R, Abumrad NA. CD36-facilitated fatty acid uptake inhibits leptin production and signaling in adipose tissue. Diabetes 2007;56:1872-1880.
7. Koonen DP, Sung MM, Kao CK, Dolinsky VW, Koves TR, Ilkayeva O, Jacobs RL, Vance DE, Light PE, Muoio DM, Febbraio M, Dyck JR. Alterations in skeletal muscle fatty acid handling predisposes middle-aged mice to

diet-induced insulin resistance. Diabetes 2010;59:1366-1375.

8. Steinbusch LK, Luiken JJ, Vlasblom R, Chabowski A, Hoebers NT, Coumans WA, Vroegrijk IO, Voshol PJ, Ouwens DM, Glatz JF, Diamant M. Absence of fatty acid transporter CD36 protects against Western-type diet-related cardiac dysfunction following pressure overload in mice. Am J Physiol Endocrinol Metab 2011;301:E618-E627.
9. Febbraio M, Abumrad NA, Hajjar DP, Sharma K, Cheng W, Pearce SF, Silverstein RL. A null mutation in murine CD36 reveals an important role in fatty acid and lipoprotein metabolism. J Biol Chem 1999;274:19055-19062.
10. Rensen PC, Van Berkel TJ. Apolipoprotein E effectively inhibits lipoprotein lipase-mediated lipolysis of chylomicron-like triglyceride-rich lipid emulsions in vitro and in vivo. J Biol Chem 1996;271:14791-14799.
11. Jong MC, Rensen PC, Dahlmans VE, van der Boom H, Van Berkel TJ, Havekes LM. Apolipoprotein C-III deficiency accelerates triglyceride hydrolysis by lipoprotein lipase in wild-type and apoE knockout mice. J Lipid Res 2001;42:1578-1585.
12. Rensen PC, Herijgers N, Netscher MH, Meskers SC, van EM, Van Berkel TJ. Particle size determines the specificity of apolipoprotein E-containing triglyceride-rich emulsions for the LDL receptor versus hepatic remnant receptor in vivo. J Lipid Res 1997;38:1070-1084.
13. Bligh EG, Dyer WJ. A rapid method of total lipid extraction and purification. Can J Biochem Physiol 1959;37:911-917.
14. Jo J, Gavrilova O, Pack S, Jou W, Mullen S, Sumner AE, Cushman SW, Periwal V. Hypertrophy and/or Hyperplasia: Dynamics of Adipose Tissue Growth. PLoS Comput Biol 2009;5:e1000324.
15. Clark AM, Sousa KM, Jennings C, MacDougald OA, Kennedy RT. Continuous-flow enzyme assay on a microfluidic chip for monitoring glycerol secretion from cultured adipocytes. Anal Chem 2009;81:2350-2356.
16. Voshol PJ, Jong MC, Dahlmans VE, Kratky D, Levak-Frank S, Zechner R, Romijn JA, Havekes LM. In muscle-specific lipoprotein lipase-overexpressing mice, muscle triglyceride content is increased without inhibition of insulin-stimulated whole-body and muscle-specific glucose uptake. Diabetes 2001;50:2585-2590.
17. Macotela Y, Boucher J, Tran TT, Kahn CR. Sex and depot differences in adipocyte insulin sensitivity and glucose metabolism. Diabetes 2009;58:803-812.
18. Stubbins RE, Najjar K, Holcomb VB, Hong J, Nunez NP. Oestrogen alters adipocyte biology and protects female mice from adipocyte inflammation and insulin resistance. Diabetes Obes Metab 2012;14:58-66.
19. Cai L, Wang Z, Ji A, Meyer JM, van der Westhuyzen DR. Scavenger receptor CD36 expression contributes to adipose tissue inflammation and cell death in diet-induced obesity. PLoS One 2012;7:e36785.
20. Collins JM, Neville MJ, Pinnick KE, Hodson L, Ruyter B, van Dijk TH, Reijngoud DJ, Fielding MD, Frayn KN. De novo lipogenesis in the differentiating human adipocyte can provide all fatty acids necessary for maturation. J Lipid Res 2011;52:1683-1692.
21. Christiaens V, Van HM, Lijnen HR, Scroyen I. CD36 promotes adipocyte differentiation and adipogenesis. Biochim Biophys Acta 2012.
22. Laurencikiene J, Skurk T, Kulyte A, Heden P, Astrom G, Sjolin E, Ryden M, Hauner H, Arner P. Regulation of lipolysis in small and large fat cells of the same subject. J Clin Endocrinol Metab 2011;96:E2045-E2049.
23. Kalderon B, Azazmeh N, Azulay N, Vissler N, Valitsky M, Bar-Tana J. Suppression of adipose lipolysis by long-chain fatty Acid analogs. J Lipid Res 2012.
24. Hertzel AV, Smith LA, Berg AH, Cline GW, Shulman GI, Scherer PE, Bernlohr DA. Lipid metabolism and adipokine levels in fatty acid-binding protein null and transgenic mice. Am J Physiol Endocrinol Metab 2006;290:E814-E823.
25. Zhou D, Samovski D, Okunade AL, Stahl PD, Abumrad NA, Su X. CD36 level and trafficking are determinants of lipolysis in adipocytes. FASEB J 2012;26:4733-4742.
26. Arner E, Westermark PO, Spalding KL, Britton T, Ryden M, Frisen J, Bernard S, Arner P. Adipocyte turnover: relevance to human adipose tissue morphology. Diabetes 2010;59:105-109.
27. Weyer C, Foley JE, Bogardus C, Tataranni PA, Pratley RE. Enlarged subcutaneous abdominal

adipocyte size, but not obesity itself, predicts type II diabetes independent of insulin resistance. Diabetologia 2000;43:1498-1506.

28. Lundgren M, Svensson M, Lindmark S, Renstrom F, Ruge T, Eriksson JW. Fat cell enlargement is an independent marker of insulin resistance and 'hyperleptinaemia'. Diabetologia 2007;50:625-633.
29. Kennedy DJ, Kuchibhotla S, Westfall KM, Silverstein RL, Morton RE, Febbraio M. A CD36-dependent pathway enhances macrophage and adipose tissue inflammation and impairs insulin signalling. Cardiovasc Res 2011;89:604-613.
30. Seppala-Lindroos A, Vehkavaara S, Hakkinen AM, Goto T, Westerbacka J, Sovijarvi A, Halavaara J, Yki-Jarvinen H. Fat accumulation in the liver is associated with defects in insulin suppression of glucose production and serum free fatty acids independent of obesity in normal men. J Clin Endocrinol Metab 2002;87:3023-3028.
31. Tiikkainen M, Tamminen M, Hakkinen AM, Bergholm R, Vehkavaara S, Halavaara J, Teramo K, Rissanen A, Yki-Jarvinen H. Liver-fat accumulation and insulin resistance in obese women with previous gestational diabetes. Obes Res 2002;10:859-867.
32. Coomans CP, Biermasz NR, Geerling JJ, Guigas B, Rensen PC, Havekes LM, Romijn JA. Stimulatory effect of insulin on glucose uptake by muscle involves the central nervous system in insulin-sensitive mice. Diabetes 2011;60:3132-3140.
33. Bays HE, Gonzalez-Campoy JM, Henry RR, Bergman DA, Kitabchi AE, Schorr AB, Rodbard HW. Is adiposopathy (sick fat) an endocrine disease? Int J Clin Pract 2008;62:1474-1483.

3 ASPIRIN REDUCES HYPERTRIGLYCERIDEMIA BY LOWERING VLDL-TRIGLYCERIDE PRODUCTION IN MICE FED A HIGH-FAT DIET

Janna A. van Diepen, Irene O.C.M. Vroegrijk,
Jimmy F.P. Berbée, Steven E. Shoelson, Johannes A. Romijn,
Louis M. Havekes, Patrick C.N. Rensen, Peter J. Voshol

Am J Physiol Endocrinol Metab 2011; 306: E1099-107

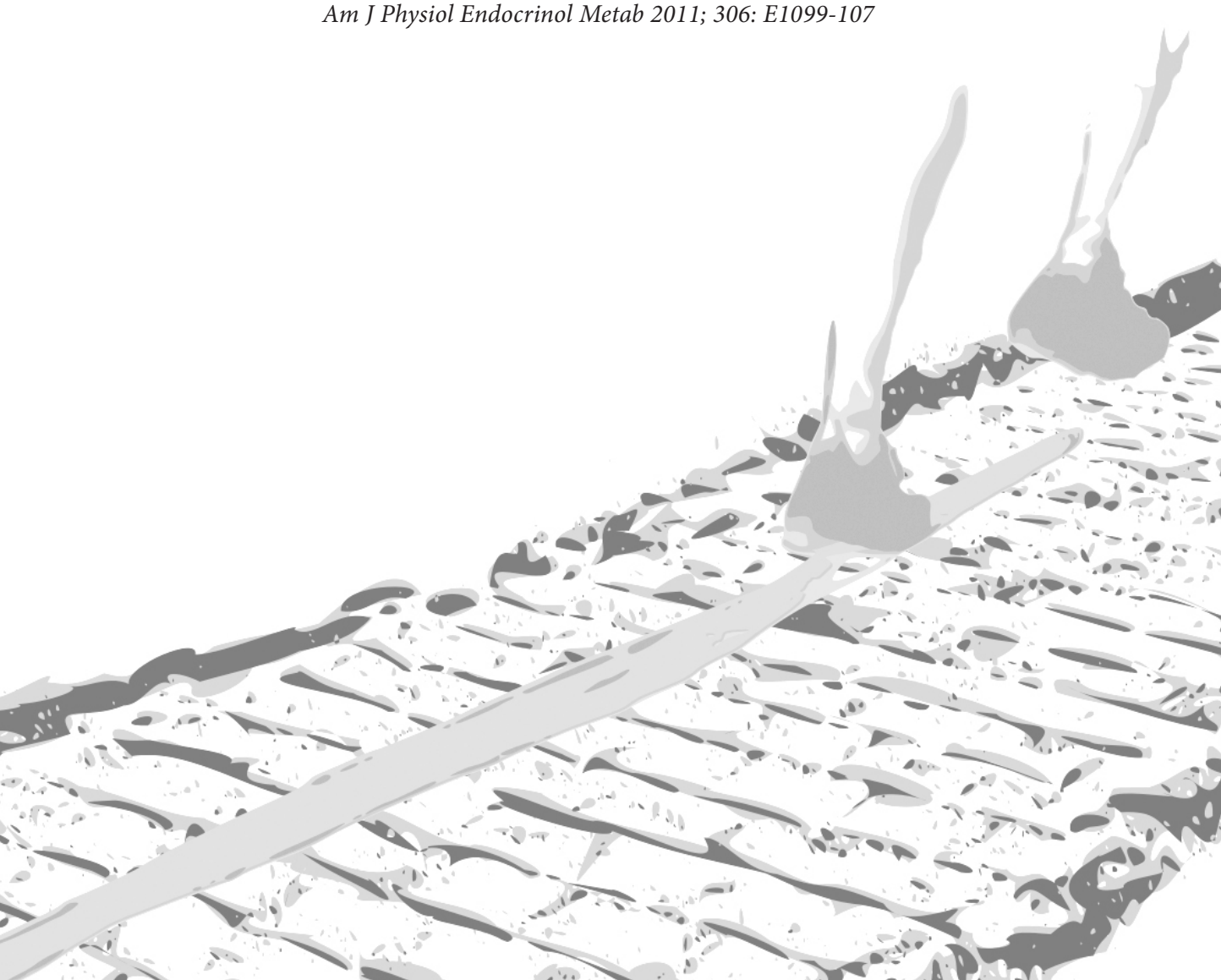

ABSTRACT

Systemic inflammation is strongly involved in the pathophysiology of the metabolic syndrome, a cluster of metabolic risk factors including hypertriglyceridemia. Aspirin treatment lowers inflammation via inhibition of NF-κB activity, but also reduces hypertriglyceridemia in humans. The aim of this study was to investigate the mechanism by which aspirin improves hypertriglyceridemia. Human apolipoprotein CI (apoCI)-expressing mice (*APOC1* mice), an animal model with elevated plasma triglyceride (TG) levels, as well as normolipidemic wild-type (WT) mice were fed a high-fat diet (HFD) and treated with aspirin. Aspirin treatment reduced hepatic NF-κB activity in HFD-fed *APOC1* and WT mice and in addition, aspirin decreased plasma TG levels (-32%; $p<0.05$) in hypertriglyceridemic *APOC1* mice. This TG-lowering effect could not be explained by enhanced VLDL-TG clearance, but aspirin selectively reduced hepatic production of VLDL-TG in both *APOC1* (-28%; $p<0.05$) and WT mice (-33%; $p<0.05$) without affecting VLDL-apoB production. Aspirin did not alter hepatic expression of genes involved in FA oxidation, lipogenesis and VLDL production, but decreased the incorporation of plasma-derived FA by the liver into VLDL-TG (-24%; $p<0.05$), which was independent of hepatic expression of genes involved in FA uptake and transport. We conclude that aspirin improves hypertriglyceridemia by decreasing VLDL-TG production without affecting VLDL particle production. Therefore, the inhibition of inflammatory pathways by aspirin could be an interesting target for the treatment of hypertriglyceridemia.

3.1 INTRODUCTION

The metabolic syndrome is a clustering of metabolic risk factors, including steatosis, insulin resistance and hyperlipidemia, predisposing to the early onset of atherosclerosis and cardiovascular morbidity and mortality. It is well established that the metabolic syndrome is associated with increased systemic inflammation.[1] Moreover, accumulating evidence suggests a strong involvement of systemic inflammation in the pathogenesis of components of the metabolic syndrome.[2] Hypertriglyceridemia, one of the components of the metabolic syndrome and an important risk factor for the development of cardiovascular disease, is strongly associated with increased inflammation.[3] Early studies show that sepsis, infection and inflammation are accompanied by hypertriglyceridemia.[4-6] More recent studies show that administration of LPS induces hypertriglyceridemia.[7,8] In addition, multiple cytokines, such as IL-6 and TNF-α, increase serum triglyceride (TG) levels.[9,10] Inhibition of inflammation might therefore be an attractive therapeutic target in patients with HFD-induced hypertriglyceridemia.

Non-steroidal anti-inflammatory drugs (NSAID) such as aspirin are known to inhibit the enzyme cyclooxygenase (COX). In addition, high doses of aspirin lower activation of inflammatory pathways by inhibition of the NF-κB pathway,[11,12] which plays a crucial role in the inflammation-mediated pathogenesis of the metabolic syndrome.[2] Interestingly, aspirin treatment diminishes hypertriglyceridemia in both obese rodents[13] and patients with type 2 diabetes mellitus.[14] However, the mechanism underlying this TG-lowering effect still has to be elucidated.

We previously found that human apolipoprotein CI (apoCI)-expressing (*APOC1*) mice have increased plasma TG, by a diminished clearance of VLDL particles through apoCI-mediated inhibition of lipoprotein lipase (LPL),[15] which is aggravated by high-fat diet (HFD) feeding (unpublished observation by I.O.C.M. Vroegrijk et al). Therefore, we reasoned that the HFD-fed *APOC1* transgenic mouse is an appropriate model to study the effectiveness of treatments targeting HFD-induced hypertriglyceridemia.

The aim of this study was to investigate the mechanism by which aspirin reverses HFD-induced hypertriglyceridemia. Therefore, we studied the effect of aspirin on VLDL-TG metabolism *in vivo* in HFD-fed hypertriglyceridemic *APOC1* mice as well as in C57Bl/6 wild-type (WT) mice, to extend any findings towards the mouse model that is most widely used for evaluation of treatments for the metabolic syndrome. Our results show that a high dose of aspirin improves hypertriglyceridemia as a consequence of a clear reduction of hepatic VLDL-TG production, mediated by a diminished hepatic incorporation of plasma-derived FA into VLDL-TG.

3.2 MATERIALS AND METHODS

Animals, diet and aspirin treatment

Transgenic *APOC1* mice with hemizygous expression of the human *APOC1* gene were generated as previously described and backcrossed at least 10 times to the C57Bl/6 background. The *APOC1* mouse model develops hypertriglyceridemia mainly due to a diminished clearance of VLDL particles through apoCI-mediated inhibition of lipoprotein lipase (LPL).[16,17] Male *APOC1* mice and WT mice (also on a C57Bl/6 background) were housed under standard conditions with a 12-hour light-dark cycle. At the age of 10–12 weeks, mice received a HFD (45 energy% derived from palm oil; D12451, Research Diet Services, Wijk bij Duurstede, The Netherlands) for a period of 6 weeks. Aspirin treatment (120 mg/kg/day in drinking water; pH 6.4) was given during the last 4 weeks on HFD and mice were subsequently used for experiments after an overnight fast at 9:00 am. Control mice received the same drinking water of pH 6.4 without the addition of aspirin. Mice were allowed free access to food and water. Animal experiments were approved by the institutional ethical committee on animal care and experimentation.

Liver NF-κB activation

Since the most common form of NF-κB is the p50/p65 heterodimer,[18] the activity of both the p50 and p65 subunits in liver tissue was determined using electrophoretic mobility shift assay (EMSA).[19] Shortly, tissues were homogenized in ice-cold Passive Lysis Buffer (Promega, Madison, WI) and centrifuged (14,000 rpm; 20 min; 4°C). Protein content of the supernatant was determined using the BCA protein assay kit (Pierce, Rockford, IL). For the EMSA, the gel shift assay system was purchased from Promega. The probe was end-labeled using T4 polynucleotide kinase and [^{32}P]ATP and purified on a Microspin G-25 column (GE Healthcare, Piscataway, NJ). For each sample, 50 μg protein was incubated with labelled probe and binding buffer (Promega) for 20 min at RT. Specific competition was done by adding unlabeled NF-κB binding probe to the reaction. The mixtures were run on 4.5% polyacrylamide gel electrophoresis in 0.5x Tris/Borate/EDTA (TBE) buffer. The gel was vacuum-dried and exposed to radiographic film.

Plasma parameters

Blood was collected from the tail vein into chilled paraoxon (Sigma, St Louis, MO)-coated capillaries to prevent ongoing lipolysis.[20] Capillaries were placed on ice, centrifuged and plasma was assayed for TG, total cholesterol (TC) and phospholipids (PL) using commercially available enzymatic kits from Roche Molecular Biochemicals (Indianapolis, IN) in 96-wells plates (Greiner Bio-One). Free fatty acids (FFA) were measured using NEFA-C kit from Wako Diagnostics (Instruchemie, Delfzijl, the Netherlands). ß-hydroxybutyrate (ß-HB) was determined using the enzymatic ß-HB Assay kit from BioVision (Mountain View, CA, USA)

Liver lipids

Lipids were extracted from livers according to a modified protocol from Bligh and Dyer.[21] Shortly, a small piece of liver was homogenized in ice-cold methanol. After centrifugation, lipids were extracted by addition of 1800 µL CH_3OH:$CHCl_3$ (3:1 v/v) to 45 µL homogenate. The $CHCl_3$ phase was dried and dissolved in 2% Triton X-100. Hepatic TG and TC concentrations were measured using commercial kits as described earlier. Liver lipids were expressed per mg protein, which was determined using the BCA protein assay kit (Pierce).

Generation of VLDL-like emulsion particles

VLDL-like TG-rich emulsion particles were prepared and characterized as described previously.[22,23] Lipids (100 mg) at a weight ratio of triolein: egg yolk phosphatidylcholine: lysophosphatidylcholine: cholesteryl oleate: cholesterol of 70: 22.7: 2.3: 3.0: 2.0, supplemented with 200 µCi of glycerol tri[9,10(n)-^{3}H]oleate ([^{3}H]TO) were sonicated at 10 µm output using a Soniprep 150 (MSE Scientific Instruments, Crawley, UK). Density gradient ultracentrifugation was used to obtain 80 nm-sized emulsion particles, which were used for subsequent experiments. TG content of the emulsions was measured as described above. Emulsions were stored at 4°C under argon and used within 7 days.

In vivo clearance of VLDL-like emulsion particles

To study *in vivo* clearance of the VLDL-like emulsion particles, overnight fasted mice were anesthetized by intraperitoneal injection of acepromazine (6.25 mg/kg Neurotranq, Alfasan International BV, Weesp, The Netherlands), midazolam (6.25 mg/kg Dormicum, Roche Diagnostics, Mijdrecht, The Netherlands), and fentanyl (0.31 mg/kg Janssen Pharmaceuticals, Tilburg, The Netherlands). Mice were injected (t=0) via the tail vein with 200 µL of [^{3}H]TO-labeled emulsion particles at a dose of 100 µg of TG per mouse. Blood samples were taken from the tail vein at 1, 2, 5, 10 and 15 minutes after injection and plasma ^{3}H-activity was counted. Plasma volumes were calculated as 0.04706 x body weight (grams) as determined from ^{125}I-BSA clearance studies as described previously.[24] After taking the last blood sample, the liver, heart, spleen, muscle and white adipose tissue (*i.e.* gonadal, subcutaneous and visceral) were collected. Organs were dissolved overnight at 60°C in Tissue Solubilizer (Amersham Biosciences, Rosendaal, The Netherlands) and ^{3}H-activity was counted. Uptake of [^{3}H]TO-derived radioactivity by the organs was calculated from the ^{3}H activity in each organ divided by plasma-specific activity of [^{3}H]TG and expressed per mg wet tissue weight.

Hepatic VLDL-TG and VLDL-apoB production

To measure VLDL production *in vivo*, mice were fasted overnight as described above. Mice were injected intravenously with Tran^{35}S label (150 µCi/mouse; MP Biomedicals, Eindhoven, The Netherlands) to label newly produced apoB. After 30 minutes, at t=0 min, Triton WR-1339 (Sigma-Aldrich) was injected intravenously (0.5 mg/g body weight, 10% solution in PBS) to block serum VLDL clearance. Blood samples were drawn before

(t=0) and 15, 30, 60 and 90 min after injection and used for determination of plasma TG concentration as described above. After 120 min, mice were exsanguinated via the retro-orbital plexus. VLDL was isolated from serum after density gradient ultracentrifugation at d<1.006 g/mL by aspiration[25] and counted for incorporated ^{35}S-activity.

Hepatic gene expression analysis

Total RNA was extracted from liver tissues using the Nucleospin RNA II kit (Macherey-Nagel, Düren, Germany) according to the instructions of the manufacturer. The quality of each mRNA sample was examined by lab-on-a-chip technology using Experion Stdsens analysis kit (Biorad, Hercules, CA). 1 μg of total RNA was reverse-transcribed with iScript cDNA synthesis kit (Bio-Rad) and obtained cDNA was purified with Nucleospin Extract II kit (Macherey-Nagel). Real-Time PCR was carried out on the IQ5 PCR machine (Biorad) using the Sensimix SYBR Green RT-PCR mix (Quantace, London, UK). mRNA levels were normalized to mRNA levels of cyclophilin (*Cyclo*) and glyceraldehyde-3-phosphate dehydrogenase (*Gapdh*). Primer sequences are listed in table 1.

Contribution of plasma FA to VLDL-TG production

To measure the contribution of plasma derived FA to the VLDL-TG production *in vivo*, mice were fasted overnight as described above. Mice received a continuous i.v. infusion of

Table 1. Primers used for quantitative real-time PCR analysis.

Gene	Forward primer	Reverse primer
Acox1	TATGGGATCAGCCAGAAAGG	ACAGAGCCAAGGGTCACATC
Apob	GCCCATTGTGGACAAGTTGATC	CCAGGACTTGGAGGTCTTGGA
Cd36	GCAAAGAACAGCAGCAAAATC	CAGTGAAGGCTCAAAGATGG
Cpt1a	GAGACTTCCAACGCATGACA	ATGGGTTGGGGTGATGTAGA
Cyclo	CAAATGCTGGACCAAACACAA	GCCATCCAGCCATTCAGTCT
Dgat1	TCCGTCCAGGGTGGTAGTG	TGAACAAAGAATCTTGCAGACGA
Fasn	TCCTGGGAGGAATGTAAACAGC	CACAAATTCATTCACTGCAGCC
Fabp1	GAGGAGTGCGAACTGGAGAC	GTAGACAATGTCGCCCAATG
Gapdh	TGCACCACCAACTGCTTAGC	GGCATGGACTGTGGTCATGAG
Mttp	CTCTTGGCAGTGCTTTTTCTCT	GAGCTTGTATAGCCGCTCATT
Ppara	ATGCCAGTACTGCCGTTTTC	GGCCTTGACCTTGTTCATGT
Slc27a2	ATCGCCTATGGTATGGGACA	ACTGGCTGGCTGAGAATTTG
Slc27a4	GCTTACTCCACGGCATGACT	GTGGCTGGTTCAGGAGGTAG
Slc27a5	ATGCAGAGCTGATGATGTGG	ATCACTGTTACGCCATGCTG
Srebf1	GGAGCCATGGATTGCACATT	CCTGTCTCACCCCCAGCATA

Acox1, acyl-Coenzyme A oxidase 1, palmitoyl; *Apob*, apolipoprotein B; *Cd36,* fatty acid translocase; *Cpt1a,* carnitine palmitoyltransferase 1a; *Dgat1*, diglyceride acyltransferase 1; *Fabp1*, fatty acid binding protein 1; *Fasn*, fatty acid synthase; *Mttp*, microsomal triglyceride transfer protein; *Ppara*, peroxisome proliferative activated receptor alpha; *Slc27a2*, fatty acid transport protein 2; *Slc27a4*, fatty acid transport protein 4; *Slc27a5*, fatty acid transport protein 5; *Srebf1*, sterol-regulatory element binding protein.

^{3}H-labeled FA ([9,10(n)-^{3}H] palmitic acid in PBS with 2% bovine serum albumin) at a rate of 100μL/h (1.6 μCi/h). After 2 hours of ^{3}H-labeled FA infusion a blood sample was taken (t=0 min), and Triton WR-1339 (Sigma-Aldrich) was injected intravenously (0.5 mg/g body weight, 10% solution in PBS) to block serum VLDL clearance. Additional blood samples were drawn 15, 30, 60 and 90 min after injection and used for determination of ^{3}H activity in the TG fraction. Lipids were extracted by adding 10 μL plasma to 3.25 mL extraction fluid (heptane/methanol/chloroform; 100:128:137 (*v/v/v*)). ^{3}H-TG were subsequently separated from ^{3}H-FA; 1mL potassium carbonate (0.1M K_2CO_3, pH 10.5) was added followed by vortexing and centrifugation (3600 rpm; 15 min), leading to an upper alkaline-methanol-aqueous phase containing saponified ^{3}H-FA and a lower chloroform-organic phase containing ^{3}H-TG.[26] A fraction (0.5 mL) of the total aqueous phase (2.45 mL) was counted for ^{3}H in scintillation fluid. The amount of ^{3}H-TG in each sample was calculated by distracting total ^{3}H-FA activity from total ^{3}H activity.

Statistical analysis

Data are presented as means ± SD. Statistical differences were calculated using the Mann-Whitney test for two independent samples with SPSS 16.0 (SPSS Inc, Chicago, IL). P<0.05 was regarded statistically significant.

3.3 RESULTS

Aspirin reduces hepatic NF-κB activation

To verify that aspirin inhibits hepatic NF-κB activity, the activities of the NF-κB subunits p50 and p65 were measured in livers of *APOC1* and WT mice fed a HFD and treated with or without aspirin using a gel shift assay (Fig. 1). Aspirin indeed reduced the activity of both p50 (-69%; P<0.05) and p65 (-48%; P<0.05) in *APOC1* mice (Fig. 1A) and the activity of p50 in WT mice (-72%; P<0.05), while the reduction in the activity of p65 did not reach statistical significance (P=0.13) (Fig. 1B).

Aspirin lowers plasma triglyceride and cholesterol levels in HFD-fed *APOC1* mice

To examine whether aspirin could reduce hypertriglyceridemia in *APOC1* mice, hyperlipidemic *APOC1* mice were fed a HFD for 6 weeks and treated with or without aspirin and plasma lipids were determined (Fig. 2). Treatment of mice with aspirin reduced plasma TG levels by -32% (3.94 ± 0.15 to 2.67 ± 0.59 mmol/L; P<0.05; Fig. 2A) and plasma TC levels by -33% (4.09 ± 0.52 to 2.76 ± 0.90 mmol/L; P<0.05; Fig. 2B). Aspirin treatment did not affect plasma PL levels (Fig. 2C) and FFA levels (Fig. 2D). The reduction in plasma TG and TC levels was not caused by a reduction in body weight, since aspirin did not affect body weight in *APOC1* mice (control: 30.5 ± 2.1 g; aspirin: 28.9 ± 3.0 g). In WT mice fed a HFD

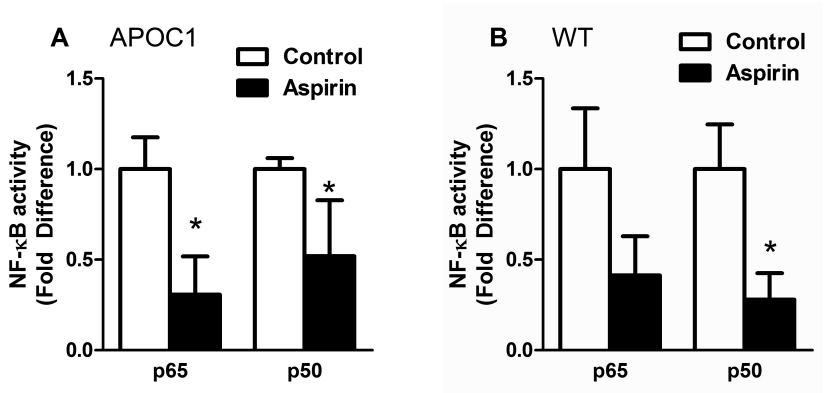

Figure 1. Aspirin reduces hepatic NF-κB activation. *APOC1* and WT mice were fed a HFD for 6 weeks and treated without or with aspirin. Mice were sacrificed after an overnight fast and hepatic NF-κB activity was measured by electrophoretic mobility shift assay in liver tissue of *APOC1 (A)* and WT (B) mice treated without (open bars) or with (closed bars) aspirin. Activities of subunits p50 and p65 were measured. Values are means ± SD (n=3-4). *P<0.05

for 6 weeks, aspirin did not affect plasma TG, TC, PL or FFA levels (Fig. 2E-H). In addition, aspirin did not affect body weight in WT mice (control: 30.3 ± 2.1 g; aspirin: 30.8 ± 1.9 g)

Aspirin attenuates VLDL-like emulsion particle-TG clearance in HFD-fed *APOC1*, but not WT mice

A reduction in fasted plasma TG levels can be explained by an increase in VLDL-TG clearance and/or a decrease in hepatic VLDL-TG production. To determine whether aspirin enhances the clearance of VLDL-TG, the plasma clearance and organ distribution of [^{3}H]-TO-labeled TG-rich VLDL-like emulsion particles was evaluated in aspirin and control treated hypertriglyceridemic *APOC1* mice (Fig. 3). Unexpectedly, aspirin inhibited, rather than enhanced, serum clearance of [^{3}H]TO (t ½ = 15.9 ± 6.6 *vs* 5.6 ± 2.6 min) (Fig. 3A) in *APOC1* mice. This reduction in [^{3}H]TO clearance upon aspirin was reflected by reduced uptake of [^{3}H]TO-derived radioactivity by the liver by -60% (123 ± 1 *vs* 308 ± 75 nmol/g; P<0.05), by skeletal muscle by -66% (11 ± 2 *vs* 31 ± 15 nmol/g; P<0.05) and by white adipose tissue (WAT), which reached statistical significance for gonadal WAT (12 ± 3 *vs* 44 ± 22 nmol/g; P<0.05) (Fig. 3B). Apparently, aspirin reduces rather than enhances TG clearance in *APOC1* mice and can, therefore, not explain the aspirin-induced reduction in VLDL-TG. In WT mice fed a HFD for 6 weeks, aspirin did not affect plasma clearance of [^{3}H]TO (Fig. 3C) or organ specific uptake of [^{3}H]TO-derived radioactivity (Fig. 3D) in WT mice. Apparently, the decreasing effect of aspirin on TG clearance may be specific for *APOC1* mice.

Aspirin lowers VLDL-TG production in HFD-fed *APOC1* and WT mice

Because the decrease in plasma TG levels in *APOC1* mice upon aspirin treatment was not caused by increased TG clearance, we investigated whether the decreased TG levels could be explained by diminished hepatic VLDL-TG production in *APOC1* mice. The rate of hepatic VLDL-TG production was measured by determining plasma TG levels after intravenous

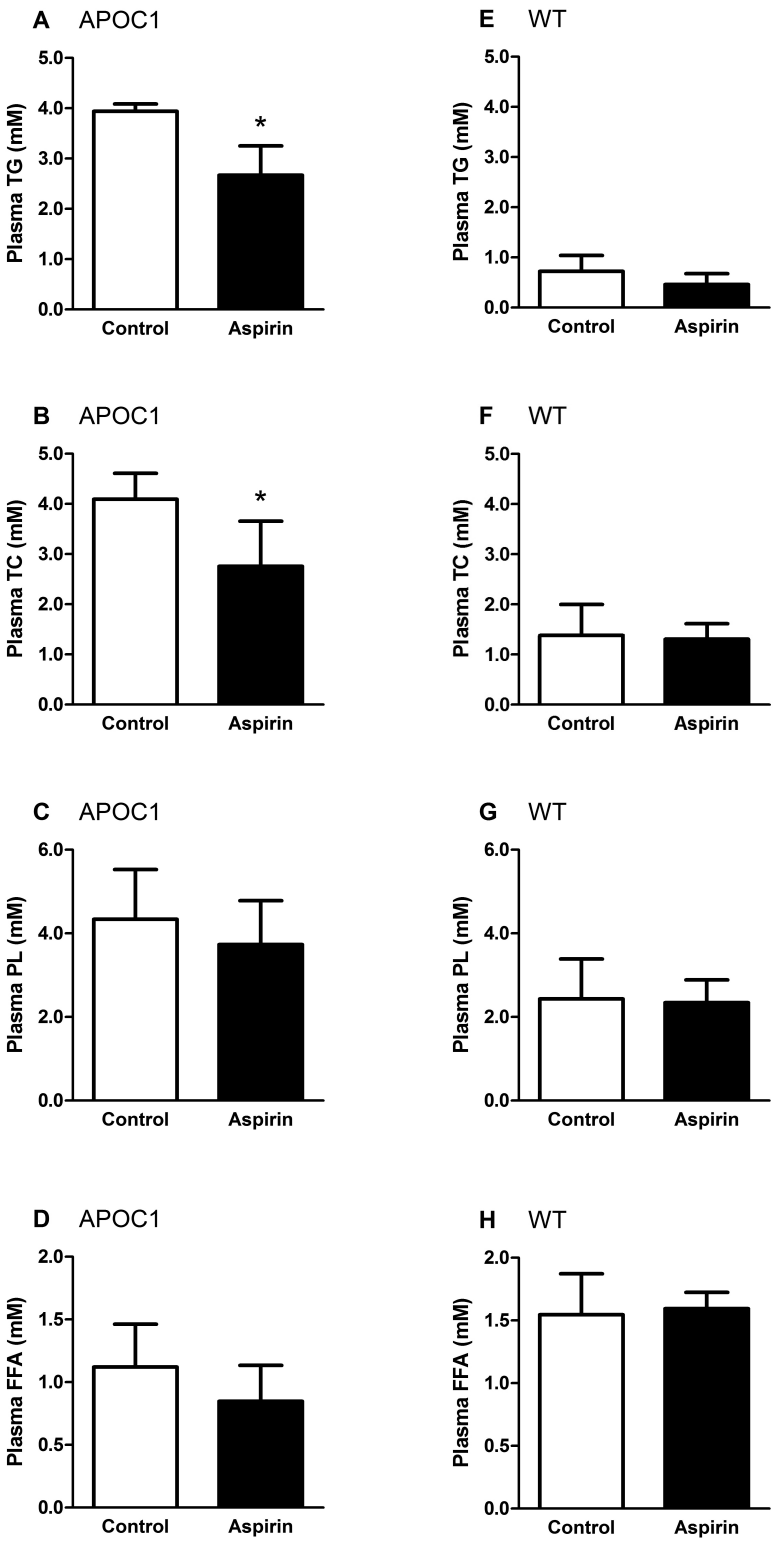

Figure 2. Aspirin lowers plasma triglyceride and cholesterol levels in HFD-fed *APOC1* mice. Plasma triglycerides (TG) (A&E), total cholesterol (TC) (B&F), phospholipids (PL) (C&G) and free fatty acid (FFA) (D&H) levels were measured in plasma of overnight-fasted HFD-fed *APOC1* and WT mice treated without or with aspirin. Values are means ± SD (n=4-5). *P<0.05.

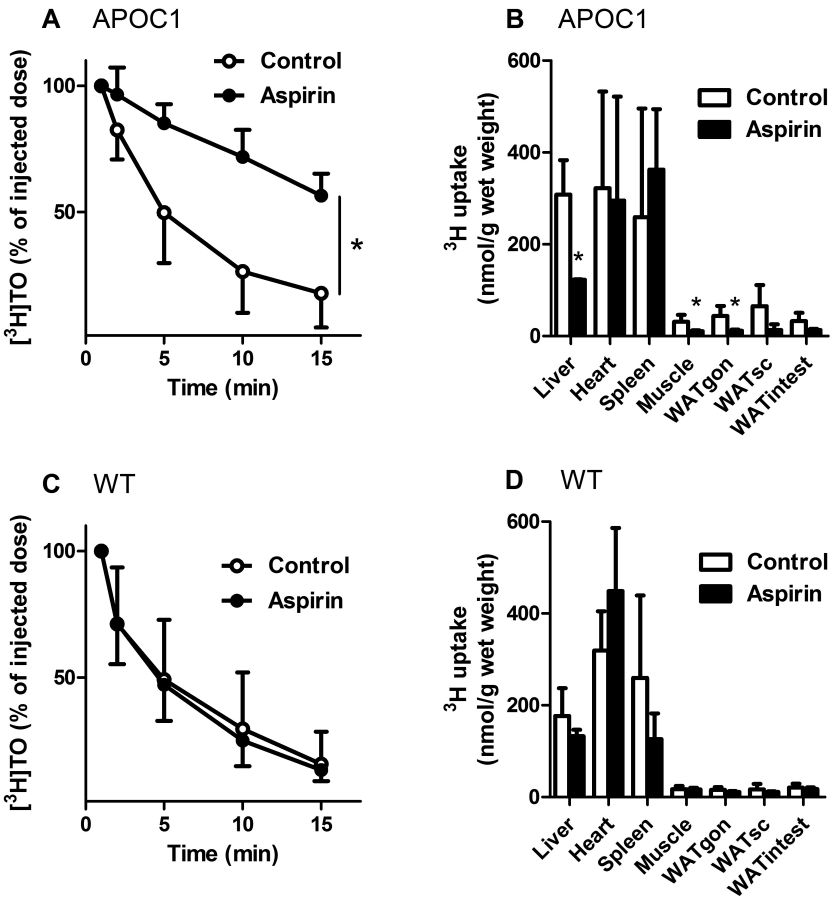

Figure 3. Aspirin attenuates TG clearance of VLDL-like emulsion particles in HFD-fed *APOC1*, but not WT mice. HFD-fed *APOC1* and WT mice that were treated without or with aspirin were fasted overnight and injected with [^{3}H]TO-labeled VLDL-like emulsion particles. Blood was collected at the indicated time points and radioactivity was measured in plasma of *APOC1* (A) and WT (C) mice treated without (open circles) or with (closed circles) aspirin. Uptake of [^{3}H]TO-derived activity by various organs was determined, and total FA uptake was calculated from the specific activity of TG in plasma, and expressed as nmol FA per mg wet tissue weight in *APOC1* (B) and WT (D) mice. Values are means ± SD (n=4). *P<0.05. WAT, white adipose tissue; intest, intestinal; sc, subcutaneous; gon, gonadal.

Triton WR1339 injection (Fig 4). We found a reduction in hepatic VLDL-TG secretion rate in *APOC1* mice treated with aspirin by -28% (3.42 ± 0.53 vs 4.95 ± 1.11 mM/h; P<0.05) (Fig. 4A), whereas aspirin did not affect the rate of VLDL-apoB production (Fig. 4B). Interestingly, similar to our observation in *APOC1* mice, aspirin did reduce the hepatic VLDL-TG secretion rate in HFD-fed WT mice by -33% (2.79 ± 0.47 mM/h vs 4.19 ± 0.48 mM/h; P<0.05; Fig. 4C), whereas VLDL-apoB production rate was also not affected (Fig. 4D). Apparently, aspirin generally reduces the VLDL-TG production in HFD-fed mice, independent of the genotype. Furthermore, since each VLDL particle contains a single apoB molecule, this observation shows that aspirin treatment inhibits hepatic VLDL-TG production, without affecting the rate of VLDL particle production.

Aspirin does not affect liver lipid levels in HFD-fed *APOC1* and WT mice

To determine whether the attenuation in hepatic VLDL-TG production was the result of decreased lipid substrate availability in the liver, the effect of aspirin on hepatic lipid content was measured (Fig. 5). However, aspirin did not affect liver TG levels (Fig. 5A) and TC levels (Fig. 5B) in *APOC1* mice. Also, aspirin did not affect liver TG (Fig. 5C) or TC (Fig. 5D) levels in WT mice.

Aspirin treatment does not affect hepatic expression of genes involved in FA oxidation, lipogenesis or VLDL production

Since changes in hepatic gene expression could underlie the reduction in VLDL-TG production, we determined the effect of aspirin on expression of genes involved in FA

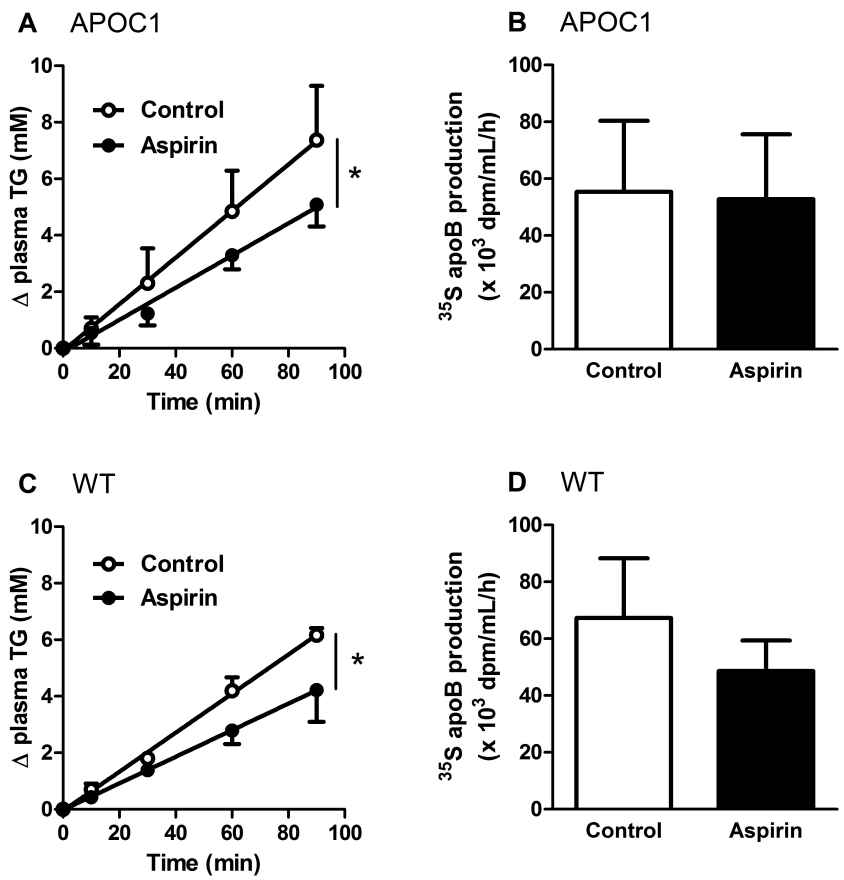

Figure 4. Aspirin decreases VLDL-TG production in HFD-fed *APOC1* and WT mice. *APOC1* and WT mice were fed a HFD and treated without or with aspirin. Overnight fasted mice were injected with Trans^{35}S and TritonWR1339 and blood samples were drawn at the indicated time points. TG concentrations were determined in *APOC1* (A) and WT (C) mice treated without (open circles) or with (closed circles) aspirin and plotted as the increase in plasma TG relative to t=0 (A). After 120 min, VLDL was isolated by ultracentrifugation, ^{35}S-activity was counted and the production rate of newly synthesized VLDL-^{35}S-apoB was determined for *APOC1* (B) and WT (D). Values are means ± SD (n=5). *P<0.05.

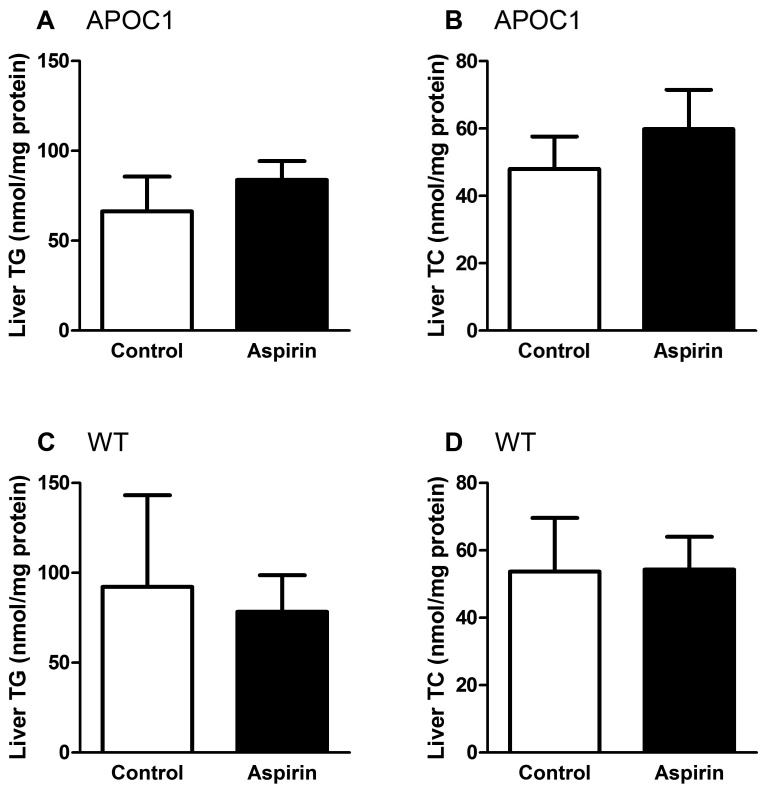

Figure 5. Aspirin does not affect liver lipids in HFD-fed *APOC1* and WT mice. Livers were collected from overnight-fasted HFD-fed *APOC1* and WT mice treated without or with aspirin. Lipids were extracted and triglyceride (TG, A&C) and total cholesterol (TC, B&D) concentrations were measured and expressed per mg protein. Values are means ± SD (n=6).

oxidation, lipogenesis and VLDL production (Table 2). In both *APOC1* and WT mice, aspirin did not affect expression of peroxisome proliferative activated receptor alpha (*Ppara*), a transcription factor that regulates genes involved in FA oxidation and ketogenesis, nor did it affect its target genes acyl-Coenzyme A oxidase 1 (*Acox1*) and carnitine palmitoyltransferase 1a (*Cpt1a*). In line with these results, aspirin did not increase plasma ß-HB levels in WT mice (data not shown), which is a plasma marker for hepatic FA oxidation and ketogenesis. This implies that the reduced VLDL-TG production upon aspirin treatment is not caused by increased hepatic FA oxidation. We additionally determined the effect of aspirin on expression of genes involved in lipogenesis. In both APOC1 and WT mice, aspirin did not affect expression of sterol regulatory element binding protein 1c (*Srebp-1c*), which regulates genes required for de novo lipogenesis, nor did it affect acyl:diacylglycerol transferase 1 (*Dgat1*), which catalyzes the final and only committed step in TG synthesis, or FA synthase (*Fas*), which plays a key role in FA synthesis. These data suggests that aspirin does not affect genetic regulation of *de novo* lipogenesis. In addition, aspirin did not affect hepatic gene expression of microsomal TG transfer protein (*Mttp*) which is involved in the assembly and secretion of VLDL. Furthermore, aspirin does not affect hepatic gene expression of

Table 2. Aspirin generally does not affect hepatic expression of genes involved in FA uptake and transport, FA oxidation, lipogenesis or VLDL secretion.

		APOC1			WT		
Gene	Protein	Control	Aspirin	p-value	Control	Aspirin	p-value
FA uptake and transport							
Fabp1	FABP1	1.00 ± 0.37	0.73 ± 0.35	0.22	1.00 ± 0.41	0.61 ± 0.25	0.14
Slc27a2	FATPa2	1.00 ± 0.45	1.23 ± 0.49	0.46	1.00 ± 0.33	0.74 ± 0.16	0.14
Slc27a4	FATPa4	1.00 ± 0.35	1.74 ± 0.51	0.13	1.00 ± 0.44	1.01 ± 0.47	0.77
Slc27a5	FATPa5	1.00 ± 0.17	1.20 ± 0.39	0.18	1.00 ± 0.40	0.96 ± 0.31	0.62
Cd36	CD36	1.00 ± 0.58	1.75 ± 0.40	0.05	1.00 ± 0.80	0.45 ± 0.22	0.23
FA oxidation							
Ppara	PPARα	1.00 ± 0.29	1.12 ± 0.46	0.62	1.00 ± 0.37	0.72 ± 0.18	0.18
Acox1	ACO	1.00 ± 0.42	1.55 ± 0.55	0.14	1.00 ± 0.36	0.59 ± 0.12	0.09
Cpt1a	CPT1a	1.00 ± 0.55	1.36 ± 0.43	0.22	1.00 ± 0.10	0.96 ± 0.11	0.46
Lipogenesis							
Dgat1	DGAT1	1.00 ± 0.37	1.20 ± 0.11	0.29	1.00 ± 0.42	1.06 ± 0.53	0.85
Fasn	FAS	1.00 ± 0.42	1.05 ± 1.09	0.81	1.00 ± 0.40	0.97 ± 0.27	0.90
Srebf1	SREBP-1c	1.00 ± 0.40	1.22 ± 0.53	0.41	1.00 ± 0.53	0.85 ± 0.68	0.72
VLDL secretion							
Apob	ApoB	1.00 ± 0.46	1.20 ± 0.26	0.73	1.00 ± 0.32	1.59 ± 0.31*	0.03
Mttp	MTP	1.00 ± 0.37	0.87 ± 0.21	0.56	1.00 ± 0.39	1.21 ± 0.12	0.34

Livers were isolated from overnight fasted *APOC1* and WT mice fed a HFD and treated without or with aspirin. mRNA was isolated and mRNA expression of the indicated genes was quantified by RT-PCR. Genes are grouped as genes involved in FA uptake and transport, FA oxidation, lipogenesis and VLDL production. Data are calculated as fold difference as compared to the control group. Values are means ± SD (n=4-5). *P<0.05 compared to control group. *Acox1,* acyl-Coenzyme A oxidase 1, palmitoyl; *Apob*, apolipoprotein B; *Cd36,* fatty acid translocase; *Cpt1a,* carnitine palmitoyltransferase 1a, liver; *Dgat1*, diglyceride acyltransferase 1; *Fabp1*, fatty acid binding protein 1, liver; *Fasn*, fatty acid synthase; *Mttp*, microsomal triglyceride transfer protein; *Ppara*, peroxisome proliferative activated receptor alpha; *Slc27a2*, fatty acid transport protein 2; *Slc27a4*, fatty acid transport protein 4; *Slc27a5*, fatty acid transport protein 5; *Srebpf1*, sterol-regulatory element binding protein.

apoB (*Apob*) in *APOC1* mice, which is in line with the observation that aspirin does not affect VLDL-apoB secretion *in vivo*. However, despite the fact that aspirin did not affect VLDL-apoB secretion in WT mice, gene expression of *Apob* was increased in WT mice.

Aspirin treatment decreases the contribution of plasma-derived FA to the VLDL-TG production

Because the decrease in VLDL-TG production was not caused by a reduced hepatic lipid content or decreased expression of genes involved in *de novo* lipogenesis that could reduce lipid availability for VLDL-TG secretion, we investigated whether the decreased VLDL-TG production could be explained by a diminished contribution of plasma derived FA for VLDL-TG secretion in WT mice (Fig. 6). The contribution of plasma derived FA

was measured by determining plasma ^{3}H-TG levels after continuous ^{3}H-FA infusion and intravenous Triton WR1339 injection. We found that aspirin reduced hepatic ^{3}H-TG secretion rate in WT mice by -24% (3.1 ± 0.4 vs 2.4 ± 0.7 x 10^{3} dpm/h; P<0.05), which suggests that aspirin reduces VLDL-TG production by reducing the incorporation of plasma-derived FA into VLDL-TG. This reduction is not caused by a reduced hepatic expression of genes involved in hepatic FA uptake and transport (Table 2), since aspirin did not affect liver-type FA binding protein (*Fabp1*), FA transport proteins 2, 4 and 5 (*Slc27a2, Slc27a4, Slc27a5*) and even increased expression of FA translocase (*Cd36*) in *APOC1*, but not WT, mice. These data imply that aspirin reduced the VLDL-TG production independent of changes in hepatic expression of genes involved in FA uptake and transport.

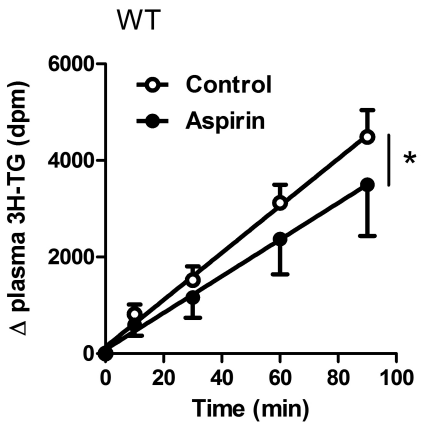

Figure 6. Aspirin reduces the contribution of plasma derived FA to the VLDL-TG production. WT mice were fed a HFD and treated without or with aspirin. Overnight fasted mice received a continuous i.v. infusion of ^{3}H-labeled FA ([9,10(n)-^{3}H] palmitic acid for 2 h, followed by an i.v. injection of TritonWR1339. Blood samples were drawn at the indicated time points and ^{3}H activity in the TG fraction was determined in mice treated without (open circles) or with (closed circles) aspirin and plotted as the increase in plasma ^{3}H-TG relative to t=0. Values are means ± SD (n=7). *P<0.05.

3.4 DISCUSSION

Treatment of obese rodents and patients with type 2 diabetes with high dose aspirin reduces hypertriglyceridemia.[13,14] However, so far, the mechanistic basis for the relation between aspirin intake and reduced plasma TG levels has been poorly understood. In the present study we focused on the effects of aspirin on VLDL-TG metabolism in HFD-induced obese hyperlipidemic *APOC1* mice and additionally evaluated the effects of aspirin on VLDL-TG metabolism in HFD-fed normolipidemic WT mice. Our results document that aspirin treatment improves hypertriglyceridemia by reducing the hepatic production of VLDL-TG as a result of an attenuated hepatic incorporation of plasma derived FA into VLDL-TG, rather than from increased clearance of VLDL-TG from the circulation.

In the present study, aspirin treatment decreased plasma TG and TC levels in HFD fed *APOC1* mice that display hypertriglyceridemia. This improvement in hyperlipidemia is in accordance with earlier studies, showing reduced serum TG concentrations upon aspirin or salicylate treatment in patients with type 2 diabetes mellitus[14] and in diabetic rats.[13]

Our data show that aspirin treatment attenuated the clearance of VLDL-like TG-rich particles in *APOC1* mice. Therefore, the decrease in plasma TG levels by aspirin cannot be explained by increased TG clearance. Earlier studies report that high dose LPS injections reduce the clearance of TG-rich lipoproteins by inhibition of the LPL activity, mediated by cytokines.[6,27] If indeed inflammation inhibits clearance of TG, inhibition of inflammation by aspirin is expected to increase TG-rich lipoprotein clearance, which is in contrast to our observation in *APOC1* mice. It should be noted that aspirin, in addition to inhibition of inflammation via NF-κB, also inhibits prostaglandin synthesis, which has been demonstrated to restore the LPS-induced inhibition of LPL.[28] Moreover, an early report has shown that aspirin treatment inhibits post-heparin LPL activity in humans.[29] It would be interesting to elucidate the mechanism by which aspirin reduces the VLDL-TG clearance, however this is beyond the scope of the current manuscript as it does not explain the reduction in hypertriglyceridemia that we observe. Moreover, the observation may be a specific feature of the *APOC1* transgenic mouse model, since we did not observe such an effect in WT mice.

Aspirin very effectively reduced hepatic secretion of VLDL-TG in *APOC1* mice, explaining the reduction in hypertriglyceridemia upon aspirin treatment. In addition, aspirin equally reduced hepatic secretion of VLDL-TG in WT mice, indicating that the effects of aspirin on the VLDL-TG production do not exclusively occur in hypertriglyceridemic mouse models such as the *APOC1* mouse. To our knowledge, we show for the first time that a decrease in inflammation corresponds with a drop in VLDL-TG production. The reduction of VLDL-TG secretion in our study is not paralleled by a reduction in apoB secretion in both *APOC1* and WT mice, suggesting that aspirin reduces the lipidation of VLDL particles rather than reducing the number of particles that are secreted by the liver. In contrast to our data on apoB secretion, a recent study by Tsai et al[30] observed that suppression of IKK with BMS345541 decreased apoB secretion *in vitro* in primary hamster hepatocytes and HepG2 cells. Even though differences between species might explain these conflicting findings, both these published *in vitro* studies and our present *in vivo* study point towards a link between the IKK/NF-κB pathway and the regulation of VLDL production. Moreover, we have recently shown that *activation* of the hepatic IKK/NF-κB pathway increases VLDL-TG production,[31] supporting the hypothesis that the effects of aspirin on the VLDL-TG production are mediated via a reduction in hepatic NF-κB activity. Nevertheless, activation of hepatic IKK/NF-κB increases hepatic *Fas* expression,[31] while aspirin in the current study did not change hepatic expression of *Fas*, neither did it change expression of other genes involved in TG synthesis, such as *Dgat1* and *Srepb-1c,* suggesting that aspirin more likely lowers VLDL-TG production by other mechanisms than via its effects on hepatic NF-κB activity.

A reduction in hepatic lipid availability by increased lipid oxidation could underlie the mechanism by which aspirin reduces hepatic VLDL-TG production. However, aspirin did not affect expression of genes involved in FA oxidation nor plasma levels of ß-HB, a marker of hepatic FA oxidation and ketogenesis. Similarly, aspirin did not affect expression of genes involved in de novo lipogenesis or VLDL production, suggesting that aspirin does not reduce VLDL-TG production by changing expression of genes involved in hepatic lipid metabolism.

It has been suggested that the decrease in plasma TG concentration that occurs upon aspirin treatment might be secondary to the fall in plasma FFA levels.[32] A reduction in FFA delivery to the liver could result in a reduced availability of FA for the release of VLDL-TG by the liver.[33] Indeed, although aspirin did not change plasma FFA levels, it changed the turnover of FA as reflected by a -24% reduction in the incorporation of plasma derived FA into VLDL-TG, showing that aspirin in fact lowers the availability of plasma derived FA for VLDL-TG production. This reduction of FA incorporation into VLDL-TG upon aspirin treatment was not caused by a reduced hepatic expression of FA transporter proteins, suggesting that aspirin reduces the FA incorporation via another mechanism. It is possible that aspirin reduces posttranscriptional processing of FA transporters independent of mRNA expression, since expression of FA transporters does not always correlate with changes in protein content or the rate of FA transport.[34] Alternatively, aspirin might increase FA uptake and transport via simple diffusion, since FA uptake has been described independent of any FA transporter.[34]

The decrease of FA turnover that we observed could be secondary to an increased insulin sensitivity of adipose tissue, thereby decreasing FA mobilization to plasma. Indeed, high dose salicylates, such as aspirin have shown to increase insulin sensitivity[13] and the reduction in VLDL-TG production in our study is similarly accompanied by an increased insulin sensitivity (unpublished observation). However, the aspirin-induced reduction in FA utilization and subsequent VLDL-TG secretion in our study were determined under fasting conditions, when the role of insulin is marginal. In fasting conditions, the lipolytic activity of adipocytes is stimulated by catecholamines. Interestingly, aspirin has been reported to reduce catecholamine-stimulated lipolysis, which is therefore a more likely explanation for our findings.[35,36] In addition, it has been shown that aspirin reduces release of FA from adipose tissue directly via inhibition of TNF-α induced lipolysis.[37] We therefore propose that the fact that aspirin reduces plasma derived FA utilization by the liver, is likely caused via direct inhibition of intracellular lipolysis in adipose tissue, which reduces plasma FA availability. Adipose tissue lipolysis might be further inhibited in the fed state by an increased sensitivity for insulin.

In conclusion, our data show that aspirin inhibits NF-κB and decreases HFD-induced hypertriglyceridemia by reducing hepatic VLDL-TG secretion rather than by accelerating the tissue distribution of VLDL-TG. The reduction in VLDL-TG is not caused by a decreased steatosis, increased FA oxidation or changes in *de novo* lipogenesis, but by an attenuation of hepatic incorporation of plasma derived FA into VLDL-TG. In scope of our findings, aspirin could potentially be a new therapeutic drug in the treatment of hypertriglyceridemia. However, chronic high-dose aspirin is associated with risk for bleeding. Salsalate on the

other hand is a non-steroidal anti-inflammatory drug with similar structure that is regarded as a safer alternative. High-dose salsalate treatment has recently shown to reduce TG levels in diabetic patients similar to high-dose aspirin treatment,[38] and could therefore potentially be a new drug for the treatment of hypertriglyceridemia.

ACKNOWLEDGEMENTS

The authors are grateful to A. Logiantara for excellent technical assistance. This work was supported by grants from the Netherlands Organization for Scientific Research (NWO Zon-MW; 917.76.301 to P.J. Voshol) and the Dutch Diabetes Research Foundation (2005.01.003 to P.J. Voshol). I.O.C.M. Vroegrijk is supported by the seventh framework program of the EU-funded "LipidomicNet" (202272). P.C.N. Rensen is an Established Investigator of the Netherlands Heart Foundation (2009T038).

REFERENCES

1. Ridker PM, Buring JE, Cook NR, Rifai N. C-reactive protein, the metabolic syndrome, and risk of incident cardiovascular events: an 8-year follow-up of 14 719 initially healthy American women. Circulation 2003;107:391-397.
2. Cai D, Yuan M, Frantz DF, Melendez PA, Hansen L, Lee J, Shoelson SE. Local and systemic insulin resistance resulting from hepatic activation of IKK-beta and NF-kappaB. Nat Med 2005;11:183-190.
3. Khovidhunkit W, Kim MS, Memon RA, Shigenaga JK, Moser AH, Feingold KR, Grunfeld C. Effects of infection and inflammation on lipid and lipoprotein metabolism: mechanisms and consequences to the host. J Lipid Res 2004;45:1169-1196.
4. Lequire VS, Hutcherson JD, Hamilton RL, Gray ME. The effects of bacterial endotoxin on lipide metabolism. I. The responses of the serum lipides of rabbits to single and repeated injections of Shear's polysaccharide. J Exp Med 1959;110:293-309.
5. Gallin JI, Kaye D, O'Leary WM. Serum lipids in infection. N Engl J Med 1969;281:1081-1086.
6. Feingold KR, Staprans I, Memon RA, Moser AH, Shigenaga JK, Doerrler W, Dinarello CA, Grunfeld C. Endotoxin rapidly induces changes in lipid metabolism that produce hypertriglyceridemia: low doses stimulate hepatic triglyceride production while high doses inhibit clearance. J Lipid Res 1992;33:1765-1776.
7. Hudgins LC, Parker TS, Levine DM, Gordon BR, Saal SD, Jiang XC, Seidman CE, Tremaroli JD, Lai J, Rubin AL. A single intravenous dose of endotoxin rapidly alters serum lipoproteins and lipid transfer proteins in normal volunteers. J Lipid Res 2003;44:1489-1498.
8. Feingold KR, Hardardottir I, Memon R, Krul EJ, Moser AH, Taylor JM, Grunfeld C. Effect of endotoxin on cholesterol biosynthesis and distribution in serum lipoproteins in Syrian hamsters. J Lipid Res 1993;34:2147-2158.
9. Nonogaki K, Fuller GM, Fuentes NL, Moser AH, Staprans I, Grunfeld C, Feingold KR. Interleukin-6 stimulates hepatic triglyceride secretion in rats. Endocrinology 1995;136:2143-2149.
10. Memon RA, Grunfeld C, Moser AH, Feingold KR. Tumor necrosis factor mediates the effects of endotoxin on cholesterol and triglyceride metabolism in mice. Endocrinology 1993;132:2246-2253.
11. Yin MJ, Yamamoto Y, Gaynor RB. The anti-inflammatory agents aspirin and salicylate inhibit the activity of I(kappa)B kinase-beta. Nature 1998;396:77-80.
12. Kopp E, Ghosh S. Inhibition of NF-kappa B by sodium salicylate and aspirin. Science 1994;265:956-959.
13. Yuan M, Konstantopoulos N, Lee J, Hansen L, Li ZW, Karin M, Shoelson SE. Reversal of obesity- and diet-induced insulin resistance with salicylates or targeted disruption of Ikkbeta. Science 2001;293:1673-1677.

14. Hundal RS, Petersen KF, Mayerson AB, Randhawa PS, Inzucchi S, Shoelson SE, Shulman GI. Mechanism by which high-dose aspirin improves glucose metabolism in type 2 diabetes. J Clin Invest 2002;109:1321-1326.
15. Berbee JF, van der Hoogt CC, Sundararaman D, Havekes LM, Rensen PC. Severe hypertriglyceridemia in human APOC1 transgenic mice is caused by apoC-I-induced inhibition of LPL. J Lipid Res 2005;46:297-306.
16. Jong MC, Dahlmans VE, van Gorp PJ, van Dijk KW, Breuer ML, Hofker MH, Havekes LM. In the absence of the low density lipoprotein receptor, human apolipoprotein C1 overexpression in transgenic mice inhibits the hepatic uptake of very low density lipoproteins via a receptor-associated protein-sensitive pathway. J Clin Invest 1996;98:2259-2267.
17. Jong MC, van Ree JH, Dahlmans VE, Frants RR, Hofker MH, Havekes LM. Reduced very-low-density lipoprotein fractional catabolic rate in apolipoprotein C1-deficient mice. Biochem J 1997;321 (Pt 2):445-450.
18. Lee JI, Burckart GJ. Nuclear factor kappa B: important transcription factor and therapeutic target. J Clin Pharmacol 1998;38:981-993.
19. Li N, Karin M. Signaling pathways leading to nuclear factor-kappa B activation. Methods Enzymol 2000;319:273-279.
20. Zambon A, Hashimoto SI, Brunzell JD. Analysis of techniques to obtain plasma for measurement of levels of free fatty acids. J Lipid Res 1993;34:1021-1028.
21. Bligh EG, Dyer WJ. A rapid method of total lipid extraction and purification. Can J Biochem Physiol 1959;37:911-917.
22. Rensen PC, van Dijk MC, Havenaar EC, Bijsterbosch MK, Kruijt JK, van Berkel TJ. Selective liver targeting of antivirals by recombinant chylomicrons--a new therapeutic approach to hepatitis B. Nat Med 1995;1:221-225.
23. Rensen PC, Herijgers N, Netscher MH, Meskers SC, van Eck M, van Berkel TJ. Particle size determines the specificity of apolipoprotein E-containing triglyceride-rich emulsions for the LDL receptor versus hepatic remnant receptor in vivo. J Lipid Res 1997;38:1070-1084.
24. Jong MC, Rensen PC, Dahlmans VE, van der Boom H, van Berkel TJ, Havekes LM. Apolipoprotein C-III deficiency accelerates triglyceride hydrolysis by lipoprotein lipase in wild-type and apoE knockout mice. J Lipid Res 2001;42:1578-1585.
25. Redgrave TG, Roberts DC, West CE. Separation of plasma lipoproteins by density-gradient ultracentrifugation. Anal Biochem 1975;65:42-49.
26. Belfrage P, Vaughan M. Simple liquid-liquid partition system for isolation of labeled oleic acid from mixtures with glycerides. J Lipid Res 1969;10:341-344.
27. Feingold KR, Marshall M, Gulli R, Moser AH, Grunfeld C. Effect of endotoxin and cytokines on lipoprotein lipase activity in mice. Arterioscler Thromb 1994;14:1866-1872.
28. Desanctis JB, Varesio L, Radzioch D. Prostaglandins inhibit lipoprotein lipase gene expression in macrophages. Immunology 1994;81:605-610.
29. Sommariva D, Bonfiglioli D, Zanaboni L, Fasoli A. Effects of acetylsalicylic acid on plasma lipids and on post-heparin lipase activities. Int J Clin Pharmacol Ther Toxicol 1981;19:112-116.
30. Tsai J, Zhang R, Qiu W, Su Q, Naples M, Adeli K. Inflammatory NF-kappaB activation promotes hepatic apolipoprotein B100 secretion: evidence for a link between hepatic inflammation and lipoprotein production. Am J Physiol Gastrointest Liver Physiol 2009;296:G1287-G1298.
31. van Diepen JA, Wong MC, Guigas B, Bos J, Stienstra R, Hodson L, Shoelson SE, Berbee JF, Rensen PC, Romijn JA, Havekes LM, Voshol PJ. Hepatocyte-specific IKK-{beta} activation enhances VLDL-triglyceride production in APOE*3-Leiden mice. J Lipid Res 2011;52:942-950.
32. Wooles WR, Borzelleca JF, Branham Jr GW. Effect of acute and prolonged salicylate administration on liver and plasma triglyceride levels and diet-induced hypercholesterolemia. Toxicol Appl Pharmacol 1967;10:1-7.
33. Laurell S. Recycling of intravenously injected palmitic acid-1-C14 as esterified fatty acid in the plasma of rats and turnover rate of plasma triglycerides. Acta Physiol Scand 1959;47:218-232.
34. Glatz JF, Luiken JJ, Bonen A. Membrane fatty acid transporters as regulators of lipid metabolism: implications for metabolic disease. Physiol Rev 2010;90:367-417.

35. Stone DB, Brown JD, Steele AA. Effect of sodium salicylate on induced lipolysis in isolated fat cells of the rat. Metabolism 1969;18:620-624.
36. Schonhofer PS, Sohn J, Peters HD, Dinnendahl V. Effects of sodium salicylate and acetylsalicylic acid on the lipolytic system of fat cells. Biochem Pharmacol 1973;22:629-637.
37. Zu L, Jiang H, He J, Xu C, Pu S, Liu M, Xu G. Salicylate blocks lipolytic actions of tumor necrosis factor-alpha in primary rat adipocytes. Mol Pharmacol 2008;73:215-223.
38. Goldfine AB, Silver R, Aldhahi W, Cai D, Tatro E, Lee J, Shoelson SE. Use of salsalate to target inflammation in the treatment of insulin resistance and type 2 diabetes. Clin Transl Sci 2008;1:36-43.

4 META060 PROTECTS AGAINST DIET-INDUCED OBESITY AND INSULIN RESISTANCE IN A HIGH-FAT DIET FED MOUSE

Irene O.C.M. Vroegrijk, Janna A. van Diepen,
Sjoerd A.A. van den Berg, Johannes A. Romijn,
Louis M. Havekes, Ko Willems van Dijk, Gary Darland,
Veera Konda, Matthew L. Tripp, Jeffrey S. Bland, Peter J. Voshol

Nutrition 2013; 29 (1): 276-283

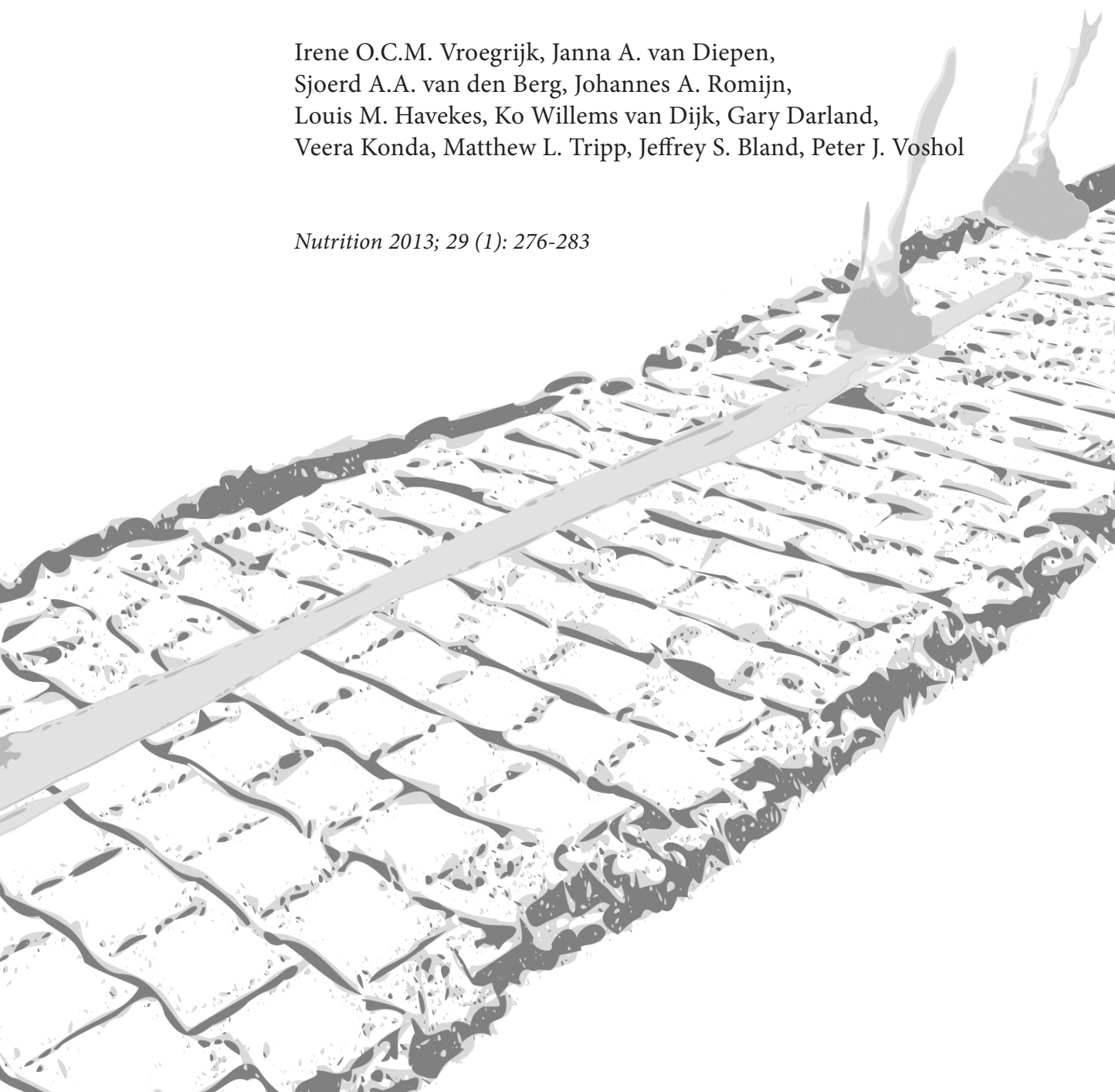

ABSTRACT

We investigated whether a reduced iso-alpha acid derived from an extract of *Humulus lupulus L.*, META060, had an effect on weight gain, body composition and metabolism in a high fat diet (HFD) fed mouse. Weight gain was monitored for up to twenty weeks in mice receiving either a low fat diet, a high fat diet, or a high fat diet supplemented with META060 or rosiglitazone. Body composition was determined using DEXA scan analysis. Indirect calorimetry measurements were performed to investigate energy balance in the mice, and oral glucose tolerance tests were administered to examine the effect of META060 on glycemic response. HFD-fed mice administered META060 for fourteen weeks had a significantly lower mean weight than that of HFD-fed mice (30.58 ± 0.5 g versus 37.88 ± 0.7 g; $P<0.05$). Indirect calorimetry measurements revealed increased metabolic flexibility in mice supplemented with META060. In addition, glucose tolerance was improved, comparable to the effects of rosiglitazone treatment. We conclude that META060 has potential therapeutic value for managing obesity and insulin resistance, and further research into the mechanism of action is warranted.

4.1 INTRODUCTION

Management of obesity has become a primary goal for healthcare practitioners in response to the rising epidemic of obesity related chronic diseases, including type 2 diabetes mellitus (T2DM) and cardiovascular disease. Pharmaceutical approaches that alter appetite, metabolism, or fat absorption include antidepressants, CNS stimulants, or peripherally acting antiobesity drugs, and all have been associated with adverse effects (reviewed in [1]). Many people seek natural therapies as an alternative to pharmaceuticals for weight management. Yerba mate, yohimbe, aloe, pyruvate, St. John's Wort, dandelion, and herbal diuretics have been used for weight loss, although significant clinical studies supporting their efficacy are lacking (reviewed in [2]).

Iso-alpha acids derived from the hop plant (*Humulus lupulus L.*) reduced plasma triglyceride and free fatty acid levels in mice [3, 4]. C57BL/6N mice fed a high fat diet (HFD) exhibited improved glucose tolerance after 14 days and reduced insulin resistance after 10 days of administration of iso-alpha acids. Furthermore, in a double-blind, placebo-controlled pilot study, diabetic subjects receiving iso-alpha acids for 8 weeks had an average 10.1% reduction in blood glucose levels and 6.4% reduction in glycated hemoglobin levels [4].

Iso-alpha acids are not particularly stable compounds, although the reduced derivatives have been found to exhibit greater stability [5]. Furthermore, reduced iso-alpha acids have recently demonstrated greater bioavailability than iso-alpha acids in humans [6].

Previous work in our lab to screen various botanical extracts for lipogenic activity resulted in the identification of a family of reduced iso-alpha acids [7]. One of the reduced iso-alpha acids, META060, has demonstrated anti-inflammatory activity *in vitro*, mediated by inhibition of NF-κB pathways [8, 9]. Several reports have suggested a link between obesity-induced inflammation and related metabolic disorders such as insulin resistance (reviewed in [10, 11]). Objectives of the current study were to determine the effects of META060 compared with rosiglitazone, a commonly used drug in the treatment of T2DM, on body weight, energy metabolism, glucose tolerance and insulin sensitivity in HFD-induced obese mice.

4.2 MATERIALS AND METHODS

Animals and diet intervention

Wild-type (WT) C57Bl/6J male mice were purchased from Charles River (Maastricht, The Netherlands). Mice were housed under standard conditions with access to water and food ad libitum. For the 14-week diet intervention, the study was started when the animals were 19 weeks of age. Mice were fed either a low fat diet (LFD) (10% energy derived from lard fat; D12450, Research Diet Services, Wijk bij Duurstede, The Netherlands), with a caloric content of 3.85 kcal/g, a high fat diet (HFD) (45% energy derived from lard fat; D12451,

Research Diet Services, Wijk bij Duurstede, The Netherlands), with a caloric content of 4.73 kcal/g, or a HFD supplemented with META060 (100 mg/kg/day) or rosiglitazone (1 mg/kg/day) (SmithKline Beecham Farma, Rijswijk, The Netherlands). META060 was supplied by Hopsteiner, and standards were purchased from ASBC. The chemical composition of META060 has been described previously [12]. META060 or Rosiglitazone were added to self-made HFD. Briefly, rosiglitazone tablets (Avandia® = rosiglitazone maleate, SmithKline Beecham Farma, Rijswijk, The Netherlands) or META060 powder were crushed in a mortar with a pestle. Subsequently, the powder was mixed with the 45% lard HFD powder diet from Research Diets Service (45% energy derived from lard fat; D12451, Research Diet Services, Wijk bij Duurstede, The Netherlands). For HFD + META060, 1.875 g of META060 per kg of HFD powder was used. For rosiglitazone, 12 mg powder was added to 1 kg of HFD powder. Pellets were made by adding 2% agar (Sigma), and were then freeze-dried to remove water and stored at -20°C. A fixed dosage was used throughout the diet intervention. Based on previously assessed food intake data we know that C57Bl/J6 mice on a HFD+META060 diet (D12451, Research Diet Services diet) eat ~2.5 g of diet per day. Each treatment group in the 14-week intervention included 12 mice, and mice were weighed weekly. Food intake was monitored weekly by weighing the food in the cages manually. After 14 weeks, animals in the LFD or HFD plus rosiglitazone groups were sacrificed, following 4 hours of fasting. Mice from the HFD group were randomly divided into 2 groups: six were shifted to HFD plus META060 (100 mg/kg/day), and the remaining six mice continued receiving a HFD for six weeks. Likewise, mice supplemented with HFD plus META060 were divided into 2 groups: six were shifted to HFD, and the remaining six mice continued receiving HFD plus META060.

For the 5-week diet intervention, 12-week-old mice were fed a HFD, a HFD supplemented with META060 (100 mg/kg/day), or a HFD supplemented with rosiglitazone (1 mg/kg/day). Each dietary group consisted of 9 animals. Body weight was measured weekly during the diet intervention. All experiments were approved by the animal ethics committee of Leiden University Medical Center.

DEXA Scan

Animals were subjected to DEXA scan analysis after 4 hours of fast. Animals were weighed and sedated by a single intraperitoneal injection of a mixture of acepromazine (6.25 mg/kg Neurotranq, Alfasan International BV, Weesp, The Netherlands), midazolam (6.25 mg/kg Dormicum, Roche Diagnostics, Mijdrecht, The Netherlands), and fentanyl (0.31 mg/kg Janssen Pharmaceuticals, Tilburg, The Netherlands). Sedated animals were scanned in toto using a small animal DEXA scanner (pDEXA, Norland Stratec Medizintechinik GmbH, Birkenfeld, Germany) and data were analyzed by the software supplied by the manufacturer. Fat mass and lean body mass were determined.

Indirect calorimetry

Groups of 8 mice were subjected to individual indirect calorimetry measurements for a period of 4 consecutive days using a Comprehensive Laboratory Animal Monitoring

System (Columbus Instruments, Columbus Ohio, US). Cages were made of clear plexiglass (30 x 10 x 9 cm (l x b x h)). Prior to the start of the experiment, animals were acclimated to the cages and the single housing for a period of 24 h. Experimental analysis started at 09:00 h and continued for 36 hours. In the next 36 hours of monitoring, animals were fasted overnight, and then food was replaced to assess metabolic flexibility. Analyzed parameters included real time food and water intake, as well as meal size, frequency and duration. Oxygen consumption (VO2) and carbon dioxide production rates (VCO2) were measured at intervals of 7 minutes. Respiratory exchange ratio (RER) as a measure for metabolic substrate choice was calculated as the ratio between VCO_2 and VO_2. Carbohydrate (CHO) and fat (FA) oxidation rates were calculated using the following formulas [13]:

CHO = ((4.585 * VCO2) – (3.226 * VO2)) * 4 / 1000

FA = ((1.695 * VO2) – (1.701 * VCO2)) * 9 /1000

Total energy expenditure was calculated from the sum of CHO and FA oxidation. Activity was monitored as 2-dimensional infrared beam breaks.

Fecal fatty acid composition and concentration

Feces were collected over 4 days during week 4 of the 5-week diet intervention. Feces were weighed, freeze-dried, and ground, and fecal fatty acids (FA) were subsequently derivatized by methyl esterification. Therefore, 2 mL methanol/hexane (4:1 v/v) containing 80 µg pentadecanoic acid (C15:0) as an internal standard (Fluka) was added to 15 mg feces. Then, 200 µL acetyl chloride (Merck) was added, and samples were incubated at 95°C. After subsequent cooling to 4°C, 5 mL 6% K2CO3 (Sigma) was added and samples were centrifuged (10 min, 4000 rpm, 4°C). The upper hexane layer was isolated and used for GC analysis of FA methyl esters (FAME). FAME were separated on a 50 m x 0.25 mm capillary GC column (CP Sil 88, Agilent technologies) in a 3800 GC gas chromatograph (Varian) equipped with a flame ionization detector. The injector and flame ionization detector were kept at 270°C. The column temperature was programmed from 170°C to 210°C. FAME were introduced by split injection (split ratio 20:1). Quantification was based on the area ratio of the individual FA to the internal standard.

Oral glucose tolerance test

Glucose and insulin levels were determined after overnight fasting during week 5 of the 5-week diet intervention, and also after 14 weeks of the 14-week diet intervention. Blood was obtained via tail bleeding, and glucose and insulin concentrations were determined. Subsequently, mice received an intragastric load of D-glucose (2 g/kg) provided as a 20% solution in PBS. Additional blood samples (30 µl) were collected via tail bleeding at 5, 15, 30, 60, 90 and 120 min after glucose loading for measurement of plasma insulin and glucose concentrations. Glucose concentration was determined with a glucose analyzer (Accu-

Check, Sensor Comfort, Roche Diagnostics GmbH, Germany) and insulin concentration was determined by immunoassay (Chrystal Chem Inc).

Statistical Analysis

Data are presented as means ± SE. Statistical differences were calculated using the unpaired *t*-test (SPSS 17, SPSS Inc, Chicago, IL) or 2-way Analysis of Variance with Bonferroni posttest (GraphPad Prism, San Diego, CA). A P-value <0.05 was regarded as statistically significant.

4.3 RESULTS

Supplementation with META060 for 14 weeks prevents HFD-induced obesity

To determine the effect of META060 on high fat diet (HFD)-induced obesity, mice were fed a low fat diet (LFD), a HFD, or a HFD supplemented with either 100 mg/kg/day META060 or 1 mg/kg/day rosiglitazone for 14 weeks. Previous studies in a mouse model of collagen-induced arthritis demonstrated an effect of META060 with 50 mg/kg/day for reducing cartilage degradation and bone erosion, and doses up to 250 mg/kg/day were well tolerated [8]. Therefore, a dose of 100 mg/kg/day was selected for the current study investigating the effect of META060 on body weight and metabolism in HFD fed mice. Rosiglitazone is an antidiabetic agent from the thiazolidinedione class of drugs. Its mechanism of action is well-known, involving activation of PPARγ, and studies in HFD fed mice demonstrated reduction of insulin levels with a dose of 1 mg/kg/day rosiglitazone [14]. Mice receiving HFD supplemented with META060 maintained similar body weights to those on a LFD over 14 weeks , and were significantly lower in weight than HFD-fed mice at week 3 and every subsequent time point up to week 14 (Fig. 1A). After 14 weeks, META060 supplemented mice weighed 19% less than HFD-fed control mice (30.58 ± 0.5 g versus 37.88 ± 0.7 g; P<0.05), and were comparable in weight to mice fed a LFD for 14 weeks (29.71 ± 0.7 g). Mice supplemented with rosiglitazone did not gain as much weight as those without supplementation, although they gained significantly more weight than HFD plus META060 or LFD fed mice (Fig. 1A). During the 14 week diet intervention no differences in food intake were observed.

To determine whether reduced weight gain in META060 supplemented mice reflected lower fat accumulation compared with HFD-only fed mice, body composition of these mice was determined by DEXA scan analysis. Total body fat of mice supplemented with META060 was significantly lower than that of HFD-fed mice (3.29 ± 1.0 g versus 12.12 ± 1.1 g; P<0.001) (Fig. 1B). At the end of the experiment, organs were dissected and weighed. META060 supplementation reduced gonadal (1.17 ± 0.2 g versus 2.40 ± 0.09 g; P<0.001) and subcutaneous (0.47 ± 0.09 g versus 1.53 ± 0.2 g; P<0.001) white adipose tissue (WAT) mass in HFD-fed mice compared to no-supplement controls (Fig. 1C).

At 15 weeks, half of the mice in the HFD group were shifted to HFD plus META060, and half of the mice in the HFD plus META060 group were shifted to HFD only. Body weight

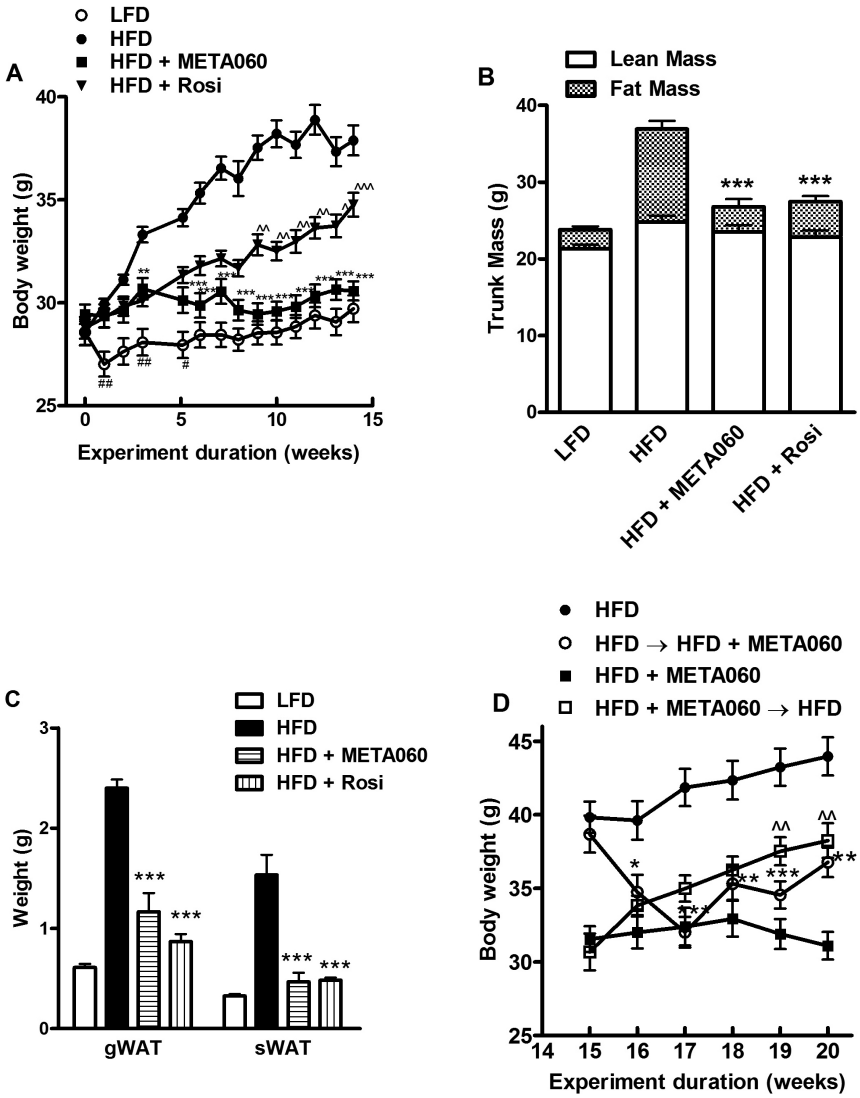

Figure 1. META060 prevents high fat diet (HFD)-induced obesity. Mice were fed a low-fat diet (LFD), a HFD, or a HFD supplemented with either 100 mg/kg/day META060 or 1 mg/kg/day rosiglitazone (Rosi) for 14 weeks. Mouse body weights were recorded every week (n = 12 per group);**P<0.01, ***P<0.001 HFD vs. HFD + META060, ^P<0.05, ^^P<0.01, ^^^P<0.001 HFD + META060 vs. HFD + Rosi, #P<0.05, ##P<0.01 HFD + META060 vs. LFD (A). After a 4 h fast, lean body mass and fat mass were determined by DEXA scan (n = 6 per group for HFD and META060 and n=12 per group for Rosi); ***P<0.001 HFD vs. HFD + META060 and HFD vs HFD + Rosi (B). After mice were sacrificed, mass of gonadal White Adipose Tissue (gWAT) and subcutaneous WAT (sWAT) was determined (n=6 per group for HFD and META060 and n=12 per group for Rosi); ***P<0.001 HFD vs. HFD + META060 and HFD vs HFD + Rosi (C). At 14 weeks, half of the mice in the HFD group were shifted to HFD + META060, and half of the mice in the HFD + META060 group were shifted to HFD only. Body weights were recorded weekly (n=6 per group); *P<0.05, **P<0.01, ***P<0.001 HFD vs. HFD → HFD + META060, ^^P<0.01 HFD + META060 vs. HFD + META060 → HFD (D). Data are presented as mean ± SE.

was monitored weekly for 5 weeks in these 4 treatment groups. While animals maintained on HFD for the entirety of the experiment continued to gain weight, those shifted to HFD plus META060 lost a significant amount of weight during weeks 16 and 17, after which they began to gain weight again (Fig. 1D). A concomitant reduction in food intake was observed in the first two weeks after switching diets, followed by a rebound to even greater levels than food intake in the HFD plus META060 group that did not switch diets (data not shown), perhaps a reflection of adjustment to palatability differences between the distinct diets.

META060 increases RER and metabolic flexibility in mice fed a HFD

To investigate how META060 protects against HFD-induced obesity, an independent, 5-week study was initiated with three treatment groups: HFD; HFD supplemented with META060 (100 mg/kg/d); or HFD supplemented with rosiglitazone (1 mg/kg/d). In the first five weeks of the 14-weeks intervention study, average weight gained in the HFD group was 5.61 ± 0.7 g, while mice supplemented with META060 gained 0.68 ± 0.3 g. In the 5-weeks study, average weight gained in the HFD group was 2.58 ± 0.4 g, and mice supplemented with META060 gained 0.54 ± 0.9 g. (Fig. 2). Despite differences in absolute weight gained, which was likely due to the difference in age of mice at the start of each study, META060 supplementation reproducibly reduced relative HFD-induced body weight gain in both experiments.

Whole body substrate utilization was examined for approximately 36 h during week 4 of the diet intervention. Four weeks of diet intervention was chosen because at this time point in the 14-week study, body weight was still increasing and a new set point had not yet been reached.

Although we did not directly compare a LFD group during the 5-week study, we know from published and experimental data that 5 weeks of HFD feeding in mice results in an

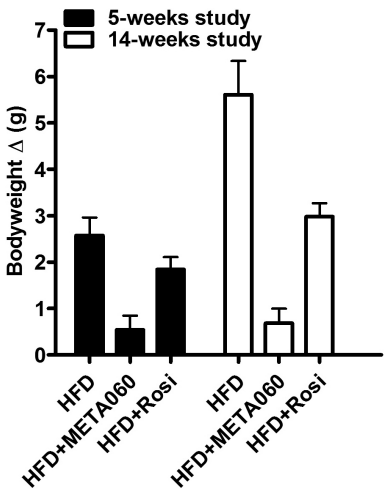

Figure 2. Comparison of 5-weeks' bodyweight increase in 5-weeks and 14-weeks studies. Mice were fed a high fat diet (HFD), HFD supplemented with META060, or HFD supplemented with rosiglitazone (Rosi) in two independent studies of varying durations, 5 weeks or 14 weeks. In both studies, mice were weighed at 5 weeks. Mean body weight difference from baseline is represented for each group ± SE (N=9-12 per group).

unaltered total energy expenditure (EE) (kcal/h), but changes respiratory exchange rate (RER) and fat (FA) and CHO oxidation. Daytime RER was 0.84±0.04 versus 0.94±0.04, and night time RER was 0.84±0.03 versus 0.93±0.04, for HFD versus LFD, respectively ($p<0.05$). Daytime FA oxidation was 0.17±0.05 versus 0.07±0.04, and night time FA-oxidation was 0.19±0.05 versus 0.08±0.06, for HFD versus LFD, respectively ($p<0.05$). META060 or Rosi intervention started from Day 0, when the animals were switched from chow to HFD as described in Materials and Methods.

Nocturnal and diurnal data were analyzed separately to distinguish between periods of low (diurnal) and high (nocturnal) physical activity. Total EE was similar across all dietary intervention groups (Fig. 3A). For food intake (FI), no significant differences were observed between the groups (data not shown). Despite similarities in total EE and FI, HFD-fed mice supplemented with META060 or rosiglitazone exhibited a significantly lower mean nocturnal FA oxidation rate than HFD only (0.16 ± 0.01 kcal/h and 0.18 ± 0.01 kcal/h versus 0.22 ± 0.01 kcal/h; $P<0.001$, $P<0.01$, respectively), and rosiglitazone had a lower mean diurnal FA oxidation rate compared to that of control (0.12 ± 0.01 kcal/h versus 0.15 ± 0.01; kcal/h $P<0.05$) (Fig. 3B). In addition, nocturnal CHO oxidation levels were increased in HFD fed mice that received META060 or rosiglitazone, compared with controls (0.36 ± 0.02 kcal/h and 0.35 ± 0.01 kcal/h versus 0.31 ± 0.01 kcal/h; $P<0.01$) (Fig. 3C). This increased carbohydrate-to-fat oxidation ratio was reflected in the RER. META060 and rosiglitazone both significantly increased RER in HFD-fed mice during the diurnal period compared to HFD-only fed mice (0.88 ± 0.00 and 0.89 ± 0.01 versus 0.86 ± 0.01; $P<0.05$, $P<0,01$ respectively), and also during the nocturnal period (0.87 ± 0.01 and 0.86 ± 0.00 versus 0.83 ± 0.01; $P<0.001$, respectively) (Fig. 4A-B). To test the ability of the animals to adjust fuel oxidation to fuel availability (metabolic flexibility), animals were fasted overnight; subsequently, the food was replaced and RER was monitored. META060 and rosiglitazone supplemented mice had a significantly higher RER when the food was replaced compared to HFD-only treated mice (0.94 ± 0.00 and 0.94 ± 0.00 versus 0.92 ± 0.00; $P<0.001$), indicating greater metabolic flexibility in META060 or rosiglitazone fed animals (Fig. 4C). Physical activity measurements did not show differences in either treatment group compared with HFD-only fed mice (data not shown).

META060 has no effect on fecal fatty acid composition and concentration

Since META060 reduced fat oxidation, we investigated whether fat absorption was impaired in META060 supplemented mice. Fecal fatty acid composition and concentration were determined in samples collected during metabolic cage experiments (data not shown). No difference was found in total fecal weight. Furthermore, quantitative gas chromatography analysis revealed equal fecal fatty acid composition and fecal fatty acid content in all treatment groups. Together with the equivalent food intake, this implies similar intestinal absorption of lipids.

META060 improves glucose tolerance in HFD fed mice

Since increased carbohydrate-to-fat oxidation ratio and increased metabolic flexibility suggest protection against HFD-induced insulin resistance, oral glucose tolerance tests

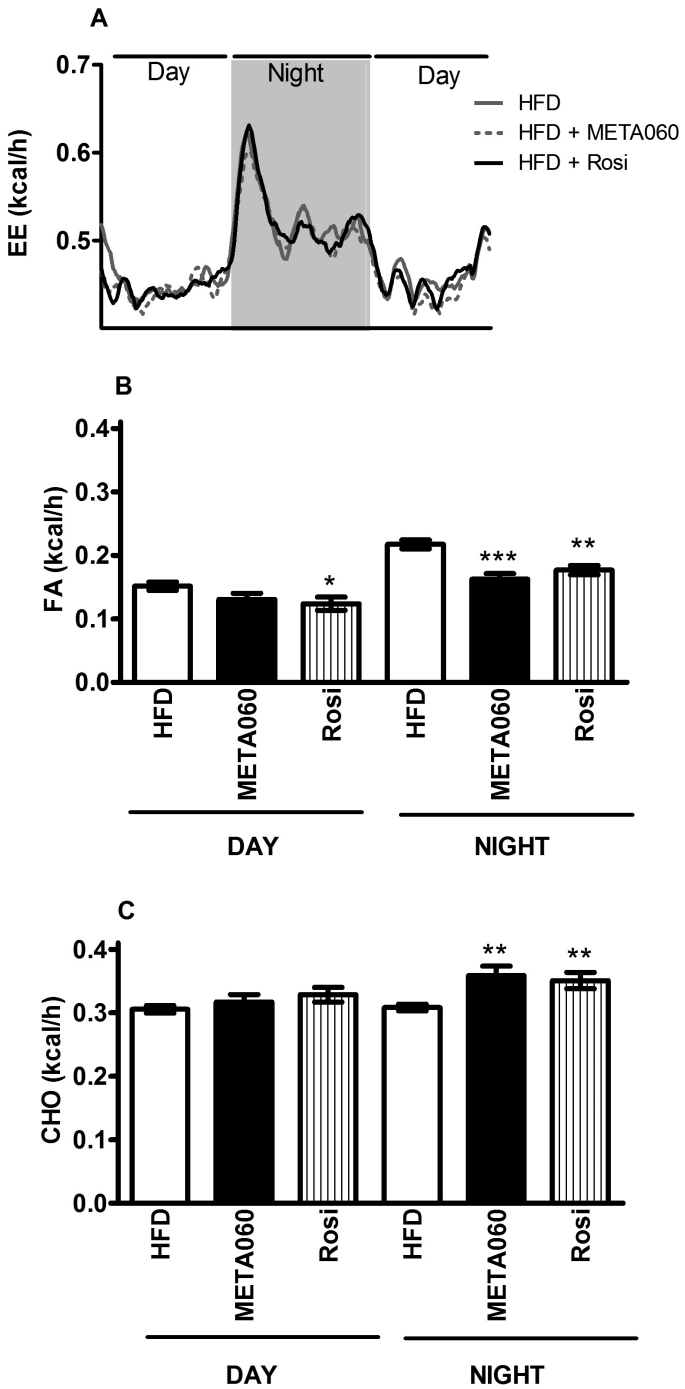

Figure 3. META060 affects substrate utilization. During week 4 of the diet intervention, O_2 consumption and CO_2 production were recorded for 36 h in HFD fed mice without supplementation or supplemented with 100 mg/kg/d META060 or 1 mg/kg/d rosiglitazone (Rosi). The night period is represented by the shaded area on the graph. EE was calculated as described in Methods (A). Fatty acid (FA) (B) and carbohydrate oxidation (CHO) (C) for day phase or night phase were calculated for HFD fed mice without supplementation or in those supplemented with META060 or Rosi. Data are presented as mean ± SE (n=8 per group);*P<0.05, **P<0.01, ***P<0.001.

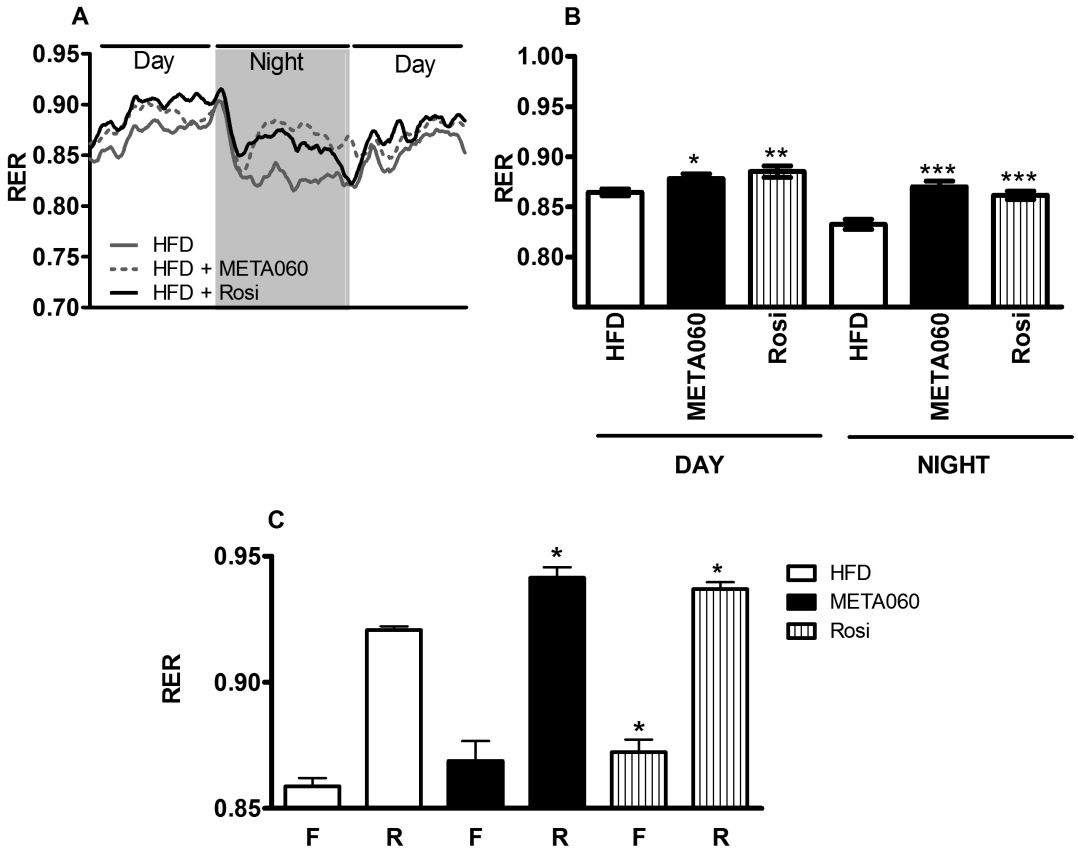

Figure 4. META060 increases respiratory exchange rate (RER) and metabolic flexibility. RER was monitored for 36 h in HFD fed mice without supplementation or supplemented with 100 mg/kg/d META060 or 1 mg/kg/d rosiglitazone (Rosi) (A). RER for day phase or night phase was calculated for each treatment group (n=8 per group); *P<0.05, **P<0.01, ***P<0.001 (B). HFD fed mice with or without supplementation with META060 or Rosi for 4 weeks were fasted overnight and then feeding was resumed. RER was calculated after fasting (F) and after refeeding (R) (n=8 per group; *P<.05) (C). Data are presented as mean ± SE.

(OGTT) were performed during week 5 of the diet intervention. After an overnight fast, blood glucose concentration was lower in META060 supplemented mice compared to that of HFD-only treated mice (4.66 ± 0.2 versus 5.34 ± 0.3; P<0.05) (Fig. 5A), while fasting insulin levels were not significantly different among treatment groups (Fig. 5D). Following glucose challenge, plasma glucose and insulin levels were determined at time intervals up to 120 min, and areas under the curve (AUC) were calculated. Glucose concentrations were significantly decreased for mice supplemented with META060 compared to HFD-fed mice at 15 min, 30 min, 90 min, and 120 min after glucose challenge, and mean AUC was 20% lower than in HFD-fed mice (P<0.05) (Fig. 5B-C). Rosiglitazone also significantly decreased plasma glucose levels at 5, 30, 60, and 90 min after glucose challenge, and mean AUC was 15% lower than in HFD-fed mice (P<0.05). These observations demonstrate that META060 and rosiglitazone improved glucose tolerance in mice fed a HFD for 5 weeks.

This may be due to increased insulin sensitivity in response to an oral glucose load, since time course and AUC for plasma insulin levels were comparable in all groups (Fig. 5E-F).

After 14 weeks of diet-intervention, fasting blood glucose concentration in META060 supplemented mice was significantly lower than that of HFD fed mice (4.5 ± 0.3 mM versus 5.9 ± 0.3 mM; $P<0.05$) (Fig. 6A). Moreover, fasting insulin concentration was also significantly reduced in META060-supplemented mice compared to that of HFD-fed mice (0.14 ± 0.05 ng/mL versus 0.42 ± 0.09 ng/mL; $P<0.001$) (Fig. 6C). This implies that after long-term META060 supplementation, insulin sensitivity in HFD-fed mice was increased. OGTT were performed on mice and blood glucose and insulin concentrations were recorded at several time points up to 120 min post-challenge. Area under the curve (AUC) for glucose was similar among all groups (Fig. 6B). However, AUC for insulin was increased in the HFD group, and only rosiglitazone supplementation had a statistically significant effect on reducing the insulin response compared to HFD (40%; $P<0.05$) (Fig. 6D).

4.4 DISCUSSION

In the current study we investigated the effects of META060 on HFD-induced obesity and insulin resistance. Supplementation with META060 reduced weight gain in HFD fed mice. This effect was significant after 3 weeks, and was sustained for up to 20 weeks. Furthermore, when META060 feeding was terminated, mice began to gain weight rapidly. META060 inhibited fat accumulation in HFD fed mice as evidenced by a reduction in adipose tissue mass in mice supplemented with META060 compared with HFD fed control mice. In addition, META060 improved glucose tolerance after 5 weeks of supplementation. Moreover, long-term META060 supplementation in HFD-fed mice clearly reduced fasting blood glucose and insulin levels. These data suggest that META060 improves glucose homeostasis similarly to rosiglitazone and prevents HFD-induced obesity and insulin resistance.

Rosiglitazone, an antidiabetic drug from the class of thiazolidinediones, increases insulin sensitivity through its action on peroxisome proliferator activated receptor gamma (PPARγ), and also has demonstrated anti-inflammatory activity through a mechanism involving nuclear factor kappa-B (NF-κB) [15,16]. While the mechanistic target(s) of META060 has not been identified, previous studies indicate that META060 has potent inhibitory effects on several kinases regulating the NF-κB pathway, including glycogen synthase kinase 3 (GSK-3) and phosphatidyl inositol-3 kinase (PI3K) [12]. In this study, META060 demonstrated effects on insulin sensitivity similar to that of rosiglitazone, prompting us to speculate whether improvement of glucose tolerance in META060 treated mice is mediated through a PPARγ dependent mechanism. However, rosiglitazone was not as effective at preventing weight gain in HFD fed mice as was META060, suggesting an alternative or additional mechanism of action for META060.

Results from metabolic experiments indicated that supplementation with META060 increased RER, metabolic flexibility, and carbohydrate-to-fat oxidation ratio in HFD fed mice.

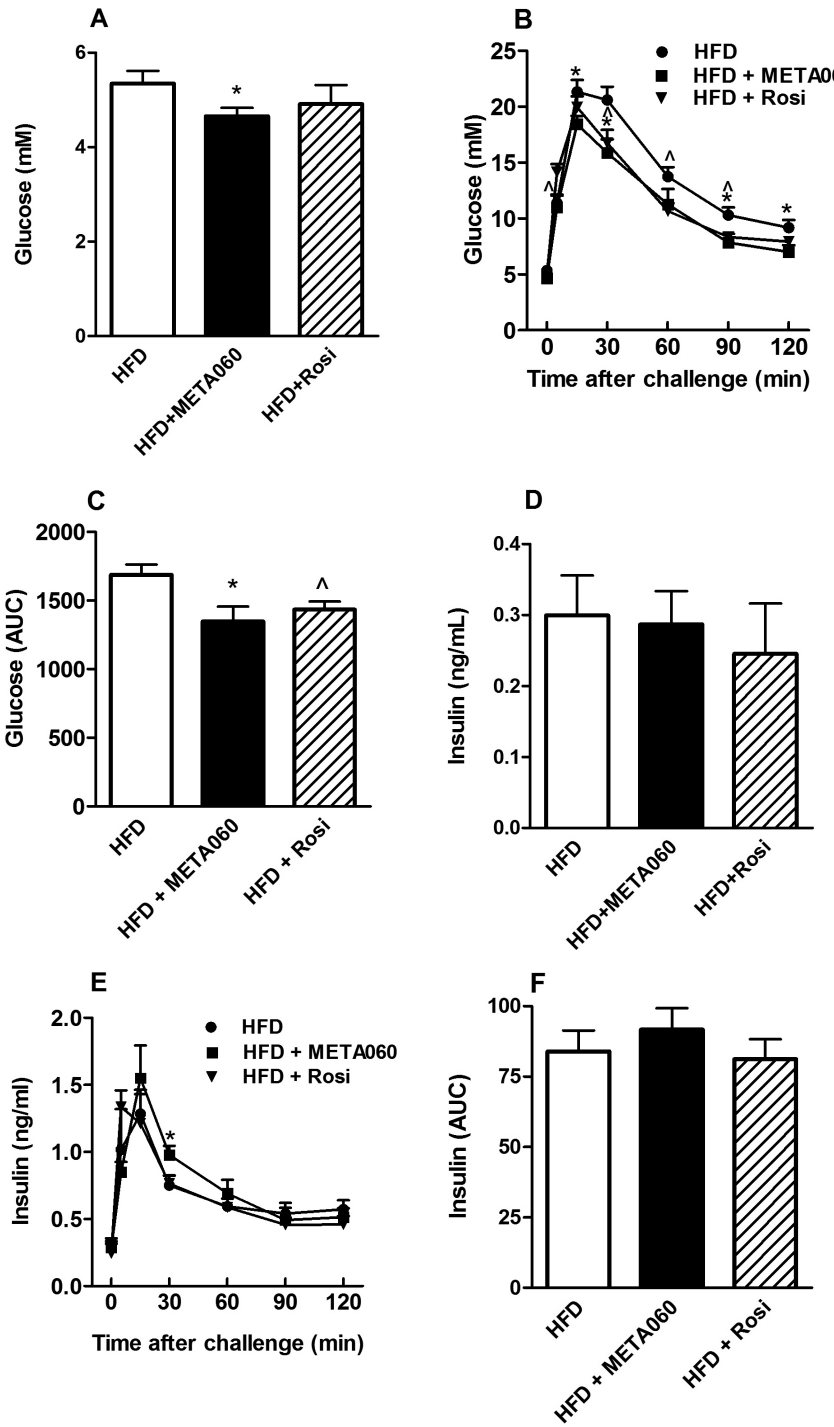

Figure 5. META060 improves glucose tolerance. Mice were fed a HFD or a HFD supplemented with 100 mg/kg/day META060 or 1 mg/kg/day rosiglitazone (Rosi). During week 5 of the diet intervention and after overnight fast, blood samples were collected, and glucose (A) and insulin (D) concentrations were determined. Oral glucose tolerance tests (OGTTs) were performed on fasted mice. Glucose (B) and insulin (E) concentrations were recorded at time points up to 120 min and areas under the curve (AUC) for glucose (C) and insulin (F) were calculated. Values are mean ± SE (n=7-9 per group). *P<0.05 HFD vs. HFD + META060, ^P<0.05 HFD vs. HFD + Rosi. 1

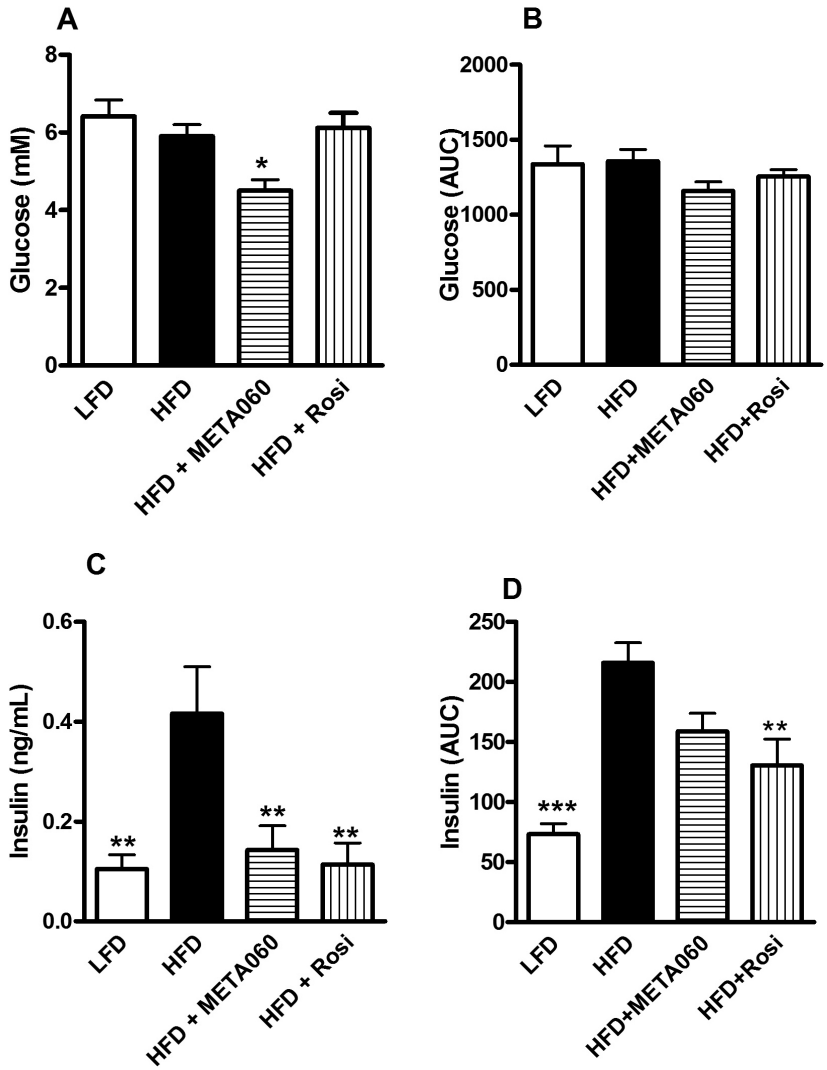

Figure 6. Long-term META060 supplementation reduces plasma glucose and insulin concentrations. Fasting plasma glucose (A) and fasting insulin concentrations (C) were determined in mice fed a LFD, a HFD, or a HFD supplemented with 100 mg/kg/day META060 for 14 weeks as described in Methods. OGTT was performed on fasted mice, and blood concentrations of glucose and insulin were determined at time points up to 120 min. Area under the curve (AUC) is presented for glucose (B) and insulin (D). Values are presented as mean ± SE (n= 5-6 per group). *P<0.05, **P<0.01, ***P<0.001.

These observations are congruent with increased insulin sensitivity and improved carbohydrate handling induced by META060. Differences in metabolism and weight may also be observed if fat intake or absorption was not consistent between treatment groups. However, the metabolic experiments also indicated that META060 did not affect total energy expenditure, food intake, nor fatty acid secretion into the feces, and thus, do not explain the reduction in weight gain of META060 supplemented mice. Therefore, metabolic measurements may not be sufficient to resolve a mechanism for global effects of META060 on mouse metabolism.

Mice used in the 5-week study were slightly younger than those in the longer term experiment, and age may have a potential impact on physical activity, food intake, energy expenditure, or other metabolic processes. While it is possible that mice of different ages may have distinct metabolic characteristics contributing to the results we observed, the effects of META060 on weight gain and glucose homeostasis were consistent in both the short term and long term experiments.

Results from *in vitro* studies in a human cecal cell line demonstrated that META060 increases GLP-1 secretion (data not shown). Since GLP-1 is an insulin sensitizing hormone, this *in vitro* effect of META060 is consistent with *in vivo* effects on glucose homeostasis. Activation of GPR120, a G protein-coupled receptor that regulates GLP-1 secretion [17-19], may function as a mechanistic target for META060 dependent GLP-1 secretion, although further studies will be required to investigate this possibility.

Future studies will focus on elucidating the mechanism of action underlying the effects of META060 on preventing weight gain in HFD fed mice and investigating whether META060 is effective in reducing weight in obese animals. META060 reduces fasting plasma glucose and insulin concentrations, and further research into its activity on insulin signaling and hepatocyte metabolism is needed. Data presented here suggest that META060 may have therapeutic value as an antidiabetic or antiobesity agent, and future investigations will evaluate its potential clinical use.

META060 supplementation significantly reduced the amount of weight gained in mice on a HFD. Indirect calorimetry measurements revealed increased metabolic flexibility in mice, and mice demonstrated improved glucose tolerance, comparable to the effects of rosiglitazone treatment. We conclude that META060 has potential therapeutic value for managing obesity and insulin resistance.

ACKNOWLEDGEMENTS

This work was supported by grants from the Netherlands Organization for Scientific Research (NWO Zon-MW; 917.76.301 to P.J.V.) and the Dutch Diabetes Research Foundation (2005.01.003 to P.J.V.). This work was also supported by the seventh framework program of the EU-funded "LipidomicNet" (proposal number 202272). We would like to thank A.C.M. Pronk and J. Bos for excellent technical assistance and Dr. Ingrid Fricks for assistance with manuscript preparation.

REFERENCES

1. Kaplan LM. Pharmacologic therapies for obesity. Gastroenterol Clin North Am 2010;39:69-79.
2. Pittler MH, Schmidt K, Ernst E. Adverse events of herbal food supplements for body weight reduction: systematic review. Obes Rev 2005;6:93-111.
3. Shimura M, Hasumi A, Minato T, Hosono M, Miura Y, Mizutani S, Kondo K, Oikawa S, Yoshida A. Isohumulones modulate blood lipid status through the activation of PPAR alpha. Biochim Biophys Acta 2005;1736:51-60.
4. Yajima H, Ikeshima E, Shiraki M, Kanaya T, Fujiwara D, Odai H, Tsuboyama-Kasaoka N,

Ezaki O, Oikawa S, Kondo K. Isohumulones, bitter acids derived from hops, activate both peroxisome proliferator-activated receptor alpha and gamma and reduce insulin resistance. J Biol Chem 2004;279:33456-33462.

5. Intelmann D, Hofmann T. On the autoxidation of bitter-tasting iso-alpha-acids in beer. J Agric Food Chem 2010;58:5059-5067.
6. Cattoor K, Remon JP, Boussery K, Van BJ, Bracke M, De KD, Deforce D, Heyerick A. Bioavailability of hop-derived iso-alpha-acids and reduced derivatives. Food Funct 2011;2:412-422.
7. Babish JG, Pacioretty LM, Bland JS, Minich DM, Hu J, Tripp ML. Antidiabetic screening of commercial botanical products in 3T3-L1 adipocytes and db/db mice. J Med Food 2010;13:535-547.
8. Konda VR, Desai A, Darland G, Bland JS, Tripp ML. META060 inhibits osteoclastogenesis and matrix metalloproteinases in vitro and reduces bone and cartilage degradation in a mouse model of rheumatoid arthritis. Arthritis Rheum 2010;62:1683-1692.
9. Tripp M, Darland G, Lerman R, Lukaczer D, Bland J, Babish, J. Hop and modified hop extracts have potent in vitro anti-inflammatory properties. In: K.E.Hummer JAH, ed. Acta Horticulturae (ISHS). 668 ed. Corvallis (Oregon): 2005:217-228.
10. Hummasti S, Hotamisligil GS. Endoplasmic reticulum stress and inflammation in obesity and diabetes. Circ Res 2010;107:579-591.
11. Olefsky JM, Glass CK. Macrophages, inflammation, and insulin resistance. Annu Rev Physiol 2010;72:219-246.
12. Desai A, Konda VR, Darland G, Austin M, Prabhu KS, Bland JS, Carroll BJ, Tripp ML. META060 inhibits multiple kinases in the NF-kappaB pathway and suppresses LPS--mediated inflammation in vitro and ex vivo. Inflamm Res 2009;58:229-234.
13. Peronnet F, Massicotte D. Table of nonprotein respiratory quotient: an update. Can J Sport Sci 1991;16:23-29.
14. Rong JX, Qiu Y, Hansen MK, Zhu L, Zhang V, Xie M, Okamoto Y, Mattie MD, Higashiyama H, Asano S, Strum JC, Ryan TE. Adipose mitochondrial biogenesis is suppressed in db/db and high-fat diet-fed mice and improved by rosiglitazone. Diabetes 2007;56:1751-1760.
15. Lehmann JM, Lenhard JM, Oliver BB, Ringold GM, Kliewer SA. Peroxisome proliferator-activated receptors alpha and gamma are activated by indomethacin and other non-steroidal anti-inflammatory drugs. J Biol Chem 1997;272:3406-3410.
16. Su CG, Wen X, Bailey ST, Jiang W, Rangwala SM, Keilbaugh SA, Flanigan A, Murthy S, Lazar MA, Wu GD. A novel therapy for colitis utilizing PPAR-gamma ligands to inhibit the epithelial inflammatory response. J Clin Invest 1999;104:383-389.
17. Hirasawa A, Tsumaya K, Awaji T, Katsuma S, Adachi T, Yamada M, Sugimoto Y, Miyazaki S, Tsujimoto G. Free fatty acids regulate gut incretin glucagon-like peptide-1 secretion through GPR120. Nat Med 2005;11:90-94.
18. Oh DY, Talukdar S, Bae EJ, Imamura T, Morinaga H, Fan W, Li P, Lu WJ, Watkins SM, Olefsky JM. GPR120 is an omega-3 fatty acid receptor mediating potent anti-inflammatory and insulin-sensitizing effects. Cell 2010;142:687-698.
19. Talukdar S, Olefsky JM, Osborn O. Targeting GPR120 and other fatty acid-sensing GPCRs ameliorates insulin resistance and inflammatory diseases. Trends Pharmacol Sci 2011;32:543-550.

5 FCR γ-CHAIN$^{-/-}$ MICE ARE PROTECTED AGAINST DIET-INDUCED OBESITY AND INSULIN RESISTANCE

Irene O.C.M. Vroegrijk, Sjoerd A.A. van den Berg,
Jan Bert van Klinken, Louis M. Havekes, Sjef J. Verbeek,
Ko Willems van Dijk, Vanessa van Harmelen.

In preparation

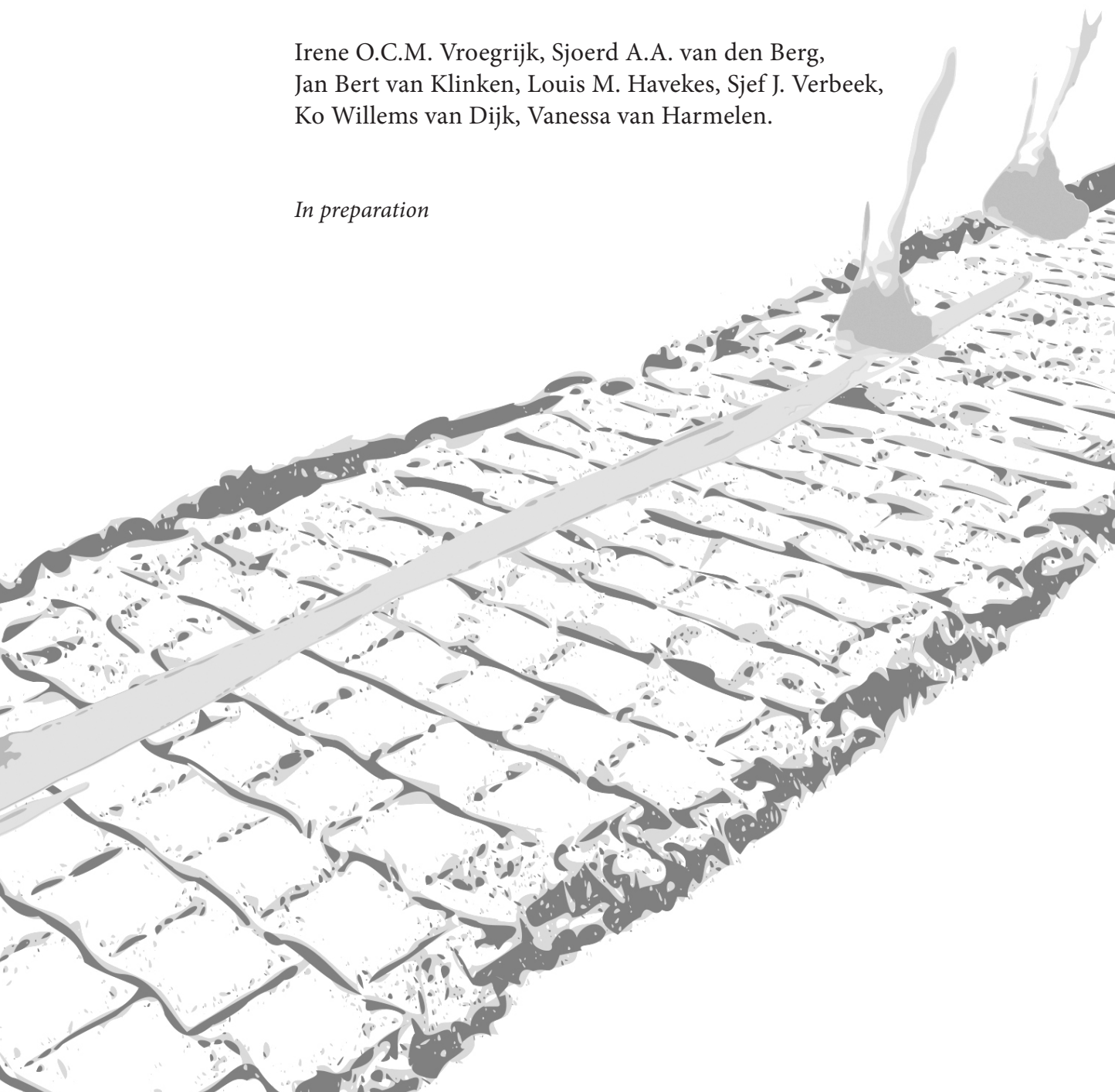

ABSTRACT

Inflammation plays a key role in the pathogenesis of diet-induced insulin resistance and type 2 diabetes. Recent studies have suggested that immunoglobulins (Ig) released by B-lymphocytes during the development of obesity play a key role in this pathology, although their mechanism of action is still unknown. Ig activate cellular responses by cross linking membrane receptors specific for the Fc portion of the Ig molecule (FcR). In this study, we have investigated whether functional FcR play a role in the development of diet-induced adipose tissue inflammation and diet-induced insulin resistance. To this end, FcR γ-chain$^{-/-}$ mice that are characterized by a decreased FcR-mediated activation by IgG and IgE antibodies, were fed a high fat diet (HFD). FcR γ-chain$^{-/-}$ mice gained less weight on HFD which was neither caused by decreased food intake nor by increased energy expenditure. However, a decreased postprandial response to a lipid load was observed, which suggests altered lipid absorption in the intestine of FcR γ-chain$^{-/-}$ mice. Basal glucose and insulin levels were decreased in FcR γ-chain$^{-/-}$ mice compared to WT controls and hyperinsulinemic euglycemic clamp analysis revealed decreased peripheral insulin resistance in FcR γ-chain$^{-/-}$ mice. The adipose tissue of FcR γ-chain$^{-/-}$ mice expressed lower levels of inflammatory genes and contained no crown-like structures. Taken together, these results demonstrate that the FcR γ-chain plays a key role in HFD induced obesity, insulin resistance and adipose tissue inflammation and are in line with a key role for Ig-mediated responses in this pathology.

5.1 INTRODUCTION

Obesity and its related metabolic disorders such as insulin resistance and type 2 diabetes are associated with low-grade systemic inflammation, characterized by increased local and systemic production of pro inflammatory cytokines and adipokines [1, 2].

Macrophage infiltration of expanding adipose tissue is one of the causes leading to increased cytokine production [3]. These macrophages are classified as 'classically' activated macrophages or M1 macrophages that have increased expression of the pro inflammatory cytokines IL-6, TNF-α and MCP-1 [4, 5]. Specific pro inflammatory subsets of T-lymphocytes have also been found to be enriched in adipose tissue from the obese. It has been suggested that T_H1 lymphocytes help recruit macrophages into adipose tissue and stimulate the M1 macrophage inflammatory activation state [6, 7].

Until recently, the role of B-lymphocytes and Ig in the development of adipose tissue inflammation and insulin resistance was poorly characterized. Duffaut et al. found an early accumulation of B-lymphocytes in adipose tissue when mice were subjected to a high fat diet (HFD) [8]. In Pima Indians, with an inherited susceptibility for diabetes type 2, gamma globulin levels were positively correlated with BMI and predicted type 2 diabetes, which suggest that activation of the humoral immune system is involved in the development of insulin resistance [9]. Moreover, Winer et al. have unequivocally shown that B-lymphocytes and antibodies play a key role in obesity associated insulin resistance. They showed that mice, which do not have mature B-lymphocytes, are protected against obesity-associated insulin resistance and in adoptive transfer experiments they demonstrated that IgG antibodies induce insulin resistance in the presence of a HFD [10]. The underlying mechanisms of the antibody effector pathways are currently still unknown. In this manuscript, we have used FcR γ-chain$^{-/-}$ mice to investigate whether functional FcR could play a role in the development of diet-induced inflammation of adipose tissue and diet-induced insulin resistance. FcR γ-chain$^{-/-}$ mice do not express the signal transducing γ-chain of FcγRI and III and FcεRI and therefore these mice have a diminished activation of IgG and IgE antibody effector pathways. Here we show that mice deficient for FcR γ-chain are protected against diet-induced obesity, diet-induced adipose tissue inflammation and diet-induced insulin resistance, indicating that functional activating FcRs might play a role in the development of the metabolic syndrome.

5.2 MATERIALS AND METHODS

Animals

The generation of FcR γ-chain deficient mice in 100% C57BL/6 background has been described previously [11]. FcR γ-chain$^{-/-}$ were bred at the Leiden University Medical Center, Leiden, The Netherlands. Wild-type (WT) control mice (C57Bl6/J background) were

purchased from Charles River (Maastricht, The Netherlands). Mice used in experiments were males, housed under standard conditions with free access to water and food. Mice were fed a high fat diet (HFD) for 11 weeks (45% energy derived from lard fat; D12451, Research Diet Services, Wijk bij Duurstede, The Netherlands) to induce obesity. Body weight was measured regularly during the diet intervention. All experiments were approved by the animal ethics committee of Leiden University Medical Center.

Plasma parameters

To determine plasma metabolite levels during week 11 of HFD feeding, tail vein blood was collected after an overnight fast, into capillary tubes coated with paraoxon (Sigma, St. Louis, MO) to prevent ongoing *in vitro* lipolysis. The tubes were placed on ice and centrifuged. Plasma triglyceride (TG), total cholesterol (TC), free fatty acid (FA), plasma phospholipids (PL), keton bodies, glucose and insulin levels were determined using commercially available kits (11488872 and 236691, Roche Molecular Biochemicals, Indianapolis, IN, NEFA-C and phospholipids B Wako Chemicals GmbH, Neuss, Germany, ab83390, Abcam, Cambrigde, UK, Instruchemie, Delfzijl, The Netherlands and Crystal Chem Inc., IL, USA, respectively).

Determination of adipocyte size and preadipocyte differentiation capacity

Adipose tissue from the gonadal (unilateral), subcutaneous (unilateral) and visceral region were removed from the mice after 11 weeks of HFD and kept in PBS. The tissue was minced and digested in 0.5g/l collagenase in HEPES buffer (pH 7.4) with 20 g/l of dialyzed bovine serum albumin (BSA, fraction V, Sigma, ST Louis, USA) for 1 h at 37°C. The disaggregated adipose tissue was filtered through a nylon mesh with a pore size of 236 µm. For the isolation of mature adipocytes, cells were obtained from the surface of the filtrate and washed several times. Cell size was determined using an imaging processing technique which automatically determines fat cell sizes from microscopic pictures of isolated adipocytes (~1000 cells/fat tissue sample). From the measured cells the adipocyte size distribution, adipocyte number and mean adipocyte diameter were determined. Subsequently the volume-weighted mean adipocyte diameter was calculated, which is a measure of the mean adipocyte diameter corrected for the amount of fat that an adipocyte can store [12]. For the isolation of preadipocytes, the infranatant of the adipose tissue filtrate was centrifuged at 200 x g for 10 min at room temperature and treated with erythrocyte lysis buffer. The cells were washed 2 times, re-suspended in DMEM/NUT.MIX.F12 medium and supplemented with 10% fetal calf serum (FCS) and 100 µg/ml penicillin-streptomycin and inoculated into 96-well plates (12 wells/adipose tissue region) at a density of 40 000 cells/ml and kept at 37°C, in 5% CO_2. The cells were expanded until confluency after which adipocyte differentiation was induced using an adipogenic medium containing DMEM/F12 with dexamethasone 0.1µM, 3-isobutyl-1-methylxanthine 25µM, insulin 17 nM, indomethacin 60µM, 10% FCS and 100 µg/ml penicillin-streptomycin. After 3 days, medium was changed to maintenance medium containing insulin 17 nM and 10%FCS. After 5 more days the cells were lipid filled and intra cellular lipid accumulation was determined using a fluorometer after incubating the cells with Nile Red.

RNA isolation and qPCR analysis

RNA from gonadal fat of mice was isolated after 11 weeks of HFD feeding using the Nucleospin RNA /Protein kit (Macherey-Nagel, Düren, Germany) according to the instructions of the manufacturer. The quality of each mRNA sample was examined by lab-on-a-chip technology using Experion Stdsens analysis kit (Biorad, Hercules, CA). 600 ng of total RNA was reverse-transcribed with iScript cDNA synthesis kit (Bio-Rad) and obtained cDNA was purified with Nucleospin Extract II kit (Macherey-Nagel). Real-Time PCR was carried out on the IQ5 PCR machine (Biorad) using the Sensimix SYBR Green RT-PCR mix (Quantace, London, UK). mRNA levels were normalized to mRNA levels of glyceraldehyde-3-phosphate dehydrogenase (Gapdh) or cyclophilin (cyclo). Primer sequences are listed in table 1.

Immunohistochemistry

Immunohistochemistry was performed on formalin fixed and paraffin embedded sections of gondal adipose tissue of mice fed a HFD for 11 weeks. For detection of macrophages/monocytes, an F4/80+ antibody (1:150) (Serotec) was used. Visualization of the complex was done using diaminobenzidene for 10 minutes. Negative and positive controls were included. Haematoxylin and Eosin (HE) stainings of sections were done using a standard protocol.

Hyperinsulinemic Euglycemic Clamp analysis

During week 11, hyperinsulinemic euglycemic clamps were performed as described earlier [13]. Briefly, after an overnight fast, animals were anesthetized and an infusion needle was placed in the tail vein. Basal glucose parameters were determined during a 60-min period, by infusion of D-[3-^{3}H]glucose to achieve steady-state levels. A bolus of insulin (3 mU) was given and a hyperinsulinemic euglycemic clamp was started with a continuous infusion of insulin (5 mU/h) and D-[3-^{3}H]glucose and a variable infusion of 12.5% D-glucose (in PBS) to maintain blood glucose levels at euglycemic levels. Blood samples were taken every

Table 1. Primers used for quantitative real-time PCR analysis.

Gene	Forward primer	Reverse primer
F4/80	CTTTGGCTATGGGCTTCCAGTC	GCAAGGAGGACAGAGTTTATCGTG
CD68	ATCCCCACCTGTCTCTCTCA	TTGCATTTCCACAGCAGAAG
MCP-1	GCATCTGCCCTAAGGTCTTCA	TTCACTGTCACACTGGTCACTCCTA
IL-6	ACCACGGCCTTCCCTACTTC	CTCATTTCCACGATTTCCCAG
IL-10	GACAACATACTGCTAACCGACTC	ATCACTCTTCACCTGCTCCACT
ACOX1	TATGGGATCAGCCAGAAAGG	ACAGAGCCAAGGGTCACATC
CPT1a	GAGACTTCCAACGCATGACA	ATGGGTTGGGGTGATGTAGA
GAPDH	TGCACCACCAACTGCTTAGC	GGCATGGACTGTGGTCATGAG
CYCLO	CAAATGCTGGACCAAACACAA	GCCATCCAGCCATTCAGTCT

F4/80, marker for macrophages; *CD68*, marker for macrophages; *MCP-1*; monocyte chemoattractant protein-1; *IL-6*, interleukin-6; *IL-10*, interleukin-10; *ACOX1*, acyl-coenzyme A oxidase 1; *CPT1a*, carnitine palmitoyltransferase 1a; *GAPDH*, glyceraldehyde-3-phosphate dehydrogenase; *CYCLO*, cyclophilin

5-10 min from the tip of the tail to monitor plasma glucose levels (AccuCheck). Seventy, eighty and ninety minutes (steady-state) after the start of the clamp, blood samples (70 µl) were taken for determination of plasma glucose, insulin and FA concentrations using commercially available kits (Instruchemie, Crystal Chem Inc., and Wako Pure Chemical Industries). Turnover rates of glucose (µmol/min/kg) were calculated during the basal period and in steady-state clamp conditions as the rate of tracer infusion (dpm/min) divided by the plasma-specific activity of ^{3}H-glucose (dpm/µmol). All metabolic parameters were expressed per kilogram of bodyweight. The hepatic glucose production (HGP) is calculated from the rate of disappearance (Rd) and glucose infusion rate (GIR) by the following equation: Rd = HGP + GIR. The Rd is measured from Steele's equation in steady state using the tracer infusion rate (Vin) and plasma-specific activity (SA) of ^{3}H-glucose (dpm/µmol) by the following formula: Rd = Vin/SA.

Indirect calorimetry

During week 5 and 10 of HFD feeding groups of 8 mice were subjected to individual indirect calorimetry measurements using a Comprehensive Laboratory Animal Monitoring System (Columbus Instruments, Columbus Ohio, US). Cages were made of clear plexiglass (30 x 10 x 9 cm (l x b x h)). A period of 24 hours prior to the start of the experiment allowed the acclimatization of the animals to the cages and the single housing. Experimental analysis started at 09:00 h and continued for 36 hours. Analyzed parameters included real time food and water intake, as well as meal size, frequency and duration. Oxygen consumption (VO2) and carbon dioxide production rates (VCO2) were measured at intervals of 7 minutes. Respiratory exchange ratio (RER) as a measure for metabolic substrate choice was calculated as the ratio between VCO_2 and VO_2. Carbohydrate (CHO) and fat (FA) oxidation rates were calculated using the following formulas [14] :

CHO = ((4.585 * VCO2) – (3.226 * VO2)) * 4 / 1000

FA = ((1.695 * VO2) – (1.701 * VCO2)) * 9 /1000

Total energy expenditure was calculated from the sum of CHO and FA oxidation. Activity was monitored as 2-dimensional infrared beam breaks.

Liver lipids

Lipids were extracted from livers of WT and FcR γ-chain$^{-/-}$ fed a HFD for 11 weeks according to a modified protocol from Bligh and Dyer [15]. Briefly, small liver pieces were homogenized in ice-cold methanol. After centrifugation, lipids were extracted by addition of 1800 µL chloroform: methanol (3:1 v/v) to 45 µL homogenate. The chloroform phase was dried and dissolved in 2% Triton X-100. Hepatic TG, TC and PL concentrations were measured using commercial kits as described earlier. Liver lipids were expressed per mg protein, which was determined using the BCA protein assay kit (Pierce).

Postprandial response

To investigate the handling of postprandial TG, mice were fed a HFD for 7 weeks. Mice were fasted 4 h (from 8.00 am to 12.00 pm) prior to the start of the experiment. Mice received an intragastric load of 200 µl olive oil (Carbonell extra virgin, Cordoba, Spain). Prior to the bolus and 1, 2, 4, and 8 h after bolus administration blood samples were obtained via tail vein bleeding for determination of plasma TG and FA as described above.

Fecal TG content

Fecal TG content was determined in feces collected during week 6 of HFD feeding. TG was extracted according to a modified protocol from Bligh and Dyer [15]. In short, 100 mg of crushed feces was homogenized in methanol:chloroform (2:1). 600 µl chloroform was added for TG extraction and samples were centrifuged. This procedure was repeated twice to maximize TG extraction. After centrifugation, the chloroform layer was collected and chloroform was evaporated. The remaining TG pellet was dissolved in 2% Triton-x-100 (Sigma). TG content was determined using a commercially available kit as described earlier.

Statistical analysis

Data are presented as means ± SD. Statistical differences were calculated using the unpaired T-test (SPSS 16, SPSS Inc, Chicago, IL). A P-value < 0.05 was regarded statistically significant.

5.3 RESULTS

FcR γ-chain$^{-/-}$ mice are protected against HFD-induced obesity

To induce obesity, male FcR γ-chain$^{-/-}$ and WT mice were fed a HFD containing 45 energy% fat for 11 weeks, and body weight of the mice was followed during the HFD intervention. FcR γ-chain$^{-/-}$ mice gained less body weight than WT mice (Fig. 1A). In line with this observation, weights of isolated fat pads were decreased in FcR-γ-chain$^{-/-}$ mice (gonadal fat -65%; P<0.001, subcutaneous fat -64%; P<0.001, visceral fat -60%; P<0.001) (Fig. 1B).

FcR γ-chain$^{-/-}$ adipocytes are smaller and have an improved differentiation capacity ex vivo

A decrease in fat pad mass can be caused by smaller adipocytes and/or by a decreased number of adipocytes. To investigate adipocyte morphology, adipocyte size distribution, volume-weighted mean adipocyte diameter and total adipocyte number were determined in isolated adipocytes from gonadal, subcutaneous and visceral fat pads from FcR γ-chain$^{-/-}$ and WT mice fed a HFD for 11 weeks. In FcR γ-chain$^{-/-}$ mice the distribution was shifted to the left for all three fat pads (Fig. 2A-C), indicating less hypertrophic adipocytes. Indeed, in FcR γ-chain$^{-/-}$ mice volume-weighted mean cell diameter was decreased in gonadal (gWAT) (-26%; P<0.001), subcutaneous (sWAT) (-29%; P<0.001) and visceral (vWAT)

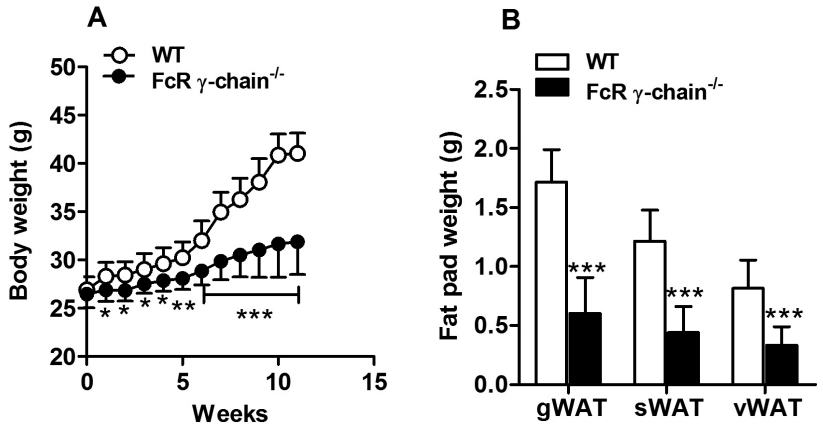

Figure 1. FcR γ-chain$^{-/-}$ mice are protected against HFD-induced obesity. Wild-type (WT) and FcR γ-chain$^{-/-}$ mice were fed a HFD for 11 weeks. Body weight of WT mice and FcR γ-chain$^{-/-}$ mice was measured at the indicated time points (A). Values are means ± SD (n= 10 per group); **P*<0.05, ***P*<0.01, ****P*<0.001. After 11 weeks of HFD, tissues were dissected and weight of WT and FcR γ-chain$^{-/-}$ fat pads was determined (B). Values are means ± SD (n= 10 per group); ****P*<0.001.

(27%; P<0.001) white adipose tissue (Fig. 2D) compared to WT mice. In addition to smaller adipocytes, also a decreased number of adipocytes was found in gWAT (-27%; P<0.001) and sWAT (-17%; P<0.05) of FcR γ-chain$^{-/-}$ mice (Fig. 2E). To investigate differentiation capacity, isolated preadipocytes from gonadal and subcutaneous fat pads of FcR γ-chain$^{-/-}$ and WT mice were differentiated in adipogenic medium and TG accumulation was measured. An increased differentiation capacity was observed for gonadal preadipocytes of FcR γ-chain$^{-/-}$ mice (+147%; P<0.05) (Fig. 2F).

FcR γ-chain$^{-/-}$ mice have decreased inflammation in white adipose tissue

To investigate whether functional FcR are important for white adipose tissue inflammation, mRNA expression of several inflammatory genes was measured in gonadal white adipose tissue (gWAT) of FcR γ-chain$^{-/-}$ and WT mice. A decreased expression of F4/80 (-46%; P<0.05), CD68 (-70%; P<0.001), monocyte chemotactic protein-1 (MCP-1) (-83%; P<0.001), interleukin 6 (IL-6) (-51%; P<0.01) and interleukin 10 (IL-10) (-58%; P<0.01) was found in FcR γ-chain$^{-/-}$ mice, which indicates decreased inflammation (Fig. 3A). Immunohistochemistry using an antibody that recognizes the macrophage antigen F4/80, showed crown like structures (CLS) in gonadal adipose tissue of WT mice, but not in gonadal adipose tissue of FcR-γ-chain$^{-/-}$ mice (Fig. 3B).

FcR γ-chain$^{-/-}$ mice have decreased HFD-induced insulin resistance

To investigate whether functional FcR play a role in diet-induced insulin resistance, plasma glucose and insulin levels of overnight fasted FcR γ-chain$^{-/-}$ and WT mice that had been on a HFD for 11 weeks were measured. Both glucose (-28%; P<0.001) and insulin (-47%; P<0.001) levels were significantly decreased in FcR-γ-chain$^{-/-}$ mice compared to WT mice

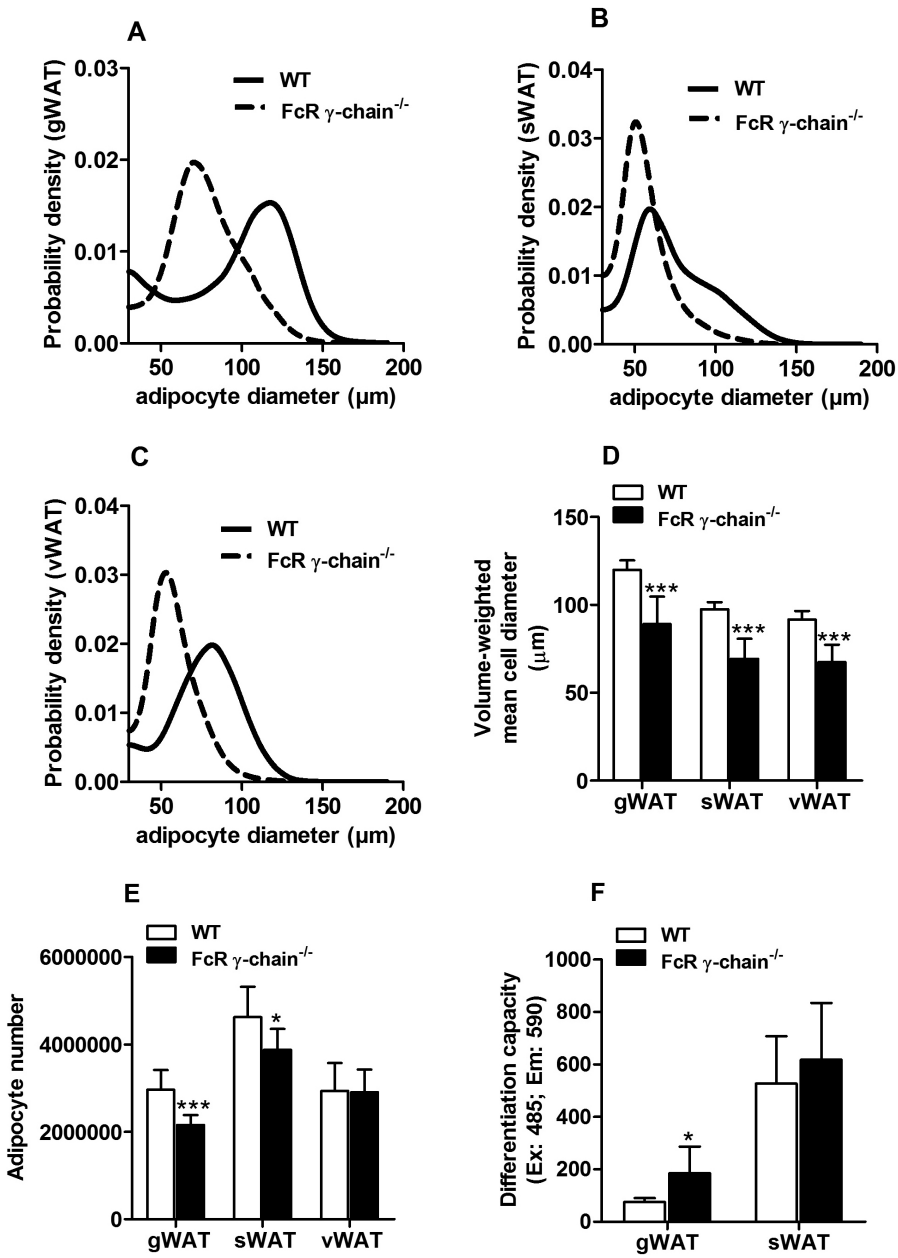

Figure 2. FcR γ-chain$^{-/-}$ adipocytes are smaller and have an improved adipogenic capacity. After 11 weeks of HFD feeding, adipocytes were isolated from gonadal (gWAT), subcutaneous (sWAT) and visceral (vWAT) white adipose tissues of wild-type (WT) and FcR γ-chain$^{-/-}$ mice. Adipocyte size distribution was determined (A-C). Values are means ± SD (n= 9-10 per group). Volume-weighted mean diameter (D), total number of adipocytes (E) and adipogenic capacity (F) was determined. Values are means ± SD (n=9-10); **P*<0.05, ****P*<0.001.

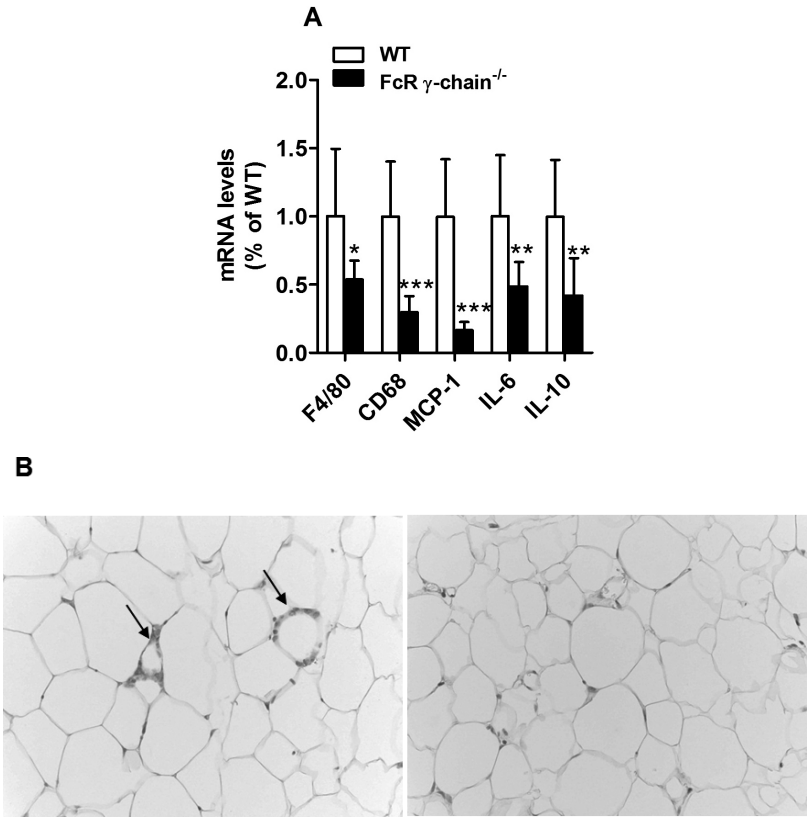

Figure 3. FcR γ-chain$^{-/-}$ mice have decreased inflammation in white adipose tissue. After 11 weeks of HFD feeding, RNA was isolated from gonadal (gWAT) white adipose tissues of wild-type (WT) and FcR γ-chain$^{-/-}$ mice. mRNA levels of F4/80, CD68, monocyte chemotactic protein-1 (MCP-1), interleukin 6 (IL-6) and interleukin 10 (IL-10) were determined (A). Values are means ± SD (n= 9-10); *P<0.05, **P<0.01, ***P<0.001. F4/80 staining in gWAT of wild-type (WT) and FcR γ-chain$^{-/-}$ mice (B).

(Fig. 4A-B), suggesting that FcR-γ-chain$^{-/-}$ mice have decreased HFD-induced insulin resistance. To further investigate the insulin sensitivity, a hyperinsulinemic euglycemic clamp was performed. This analysis revealed a significant increase in glucose disposal rate in FcR γ-chain$^{-/-}$ mice during the hyperinsulinemic period (+20 %; P<0.05) (Fig. 4C), indicating that HFD-induced peripheral insulin resistance is decreased in these mice compared to WT controls. Insulin mediated suppression of HGP was similar in both groups (Fig. 4D), indicating similar hepatic insulin sensitivity after HFD.

FcR γ-chain$^{-/-}$ mice have equal food intake and energy expenditure

To investigate how FcR γ-chain$^{-/-}$ mice are protected against diet-induced obesity indirect calorimetry measurements were performed in the mice during week 5 and 10 of the HFD intervention. Fig. 5 shows results of week 5, which were similar to the results of week 10. The batch of mice that was used for indirect calorimetry measurements did not differ significantly in body weight at week 5, only body weight gain differed significantly (body weight was 30.6

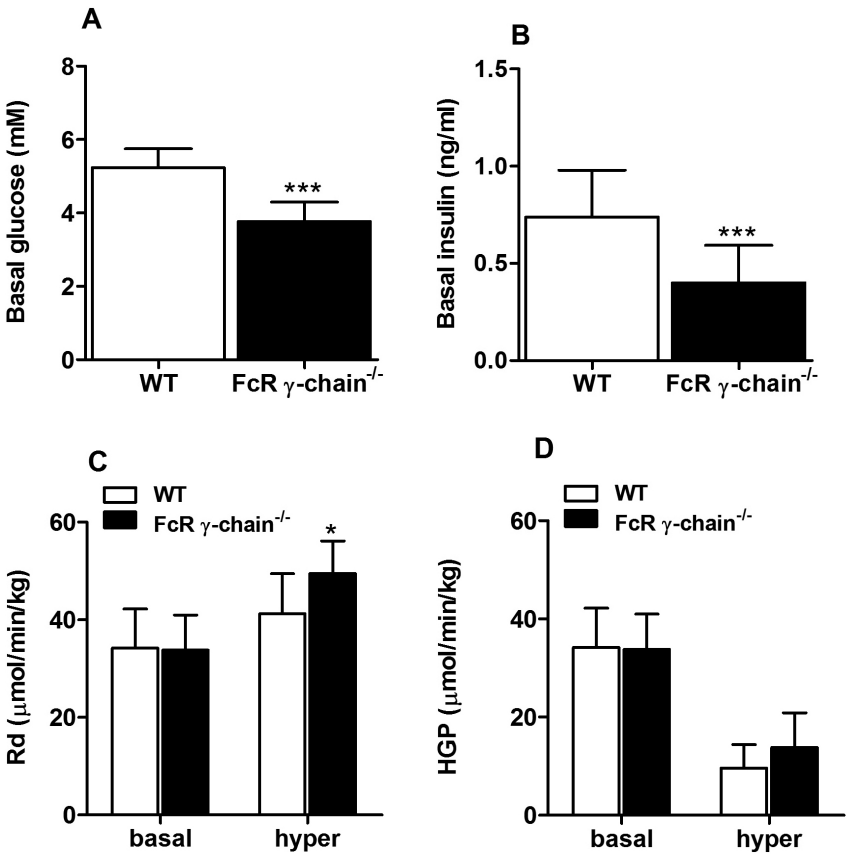

Figure 4. FcR γ-chain$^{-/-}$ mice are protected against HFD-induced insulin resistance. A second set of wild-type (WT) and FcR γ-chain$^{-/-}$ mice was fed a HFD for 11 weeks and after an overnight fast plasma glucose (A) and insulin levels (B) were determined. Values are means ± SD (n=8); ***P<0.001. A hyperinsulinemic euglycemic clamp was performed in wild-type (WT) and FcR γ-chain$^{-/-}$ mice. Rate of disappearance during basal and hyperinsulinemic period (C) and hepatic glucose production during hyperinsulinemic period (D) were determined. Values are means ± SD (n=8); *P<0.05.

± 2.2 vs. 31.3 ± 1.1, body weight gain was 3.0 ± 0.8 vs. 5.0 ± 0.8; P<0.001). Differences in calorimetry during week 5 could thus not be due to differences in body weight. Nocturnal and diurnal data were analyzed separately to distinguish between periods of low (diurnal) and high (nocturnal) physical activity. During the diurnal period no differences were observed in total energy expenditure (EE), respiratory exchange ratio (RER), absolute fatty acid (FA_{ox}) and absolute carbohydrate (CH_{ox}) oxidation rates both at week 5 and 10. Food intake tended to be lower in the FcR γ-chain$^{-/-}$ mice (p=0.08) during week 10, but was not different during week 5 (Fig. 5A-E). Ambulatory physical activity during the diurnal period was not different between groups (data not shown) both at week 5 and 10. During the nocturnal period, ambulatory physical activity was higher in FcR γ-chain$^{-/-}$ mice, both at week 5 and 10 (week 5: +33%, week 10: +47%; P<0.05). This higher physical activity did not result in an increased EE in FcR γ-chain$^{-/-}$ mice. Measured food intake and EE were not different, however the average

RER was increased in FcR γ-chain$^{-/-}$ mice, both at week 5 and 10 (week 5: +3%, week 10: +2%; P<0.05) which was reflected in a somewhat lower absolute FA_{ox} rate and a somewhat higher CH_{ox} rate (Fig. 5A-E). This higher CH_{ox} rate in FcR γ-chain$^{-/-}$ mice compared to WT controls corresponds to the increased insulin sensitivity that was observed.

In addition, the energy balance was determined for FcR γ-chain$^{-/-}$ and WT mice by calculating [food intake (kcal/24h)] – [energy expenditure (kcal/24h)]. No significant

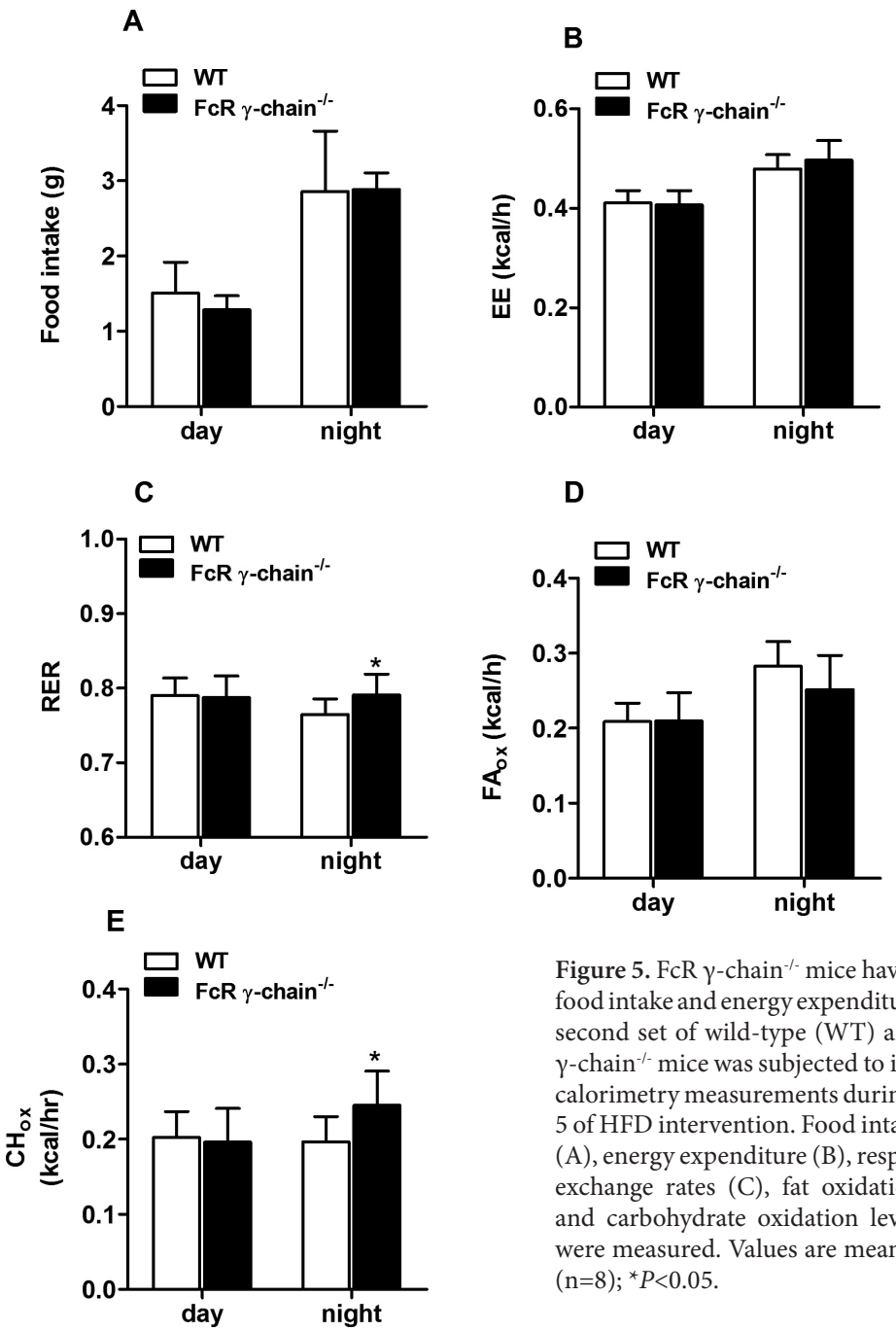

Figure 5. FcR γ-chain$^{-/-}$ mice have equal food intake and energy expenditure. The second set of wild-type (WT) and FcR γ-chain$^{-/-}$ mice was subjected to indirect calorimetry measurements during week 5 of HFD intervention. Food intake (FI) (A), energy expenditure (B), respiratory exchange rates (C), fat oxidation (D) and carbohydrate oxidation levels (E) were measured. Values are means ± SD (n=8); **P*<0.05.

differences in energy balance were observed, both during week 5 and 10 (week 5: +8.9 ± 1.8 vs. +10.0 ± 5.5, week 10: +3.4 ± 1.8 vs. +4.4 ± 3.8).

FcR γ-chain$^{-/-}$ mice have decreased plasma lipid levels and decreased liver lipid levels

To further unravel the mechanisms underlying the decreased adiposity of the FcR γ-chain$^{-/-}$ mice, plasma lipid parameters were determined during week 11 of HFD feeding. Plasma TG, TC and PL levels were significantly decreased in FcR γ-chain$^{-/-}$ mice (-26%; P<0.05, -39% and -24 %; P<0.001) (Table 2). In addition liver lipids were measured, demonstrating decreased liver TG content in FcR γ-chain$^{-/-}$ mice (-60%; P<0.001) (Fig. 6A). mRNA levels of acyl-Coenzyme A oxidase 1 (Acox1) and carnitine palmitoyltransferase 1a (Cpt1a), 2 genes involved in β-oxidation, were decreased in FcR γ-chain$^{-/-}$ mice (-66%; P<0.001 and -59%; P<0.01) (Fig. 6B). Furthermore, keton bodies in plasma were measured during week 9 and 11 of the HFD intervention in 2 batches of mice. Equal or decreased levels of keton bodies were observed, respectively (1.06 ± 0.25 versus 1.02 ± 0.28 and 0.90 ± 0.27 versus 1.23 ± 0.14; P<0.01). Together these results indicate decreased β-oxidation in FcR γ-chain$^{-/-}$ mice.

FcR γ-chain$^{-/-}$ mice have decreased postprandial response

Decreased adiposity in FcR γ-chain$^{-/-}$ mice might also be caused by absorption problems. To investigate this hypothesis, FcR γ-chain$^{-/-}$ and WT mice were given an oral bolus of 200 µl olive oil after 7 weeks of HFD and plasma TG levels were monitored in time. FcR γ-chain$^{-/-}$ mice had a decreased postprandial response compared to WT mice (Fig. 7A). However, no

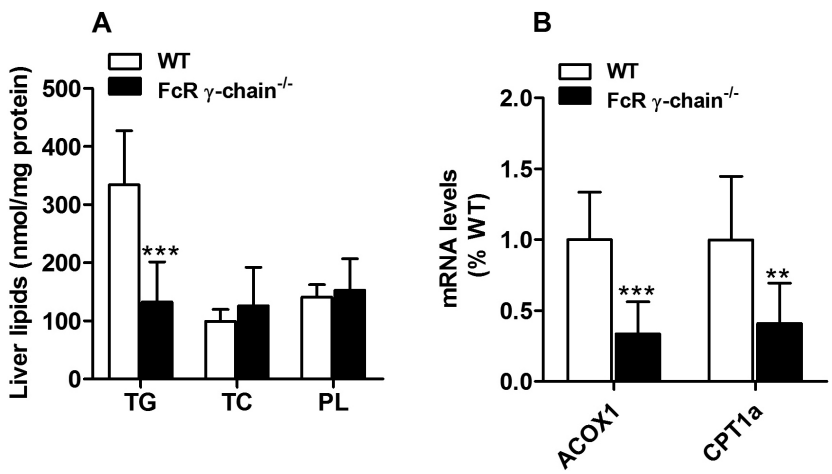

Figure 6. FcR γ-chain$^{-/-}$ mice have decreased plasma lipid levels and decreased liver lipid levels. After 11 weeks of HFD, liver was dissected of wild-type (WT) and FcR γ-chain$^{-/-}$ mice and liver lipids were determined (A). Values are means ± SD (n=5); ***P<0.001. RNA was isolated from WT and FcR γ-chain$^{-/-}$ livers and mRNA levels of acyl-Coenzyme A oxidase 1 (Acox1) and carnitine palmitoyltransferase 1a (Cpt1a) were measured (B). Values are means ± SD (n=9-10); **P<0.01, ***P<0.001.

Table 2. FcR γ-chain$^{-/-}$ mice have decreased plasma lipid levels on high fat diet.

	WT	FcR γ-chain$^{-/-}$
TG (mM)	1.10 ± 0.30	0.81 ± 0.21*
TC (mM)	4.23 ± 0.30	2.56 ± 0.40***
PL (mM)	2.99 ± 0.36	2.26 ± 0.38***
FA (mM)	1.08 ± 0.22	1.21 ± 0.24

Plasma was obtained from overnight fasted mice during week 11 of high fat diet intervention (n=10). Plasma triglycerides (TG), total cholesterol (TC), phospholipids (PL) and free fatty acids (FA) were measured. Values are means ± SD. *P<0.05, ***P<0.001.

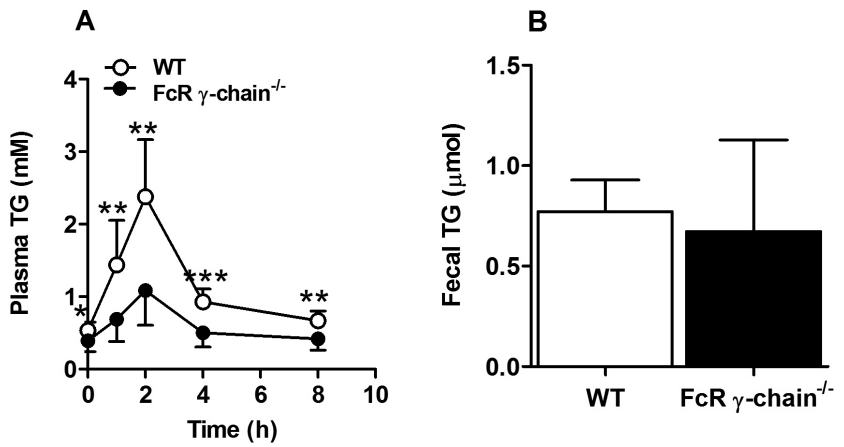

Figure 7. FcR γ-chain$^{-/-}$ mice have decreased postprandial response. After 7 weeks of HFD, the postprandial response triglyceride (TG) was determined in a third set of wild-type (WT) and FcR γ-chain$^{-/-}$ mice (A). Values are means ± SD (n=9); *P<0.05, **P<0.01, ***P<0.001. During week 6 of HFD intervention feces was collected of these mice and TG content was determined in fecal samples of WT and FcR γ-chain$^{-/-}$ mice (B). Values are means ± SD (n=7-9).

differences in fecal TG content were observed (Fig. 7B). These data indicate that intestinal lipid absorption kinetics are affected in FcR γ-chain$^{-/-}$ mice.

5.4 DISCUSSION

The study presented here is to our knowledge the first to indicate that FcR associated antibody effector pathways are involved in the development of diet-induced insulin resistance. We show that after a HFD, FcR γ-chain$^{-/-}$ mice become less obese and develop less adipose tissue inflammation and peripheral insulin resistance compared to WT controls. As the FcR γ-chain is crucial for full activation of IgG and IgE antibody effector pathways, our results demonstrate that FcR associated antibody effector pathways might play a key role in

these processes. Our results are in line with a role of Ig in the development of HFD-induced insulin resistance, which has recently been shown by Winer et al. [10].

The FcR γ-chain$^{-/-}$ mice showed a reduced body weight gain and decreased adipocyte size as compared to HFD-fed WT mice. Since body weight and adipocyte size per se are determinants of insulin sensitivity, these effects can explain at least part of the observed decreased HFD-induced insulin resistance. However, the calorimetry measurements demonstrated a higher CH_{ox} rate in FcR γ-chain$^{-/-}$ mice during week 5 when the FcR γ-chain$^{-/-}$ and WT mice did not differ in body weight. As a high CH_{ox} rate corresponds to increased insulin sensitivity, these data may suggest that the Fc γ-chain per se plays a role in diet-induced insulin resistance and is not only a consequence of the effects on body weight. In the study of Winer et al., B-lymphocyte deficient mice showed improved glucose tolerance and insulin sensitivity compared to HFD-fed WT mice, although they did not differ from WT mice in weight gain nor adipocyte size upon HFD feeding. Their study suggests that B-lymphocyte derived Ig are responsible for a body weight-independent effect on HFD-induced insulin resistance [10]. In another recent study using B-lymphocyte deficient mice on BalbC background (BcKO mice), body fat stores were assessed after a HFD and the BcKO mice did show reduced inguinal and epididymal fat stores compared to their heterozygous littermate controls [16].

The fact that FcR γ-chain$^{-/-}$ mice are relatively protected against HFD-induced obesity cannot be explained by differences in food intake nor energy expenditure. However, intestinal lipid absorption may be affected in FcR γ-chain$^{-/-}$ mice as indicated by a decreased postprandial response to an olive oil load. In line with a reduction of the intestinal lipid flux, circulating plasma TG and liver TG were both decreased and genes involved in β-oxidation were also decreased. Despite the reduced postprandial TG response, fecal fat secretion was not different from WT mice. Combined, these observations may indicate that the lipids that were not absorbed postprandially as plasma TG in the FcR γ-chain$^{-/-}$ mice, were still being metabolized in the intestine, most likely by the intestinal microbiota. Since intestinal microbiota are predominantly anaerobic, energy expended via this pathway will not be measured by gas-based calorimetry equipment. Although the TG/FA breakdown products from the intestinal microbiota (such as short chain FA) will be absorbed and used as fuel, the net energy output will be much lower as the microbial conversion reactions cost a lot of energy. This loss of energy may also contribute to the reduced body weight gain in HFD-fed FcR γ-chain$^{-/-}$ mice.

Recently, it was found that in the absence of IgA, the major antibody class in the gut, and in the presence of microbiota, the intestinal epithelium down regulates its metabolic functions and up regulates its immune functions, which ultimately results in lipid malabsorption. These effects were also observed in B-lymphocyte deficient mice. Moreover, duodenal samples of immunodeficient humans display a down regulation of metabolic genes and an up regulation of genes involved in immunity in intestinal epithelium [16]. The TG absorption problems found in the FcR γ-chain$^{-/-}$ mice, which also represent an immune-compromised model, are completely in line with these observations. However, we do not know whether IgA is involved in the observed phenotype of the FcR γ-chain$^{-/-}$ mice, since in mice the FcR for IgA – i.e FcαR- has never been identified, in contrast to in humans. Humans express a γ-chain associated high

affinity receptor for IgA, FcαRI (CD89). However, this FcαRI, expressed on myeloid cells such as macrophages, neutrophils and eosinophils, has never been found in mice [17].

Besides its association with different FcR, the FcR γ-chain is also associated with several receptors involved in innate immunity including NKR-P1C, PIR-A and IL3R. NKR-P1C is expressed on natural killer cells and mediates cytotoxicity against tumor cells [18]. The paired immunoglobulin like receptor-A (PIR-A), which is present on monocytes and macrophages, dendritic cells, mast cells and certain B lymphocytes subsets expressing natural antibodies, is able to activate these cells upon interaction with major histocompatibility complex (MHC) class 1 molecules [19]. Additionally, the γ-chain is a constitutive component of IL-3R and is necessary for IL-3-induced production of IL-4 by basophils [20]. Together these findings indicate that besides a signaling role in the antibody mediated effector mechanisms, the FcR γ-chain plays also an important role in innate immunity, which could contribute to the metabolic phenotype of the FcR γ-chain$^{-/-}$ mice that we observed.

However, we postulate that the FcR γ-chain$^{-/-}$ mice is a suitable model to study antibody effector mechanisms despite its association to other receptor types. In case FcR are involved in HFD-induced obesity and insulin resistance, the FcR γ-chain$^{-/-}$ mice should show a phenotype. Our experiments indicate that FcR γ-chain$^{-/-}$ mice indeed have a phenotype, which is a first indication for a major role for FcR mediated Ig effector pathways in HFD-induced obesity and insulin resistance and therefore they provide multiple avenues for future studies.

In conclusion, our data provide direct evidence for a role of the FcR γ-chain in HFD-induced obesity and insulin resistance. Although, we cannot exclude that non-FcR mediated mechanisms are responsible for this effect, our data suggests a major role for FcR mediated Ig effector pathways in HFD obesity and insulin resistance Our data also clearly indicate that FcR γ-chain mediated pathways are important in multiple tissues involved in HFD-induced pathology, including adipose tissue and the intestine.

ACKNOWLEDGEMENTS

The authors would like to thank A.C.M. Pronk, F. el Bouazzaoui and D.C.F. Salvatori for excellent technical assistance.

This work was supported by grants from: 1) the seventh framework program of the EU-funded "LipidomicNet" (proposal number 202272), 2) the Center for Translational Molecular Medicine (www.ctmm.nl), project PREDICCt (grant 01C-104), 3) the Center of Medical Systems Biology (CMSB) and 4) the Netherlands Consortium for Systems Biology (NCSB) established by The Netherlands Genomics Initiative/Netherlands Organization for Scientific Research (NGI/NWO).

REFERENCES

1. Hotamisligil GS. Inflammation and metabolic disorders. Nature 2006;444:860-867.
2. Olefsky JM, Glass CK. Macrophages, inflammation, and insulin resistance. Annu Rev Physiol 2010;72:219-246.
3. Weisberg SP, McCann D, Desai M, Rosenbaum M, Leibel RL, Ferrante AW, Jr. Obesity is associated with macrophage accumulation in adipose tissue. J Clin Invest 2003;112:1796-1808.
4. Lumeng CN, Bodzin JL, Saltiel AR. Obesity induces a phenotypic switch in adipose tissue macrophage polarization. J Clin Invest 2007;117:175-184.
5. Prieur X, Mok CY, Velagapudi VR, Nunez V, Fuentes L, Montaner D, Ishikawa K, Camacho A, Barbarroja N, O'Rahilly S, Sethi JK, Dopazo J, Oresic M, Ricote M, Vidal-Puig A. Differential lipid partitioning between adipocytes and tissue macrophages modulates macrophage lipotoxicity and M2/M1 polarization in obese mice. Diabetes 2011;60:797-809.
6. Nishimura S, Manabe I, Nagasaki M, Eto K, Yamashita H, Ohsugi M, Otsu M, Hara K, Ueki K, Sugiura S, Yoshimura K, Kadowaki T, Nagai R. CD8+ effector T cells contribute to macrophage recruitment and adipose tissue inflammation in obesity. Nat Med 2009;15:914-920.
7. Winer S, Chan Y, Paltser G, Truong D, Tsui H, Bahrami J, Dorfman R, Wang Y, Zielenski J, Mastronardi F, Maezawa Y, Drucker DJ, Engleman E, Winer D, Dosch HM. Normalization of obesity-associated insulin resistance through immunotherapy. Nat Med 2009;15:921-929.
8. Duffaut C, Galitzky J, Lafontan M, Bouloumie A. Unexpected trafficking of immune cells within the adipose tissue during the onset of obesity. Biochem Biophys Res Commun 2009;384:482-485.
9. Lindsay RS, Krakoff J, Hanson RL, Bennett PH, Knowler WC. Gamma globulin levels predict type 2 diabetes in the Pima Indian population. Diabetes 2001;50:1598-1603.
10. Winer DA, Winer S, Shen L, Wadia PP, Yantha J, Paltser G, Tsui H, Wu P, Davidson MG, Alonso MN, Leong HX, Glassford A, Caimol M, Kenkel JA, Tedder TF, McLaughlin T, Miklos DB, Dosch HM, Engleman EG. B cells promote insulin resistance through modulation of T cells and production of pathogenic IgG antibodies. Nat Med 2011;17:610-617.
11. Arase H, Ono S, Arase N, Park SY, Wakizaka K, Watanabe H, Ohno H, Saito T. Developmental arrest of NK1.1+ T cell antigen receptor (TCR)-alpha/beta+ T cells and expansion of NK1.1+ TCR-gamma/delta+ T cell development in CD3 zeta-deficient mice. J Exp Med 1995;182:891-895.
12. Jo J, Gavrilova O, Pack S, Jou W, Mullen S, Sumner AE, Cushman SW, Periwal V. Hypertrophy and/or Hyperplasia: Dynamics of Adipose Tissue Growth. PLoS Comput Biol 2009;5:e1000324.
13. Voshol PJ, Jong MC, Dahlmans VE, Kratky D, Levak-Frank S, Zechner R, Romijn JA, Havekes LM. In muscle-specific lipoprotein lipase-overexpressing mice, muscle triglyceride content is increased without inhibition of insulin-stimulated whole-body and muscle-specific glucose uptake. Diabetes 2001;50:2585-2590.
14. Peronnet F, Massicotte D. Table of nonprotein respiratory quotient: an update. Can J Sport Sci 1991;16:23-29.
15. Bligh EG, Dyer WJ. A rapid method of total lipid extraction and purification. Can J Biochem Physiol 1959;37:911-917.
16. Shulzhenko N, Morgun A, Hsiao W, Battle M, Yao M, Gavrilova O, Orandle M, Mayer L, Macpherson AJ, McCoy KD, Fraser-Liggett C, Matzinger P. Crosstalk between B lymphocytes, microbiota and the intestinal epithelium governs immunity versus metabolism in the gut. Nat Med 2011;17:1585-1593.
17. Monteiro RC. Role of IgA and IgA fc receptors in inflammation. J Clin Immunol 2010;30:1-9.
18. Arase N, Arase H, Park SY, Ohno H, Ra C, Saito T. Association with FcRgamma is essential for activation signal through NKR-P1 (CD161) in natural killer (NK) cells and NK1.1+ T cells. J Exp Med 1997;186:1957-1963.
19. Takai T. Paired immunoglobulin-like receptors and their MHC class I recognition. Immunology 2005;115:433-440.
20. Hida S, Yamasaki S, Sakamoto Y, Takamoto M, Obata K, Takai T, Karasuyama H, Sugane K, Saito T, Taki S. Fc receptor gamma-chain, a constitutive component of the IL-3 receptor, is required for IL-3-induced IL-4 production in basophils. Nat Immunol 2009;10:214-222.

6 GENERAL DISCUSSION

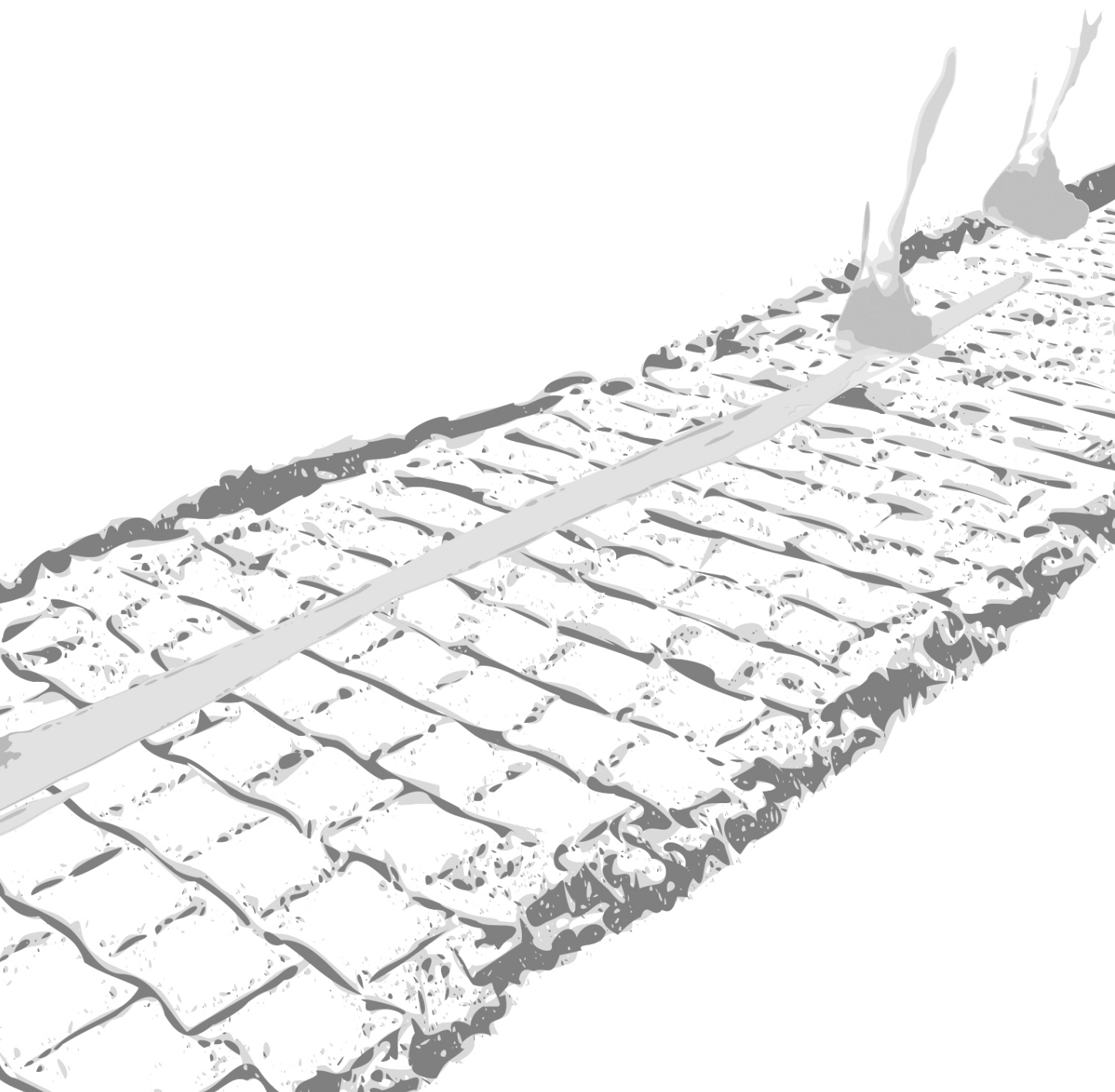

The metabolic syndrome, a multi-component condition including obesity, insulin resistance, dyslipidemia and hypertension, is associated with an increased risk for cardiovascular diseases and diabetes. The prevalence of the metabolic syndrome, currently around 30%, is rising worldwide and this rise parallels the increase in the prevalence of overweight and obesity. In 2009, 47% of all Dutch adults had overweight of which 12% were obese [1].

Chronic low-grade inflammation is thought to function as the link between the various components of the metabolic syndrome and the development of the associated pathologies. Disturbances in triglyceride (TG) and fatty acid (FA) metabolism can drive the inflammatory response and vice versa, the inflammatory response can drive disturbances in TG/FA metabolism. However, the mechanisms underlying these interactions between TG/FA metabolism and inflammation remain to be fully understood. In this thesis, we have investigated how modulation of TG/FA metabolism and inflammatory pathways interact in the development of obesity and insulin resistance, which are both primary risk factors for the development of type 2 diabetes.

6.1 ROLE OF FA TRANSPORT IN ADIPOSE TISSUE DEVELOPMENT AND INFLAMMATION

Adipose tissue is the first visually affected organ in the development of obesity and the metabolic syndrome. Excessive calories are stored in adipose tissue as TG. Energy storage in adipocytes is partly regulated by FA transporters in adipocytes that facilitate FA entry.

In chapter 2 we found that the FA transporter CD36 is important for adipocyte recruitment and adipocyte functionality. $CD36^{-/-}$ mice become less obese on high fat diet (HFD), although their body weight is still increased compared to mice fed a normal chow diet. Adipose tissue of $CD36^{-/-}$ mice has some healthy aspects compared to adipose tissue of wild-type (WT) mice, since we found that the adipocytes of $CD36^{-/-}$ mice are more insulin sensitive and the adipose tissue of $CD36^{-/-}$ mice is less inflamed. Nevertheless, the adipose tissue of these animals should be considered as dysfunctional. The adipocytes of $CD36^{-/-}$ mice cannot store surplus FA and also the recruitment of new adipocytes is impaired. As a result the FA are trans located to the liver and stored ectopically, which results in hepatic insulin resistance.

Differences in storage capacity of adipose tissue are important in the development of the metabolic syndrome. Human cohort studies indicate that there are individuals who are obese but seem to remain metabolically healthy. These individuals have a healthy lipid profile, e.g. lower TG, higher high density lipoprotein (HDL) cholesterol, lower fasting glucose and insulin concentrations and better glucose tolerance compared to unhealthy obese individuals, despite a similar level of total body fat [2]. Several studies have shown that the expandability of subcutaneous fat is critical for maintaining healthy obesity [3]. If this capacity to expand is large, an individual is more likely to remain healthy, even when obese. If the expandability of subcutaneous fat is low, excess fat is likely to be stored intra-abdominally (in visceral fat) or in non-adipose tissues (ectopic fat deposition), which is associated with an adverse metabolic profile

Different factors could play a role in the capacity of the subcutaneous fat to expand. Fat mass, fat distribution and adipocyte numbers are for a large part genetically determined. Twin and population studies have indicated that 25-70% of the variability in these traits can be explained by genetics. For example, variation in the LPL gene and mutations in the β3-adrenergic receptor gene have been associated with visceral obesity [4].

Additional important factors that could play a role in maintaining healthy adipose tissue are nutrition and exercise. A controlled-feeding trial demonstrated that consumption of a diet enriched in saturated FA (SFA) led to an increased expression of genes involved in inflammatory processes, while a diet enriched in monounsaturated FA (MUFA) led to decreased expression of inflammatory genes in adipose tissue of overweight subjects [5]. Thus, the type of dietary FA seems to affect inflammation in adipose tissue.

Physical activity also likely contributes to healthy obesity. It has been found that active obese men (fat fit men) have increased HDL cholesterol levels, decreased TG levels, decreased alanine aminotransferase (ALT) levels (which is a marker for liver damage), and improved insulin sensitivity, as measured by HOMA-index, compared to unfit obese men (fat unfit men). In addition, visceral fat and liver fat were decreased in fat fit men compared to fat unfit men. It has been postulated that men who are fit and fat have a greater capacity to store fat in subcutaneous adipose tissue [6].

If the expandability capacity of subcutaneous adipose tissue is decreased, excessive FA are more likely to be stored as visceral fat or in non-adipose tissues as ectopic fat. In its most extreme form this is illustrated by patients with lipodystrophy, who despite a normal BMI display features of the metabolic syndrome such as insulin resistance and hypertriglyceridemia. These patients have genetic defects in the development of adipose tissue and are characterized by extremely fatty livers. Insight in the genetics of lipodystrophy provides direct insight in adipose tissue development and function, and contributes to a better understanding of the onset of the pathology associated with the metabolic syndrome [7].

A less extreme form of lipodystrophy may affect individuals who despite a normal weight and BMI, display signs of insulin resistance and dyslipidemia. These individuals have been identified as metabolically obese normal weight (MONW) individuals [8]. MONW individuals are characterized by an increased visceral fat mass, which is associated with decreased insulin sensitivity [9]. Seppala-Linderoos et al. have found increased hepatic TG content in nonobese men who have high levels of plasma insulin and TG [10].

Physical inactivity may be an important characteristic of MONW individuals [11]. An inverse relationship between maximal oxygen uptake (V_{O2max}) and insulin insensitivity has been shown [12]. Several studies have demonstrated that regular exercise, either in combination with a healthy diet ameliorates metabolic abnormalities and reverses adverse fat distribution [13-16]. These studies illustrate the necessity of some basal level of physical activity even for those that are not obviously overweight.

6.2 ROLE OF INFLAMMATION IN TRIGLYCERIDE METABOLISM AND INSULIN RESISTANCE

Adipose tissue expansion and obesity are associated with the development of low-grade inflammation [17]. Expansion of adipose tissue is beyond a certain point physically limited by nutrient and oxygen supply. The subsequent hypoxia, endoplasmatic reticulum stress and apoptosis may lead to infiltration of immune cells into adipose tissue such as macrophages [18], activated T-lymphocytes [19 20-22] and activated B-lymphocytes [20,23]. Under normal physiological conditions, this response is self-limited and geared towards a new metabolic and inflammatory equilibrium. However, under conditions of chronic overnutrition, the low-grade inflammation can also become chronic. This chronic low-grade inflammation has been termed metabolic inflammation, since it is hypothesized that this inflammation is triggered by a surplus of nutrients. Metabolic inflammation is characterized by increased plasma levels of pro inflammatory cytokines, insulin resistance and a deregulation of TG/FA metabolism [24]. Inflammation, insulin resistance, and deregulation of TG/FA metabolism are part of a vicious cycle that drives the progression of diabetes and cardiovascular diseases.

Inflammation itself can directly affect lipoprotein metabolism as illustrated by the observation that patients with acute infections have elevated VLDL TG levels [25]. In addition, administration of lipopolysaccharide (LPS), a strongly pro inflammatory component of the cell wall of Gram-negative bacteria, and cytokines produce hypertriglyceridemia [26]. Conversely, disturbances of lipid metabolism can also produce a pro-inflammatory state. SFA can stimulate inflammatory pathways via Toll Like Receptor (TLR) 4 [27] or via increased reactive oxygen species (ROS) production. Recently it was found that SFA-induced ROS can activate the inflammasome complex, which results in increased release of the pro inflammatory cytokine IL-1β [28].

In chapter 3 and 4 of this thesis, we have investigated the effect of anti-inflammatory compounds on TG metabolism (chapter 3) and glucose tolerance (chapter 4). In chapter 3 we show that high-dose aspirin, which decreases total hepatic NF-κB activity, also reduces hepatic VLDL-TG production in HFD-fed mice, thereby reducing the plasma TG levels of hypertriglyceridemic mice. In chapter 4 we showed that a botanical agent that has shown anti-inflammatory activity in vitro, was able to reduce body weight gain and diminish glucose intolerance in mice fed a HFD. Anti-inflammatory agents might therefore be interesting to treat symptoms of the metabolic syndrome.

High-dose aspirin has been shown to improve insulin sensitivity in obese type 2 diabetics [29]. In this study also a reduction of plasma TG was observed. Since prolonged use of high-dose aspirin can lead to gastrointestinal bleedings, clinical trials are being performed with salsalate, another anti-inflammatory agent based on the active compound salicylic acid, with fewer side effects than aspirin. Recently, high-dose salsalate treatment has shown to improve glycemic control, to decrease CRP levels and to decrease TG levels in type 2 diabetic patients [30]. Botanical compounds like META060 that we have tested in chapter 4 are anticipated to have even fewer side effects.

Even when unwanted potential side effects of anti-inflammatory compounds can be avoided, one could argue that reducing the inflammatory response in itself may be dangerous, since the capacity to destroy potential pathogens is also diminished. In this respect, adverse effects of anti-TNF-α have been reported. Treatment with TNF-α blockers has long been established for patients with rheumatoid arthritis (RA) and Crohn's disease. Because of the tight association between inflammation and insulin resistance and the positive effects on glucose and insulin levels in patients with RA [31, 32] anti-TNF-α agents have been tested in individuals with the metabolic syndrome. Etanercept, an anti-TNF-α agent, was found to improve fasting glucose levels in individuals with the metabolic syndrome [33]. Extensive use of anti-TNF-α agents in treatment of the metabolic syndrome was however not recommended, since increased risk of infection has been reported in patients with RA and Crohn's disease [34]. A more promising anti-inflammatory agent is Anakinra. Anakinra is an IL-1 receptor antagonist (IL-1ra) that counterbalances the pro inflammatory cytokine IL-1β. Administration of Anakinra resulted in improved glycemic control due to improved β-cell function in type 2 diabetic patients, although insulin sensitivity was unchanged [35]. In line with these results it was shown that in non-diabetic subjects treatment with IL-1ra improved β-cell function, but insulin sensitivity remained similar [36]. In contrast to treatment with anti-TNF-α, no significant increase in incidence of infection in RA patients treated with Anakinra have been reported [37]. Also for salsalate, there are no known effects for increased risk of infection [30].

Although anti-inflammatory agents are thus promising in treating insulin resistance and hypertriglyceridemia, a large randomized clinical trial has shown that intensive lifestyle intervention, i.e. weight loss due to caloric restriction and physical exercise, is also able to reduce inflammation as demonstrated by lower CRP levels [38]. In comparison with metformin, intensive lifestyle intervention was able to prevent diabetes to a greater extent in patients with impaired glucose tolerance [39]. Thus, anti-inflammatory agents may be useful to reduce the inflammatory burden on the short term, whereas intensive lifestyle intervention and maintenance of this novel life style could do so on the long term.

6.3 ROLE OF THE ADAPTIVE IMMUNE SYSTEM IN METABOLIC INFLAMMATION

Recent studies have shown that the adaptive immune system plays a clear role in metabolic inflammation. Increased amounts of T_H1 and $CD8^+$ T-lymphocytes in adipose tissues of obese individuals have been reported [21, 22]. Yang et al. found that T-lymphocytes that reside in adipose tissue of diet-induced obese mice have a restricted T Cell Receptor (TCR) profile [40], which suggest that there is ongoing antigen exposure eliciting an active adaptive immune response. Recently, it was found that transfer of IgG antibodies of diet-induced obese mice to B-lymphocyte deficient mice induces adipose tissue inflammation and insulin resistance in these mice [41].

In chapter 5, we revealed that functional activating Fc receptors (FcR) likely play a role in diet-induced obesity and associated diet-induced adipose tissue inflammation and insulin resistance. Membrane receptors for the Fc portion of antibody molecules can be found on

many hematopoietic cells, including macrophages. Cross-linking of these receptors activates cellular responses that are important for inflammation and immunity. The observation that functional FcR are likely involved in diet-induced obesity and inflammation suggest that antibodies are able to elicit a pro inflammatory response via cross-linking with FcR, which subsequently contributes to metabolic abnormalities seen in obese subjects.

Currently it is unclear against which antigens these antibodies are directed. Also it is unclear how B-lymphocytes acquire antigens. It could be that antigens arise from stressed apoptotic adipocytes, since it was observed that IgG antibodies localize with crown-like structures [41]. Invariant natural killer T (iNKT) cells may also play a role in B-lymphocyte activation. iNKT cells react to lipid stimuli and are able to activate antibody production by B-lymphocytes [42]. Recently it was found that mice fed a HFD have an increased amount of activated iNKT cells. It was also discovered that iNTK cell-deficiency protects against diet-induced insulin resistance and adipose tissue inflammation. Since similar results were obtained with db/db mice fed a chow diet, it is unlikely that exogenous lipids activate iNKT cells. Instead, the authors suggest that dyslipidemia in obesity results in iNKT cells loaded with self-lipids. These lipids could be presented to iNKT cells by antigen presenting cells such as macrophages [43]. The increased amount of activated iNKT cells in obese mice may contribute to an increased B-lymphocyte activation, which subsequently leads to adverse metabolic effects.

The observation that the adaptive immune system is involved in the onset of insulin resistance offers new therapeutic possibilities. HFD-fed mice treated with CD3 specific antibody, which inactivates pro inflammatory T_H1 lymphocytes and selectively increases Treg lymphocytes, showed improved glucose tolerance [22]. In addition, deletion of B-lymphocytes with CD20 specific monoclonal antibody in HFD-fed mice also resulted in improved glucose tolerance [41]. More B-lymphocyte or antibody modulating agents such as inhibitors against CD19 and CD22 are available for usage in humans. Specific deletion of iNKT cells by an iNKT cell-specific antibody in individuals prone to develop the metabolic syndrome could also be protective in these individuals. However, just as mentioned in the previous section on anti-inflammatory compounds, a possible side effect of interference in the adaptive immune system may be enhanced susceptibility to invading pathogens. Therefore a target-tissue approach might be important. For instance, agents that specifically target the pro inflammatory response in adipose tissue would attenuate adipose tissue inflammation and associated insulin resistance, without disrupting other immune functions in the body of an individual.

6.4 ROLE OF THE GUT IN METABOLIC INFLAMMATION

Recently, attention has been drawn to the role of microbiota and epithelial barrier function of the gut in metabolic inflammation. It was found that innate immune suppression, by deletion of components of the inflammasome, can lead to altered gut microbiota, which results in transfer of bacterial products to the portal circulation where TLR 4 and 9 are activated, which

ultimately leads to enhanced pro inflammatory signaling [44]. Another study showed that gut microbiota per se can induce obesity and insulin resistance in mice that are genetically protected against obesity and insulin resistance (the mice used in this study were TLR 2 deficient) by increasing the gut permeability, which leads to increased LPS absorption [45].

We observed that both CD36-deficient mice as well as FcR γ-chain deficient mice have increased intestinal length (data not shown), indicating that alterations in lipid metabolism and inflammation are associated with alterations in the intestine. Human and mice studies have indicated that there is an association between immune suppression and lipid malabsorption [46].

Since microbiota and the epithelial barrier function can be changed by diet, the role of altered microbiota/epithelial barrier function is another factor that should be taken into account when studying the onset of the metabolic syndrome. Already, a few years ago it was shown that weight loss by following a fat or carbohydrate restricted low calorie diet, could induce a shift in bacterial phyla of obese people [47]. Recently, it was found by Everard et al. that the botanical compound META060 that we have used in chapter 4 increased expression of two key intestinal tight junction proteins, thereby reducing the gut permeability [48]. Prebiotics, non-digestible nutrients such as dietary fibre and frutan, are also able to change gut microbiota. In obese individuals, fructan administration has shown a positive effect on BMI. Additional studies have demonstrated favorable effects of fructans on gastro-intestinal peptides such as PYY and GLP-1, which may contribute to the positive effects of fructan. Which gut microbial species are responsible for these positive effects is currently unknown, since many are changed upon treatment with prebiotica [49].

6.5 CONCLUDING REMARKS

The increasing prevalence of the metabolic syndrome world-wide urges the development of new drugs and therapies that reduce the progress of metabolic disturbances such as hypertriglyceridemia and insulin resistance. In the last decades it has become clear that FA metabolites and chronic inflammation are involved in the pathology of the metabolic syndrome. The epithelial barrier function of the gut also has to be taken into account when studying the metabolic syndrome. For the development of new drugs and therapies it is essential to evaluate how FA metabolites and inflammatory pathways contribute to the development of hypertriglyceridemia and insulin resistance. In this thesis we showed that CD36 plays a role in proper storage of FA in mature adipocytes as well as in recruitment of new adipocytes, thereby reducing ectopic fat deposition. Also, we identified that FcR antibody effector pathways may be involved in the development of obesity and insulin resistance, which suggest new diagnostic and therapeutic possibilities for managing the metabolic syndrome. Furthermore we found that inhibition of inflammatory pathways reduces hypertriglyceridemia and insulin resistance. Although anti-inflammatory agents might be helpful in treatment of the metabolic syndrome, caution is needed, since an inflammatory

response is necessary for destroying pathogens. Therefore, lifestyle-changing programs that help patients with improving (and maintaining) their dietary habits and adapting to a more physical active lifestyle deserve attention as well, since these interventions have proven to be successful in managing the metabolic syndrome.

REFERENCES

1. www.rivm.nl. 2009.
2. Brochu M, Tchernof A, Dionne IJ, Sites CK, Eltabbakh GH, Sims EA, Poehlman ET. What are the physical characteristics associated with a normal metabolic profile despite a high level of obesity in postmenopausal women? J Clin Endocrinol Metab 2001;86:1020-1025.
3. Karelis AD, St-Pierre DH, Conus F, Rabasa-Lhoret R, Poehlman ET. Metabolic and body composition factors in subgroups of obesity: what do we know? J Clin Endocrinol Metab 2004;89:2569-2575.
4. Wajchenberg BL. Subcutaneous and visceral adipose tissue: their relation to the metabolic syndrome. Endocr Rev 2000;21:697-738.
5. van Dijk SJ, Feskens EJ, Bos MB, Hoelen DW, Heijligenberg R, Bromhaar MG, de Groot LC, de Vries JH, Muller M, Afman LA. A saturated fatty acid-rich diet induces an obesity-linked proinflammatory gene expression profile in adipose tissue of subjects at risk of metabolic syndrome. Am J Clin Nutr 2009;90:1656-1664.
6. O'Donovan G, Kearney E, Sherwood R, Hillsdon M. Fatness, fitness, and cardiometabolic risk factors in middle-aged white men. Metabolism 2012;61:213-220.
7. Huang-Doran I, Sleigh A, Rochford JJ, O'Rahilly S, Savage DB. Lipodystrophy: metabolic insights from a rare disorder. J Endocrinol 2010;207:245-255.
8. Ruderman N, Chisholm D, Pi-Sunyer X, Schneider S. The metabolically obese, normal-weight individual revisited. Diabetes 1998;47:699-713.
9. Park KS, Rhee BD, Lee KU, Kim SY, Lee HK, Koh CS, Min HK. Intra-abdominal fat is associated with decreased insulin sensitivity in healthy young men. Metabolism 1991;40:600-603.
10. Seppala-Lindroos A, Vehkavaara S, Hakkinen AM, Goto T, Westerbacka J, Sovijarvi A, Halavaara J, Yki-Jarvinen H. Fat accumulation in the liver is associated with defects in insulin suppression of glucose production and serum free fatty acids independent of obesity in normal men. J Clin Endocrinol Metab 2002;87:3023-3028.
11. Dvorak RV, DeNino WF, Ades PA, Poehlman ET. Phenotypic characteristics associated with insulin resistance in metabolically obese but normal-weight young women. Diabetes 1999;48:2210-2214.
12. Nyholm B, Mengel A, Nielsen S, Skjaerbaek C, Moller N, Alberti KG, Schmitz O. Insulin resistance in relatives of NIDDM patients: the role of physical fitness and muscle metabolism. Diabetologia 1996;39:813-822.
13. Albu JB, Heilbronn LK, Kelley DE, Smith SR, Azuma K, Berk ES, Pi-Sunyer FX, Ravussin E. Metabolic changes following a 1-year diet and exercise intervention in patients with type 2 diabetes. Diabetes 2010;59:627-633.
14. Borel AL, Nazare JA, Smith J, Almeras N, Tremblay A, Bergeron J, Poirier P, Despres JP. Visceral and not subcutaneous abdominal adiposity reduction drives the benefits of a 1-year lifestyle modification program. Obesity (Silver Spring) 2012;20:1223-1233.
15. Johnson NA, Sachinwalla T, Walton DW, Smith K, Armstrong A, Thompson MW, George J. Aerobic exercise training reduces hepatic and visceral lipids in obese individuals without weight loss. Hepatology 2009;50:1105-1112.
16. Ross R, Dagnone D, Jones PJ, Smith H, Paddags A, Hudson R, Janssen I. Reduction in obesity and related comorbid conditions after diet-induced weight loss or exercise-induced weight loss in men. A randomized, controlled trial. Ann Intern Med 2000;133:92-103.
17. Hotamisligil GS, Erbay E. Nutrient sensing and inflammation in metabolic diseases. Nat Rev Immunol 2008;8:923-934.
18. Weisberg SP, McCann D, Desai M, Rosenbaum M, Leibel RL, Ferrante AW, Jr. Obesity is associated with macrophage accumulation in adipose tissue. J Clin Invest 2003;112:1796-1808.

19. Kintscher U, Hartge M, Hess K, Foryst-Ludwig A, Clemenz M, Wabitsch M, Fischer-Posovszky P, Barth TF, Dragun D, Skurk T, Hauner H, Bluher M, Unger T, Wolf AM, Knippschild U, Hombach V, Marx N. T-lymphocyte infiltration in visceral adipose tissue: a primary event in adipose tissue inflammation and the development of obesity-mediated insulin resistance. Arterioscler Thromb Vasc Biol 2008;28:1304-1310.

20. Duffaut C, Galitzky J, Lafontan M, Bouloumie A. Unexpected trafficking of immune cells within the adipose tissue during the onset of obesity. Biochem Biophys Res Commun 2009;384:482-485.

21. Nishimura S, Manabe I, Nagasaki M, Eto K, Yamashita H, Ohsugi M, Otsu M, Hara K, Ueki K, Sugiura S, Yoshimura K, Kadowaki T, Nagai R. CD8+ effector T cells contribute to macrophage recruitment and adipose tissue inflammation in obesity. Nat Med 2009;15:914-920.

22. Winer S, Chan Y, Paltser G, Truong D, Tsui H, Bahrami J, Dorfman R, Wang Y, Zielenski J, Mastronardi F, Maezawa Y, Drucker DJ, Engleman E, Winer D, Dosch HM. Normalization of obesity-associated insulin resistance through immunotherapy. Nat Med 2009;15:921-929.

23. Jagannathan M, McDonnell M, Liang Y, Hasturk H, Hetzel J, Rubin D, Kantarci A, Van Dyke TE, Ganley-Leal LM, Nikolajczyk BS. Toll-like receptors regulate B cell cytokine production in patients with diabetes. Diabetologia 2010;53:1461-1471.

24. Olefsky JM, Glass CK. Macrophages, inflammation, and insulin resistance. Annu Rev Physiol 2010;72:219-246.

25. Sammalkorpi K, Valtonen V, Kerttula Y, Nikkila E, Taskinen MR. Changes in serum lipoprotein pattern induced by acute infections. Metabolism 1988;37:859-865.

26. Khovidhunkit W, Kim MS, Memon RA, Shigenaga JK, Moser AH, Feingold KR, Grunfeld C. Effects of infection and inflammation on lipid and lipoprotein metabolism: mechanisms and consequences to the host. J Lipid Res 2004;45:1169-1196.

27. Shi H, Kokoeva MV, Inouye K, Tzameli I, Yin H, Flier JS. TLR4 links innate immunity and fatty acid-induced insulin resistance. J Clin Invest 2006;116:3015-3025.

28. Wen H, Gris D, Lei Y, Jha S, Zhang L, Huang MT, Brickey WJ, Ting JP. Fatty acid-induced NLRP3-ASC inflammasome activation interferes with insulin signaling. Nat Immunol 2011;12:408-415.

29. Hundal RS, Petersen KF, Mayerson AB, Randhawa PS, Inzucchi S, Shoelson SE, Shulman GI. Mechanism by which high-dose aspirin improves glucose metabolism in type 2 diabetes. J Clin Invest 2002;109:1321-1326.

30. Goldfine AB, Fonseca V, Jablonski KA, Pyle L, Staten MA, Shoelson SE. The effects of salsalate on glycemic control in patients with type 2 diabetes: a randomized trial. Ann Intern Med 2010;152:346-357.

31. Gonzalez-Gay MA, De Matias JM, Gonzalez-Juanatey C, Garcia-Porrua C, Sanchez-Andrade A, Martin J, Llorca J. Anti-tumor necrosis factor-alpha blockade improves insulin resistance in patients with rheumatoid arthritis. Clin Exp Rheumatol 2006;24:83-86.

32. Kiortsis DN, Mavridis AK, Vasakos S, Nikas SN, Drosos AA. Effects of infliximab treatment on insulin resistance in patients with rheumatoid arthritis and ankylosing spondylitis. Ann Rheum Dis 2005;64:765-766.

33. Stanley TL, Zanni MV, Johnsen S, Rasheed S, Makimura H, Lee H, Khor VK, Ahima RS, Grinspoon SK. TNF-alpha antagonism with etanercept decreases glucose and increases the proportion of high molecular weight adiponectin in obese subjects with features of the metabolic syndrome. J Clin Endocrinol Metab 2011;96:E146-E150.

34. Mori S, Sugimoto M. Is continuation of anti-tumor necrosis factor-alpha therapy a safe option for patients who have developed pulmonary mycobacterial infection? : Case presentation and literature review. Clin Rheumatol 2012;31:203-210.

35. Larsen CM, Faulenbach M, Vaag A, Volund A, Ehses JA, Seifert B, Mandrup-Poulsen T, Donath MY. Interleukin-1-receptor antagonist in type 2 diabetes mellitus. N Engl J Med 2007;356:1517-1526.

36. van Asseldonk EJ, Stienstra R, Koenen TB, Joosten LA, Netea MG, Tack CJ. Treatment with Anakinra improves disposition index but not insulin sensitivity in nondiabetic subjects with the metabolic syndrome: a randomized, double-blind, placebo-controlled study. J Clin Endocrinol Metab 2011;96:2119-2126.

37. Dinarello CA. The many worlds of reducing interleukin-1. Arthritis Rheum 2005;52:1960-1967.
38. Haffner S, Temprosa M, Crandall J, Fowler S, Goldberg R, Horton E, Marcovina S, Mather K, Orchard T, Ratner R, Barrett-Connor E. Intensive lifestyle intervention or metformin on inflammation and coagulation in participants with impaired glucose tolerance. Diabetes 2005;54:1566-1572.
39. Knowler WC, Barrett-Connor E, Fowler SE, Hamman RF, Lachin JM, Walker EA, Nathan DM. Reduction in the incidence of type 2 diabetes with lifestyle intervention or metformin. N Engl J Med 2002;346:393-403.
40. Yang H, Youm YH, Vandanmagsar B, Ravussin A, Gimble JM, Greenway F, Stephens JM, Mynatt RL, Dixit VD. Obesity increases the production of proinflammatory mediators from adipose tissue T cells and compromises TCR repertoire diversity: implications for systemic inflammation and insulin resistance. J Immunol 2010;185:1836-1845.
41. Winer DA, Winer S, Shen L, Wadia PP, Yantha J, Paltser G, Tsui H, Wu P, Davidson MG, Alonso MN, Leong HX, Glassford A, Caimol M, Kenkel JA, Tedder TF, McLaughlin T, Miklos DB, Dosch HM, Engleman EG. B cells promote insulin resistance through modulation of T cells and production of pathogenic IgG antibodies. Nat Med 2011;17:610-617.
42. Matsuda JL, Mallevaey T, Scott-Browne J, Gapin L. CD1d-restricted iNKT cells, the 'Swiss-Army knife' of the immune system. Curr Opin Immunol 2008;20:358-368.
43. Wu L, Parekh VV, Gabriel CL, Bracy DP, Marks-Shulman PA, Tamboli RA, Kim S, Mendez-Fernandez YV, Besra GS, Lomenick JP, Williams B, Wasserman DH, Van KL. Activation of invariant natural killer T cells by lipid excess promotes tissue inflammation, insulin resistance, and hepatic steatosis in obese mice. Proc Natl Acad Sci U S A 2012.
44. Henao-Mejia J, Elinav E, Jin C, Hao L, Mehal WZ, Strowig T, Thaiss CA, Kau AL, Eisenbarth SC, Jurczak MJ, Camporez JP, Shulman GI, Gordon JI, Hoffman HM, Flavell RA. Inflammasome-mediated dysbiosis regulates progression of NAFLD and obesity. Nature 2012;482:179-185.
45. Caricilli AM, Picardi PK, de Abreu LL, Ueno M, Prada PO, Ropelle ER, Hirabara SM, Castoldi A, Vieira P, Camara NO, Curi R, Carvalheira JB, Saad MJ. Gut microbiota is a key modulator of insulin resistance in TLR 2 knockout mice. PLoS Biol 2011;9:e1001212.
46. Shulzhenko N, Morgun A, Hsiao W, Battle M, Yao M, Gavrilova O, Orandle M, Mayer L, Macpherson AJ, McCoy KD, Fraser-Liggett C, Matzinger P. Crosstalk between B lymphocytes, microbiota and the intestinal epithelium governs immunity versus metabolism in the gut. Nat Med 2011;17:1585-1593.
47. Ley RE, Turnbaugh PJ, Klein S, Gordon JI. Microbial ecology: human gut microbes associated with obesity. Nature 2006;444:1022-1023.
48. Everard A, Geurts L, Van RM, Delzenne NM, Cani PD. Tetrahydro iso-Alpha Acids from Hops Improve Glucose Homeostasis and Reduce Body Weight Gain and Metabolic Endotoxemia in High-Fat Diet-Fed Mice. PLoS One 2012;7:e33858.
49. Delzenne NM, Neyrinck AM, Cani PD. Modulation of the gut microbiota by nutrients with prebiotic properties: consequences for host health in the context of obesity and metabolic syndrome. Microb Cell Fact 2011;10 Suppl 1:S10.

SUMMARY

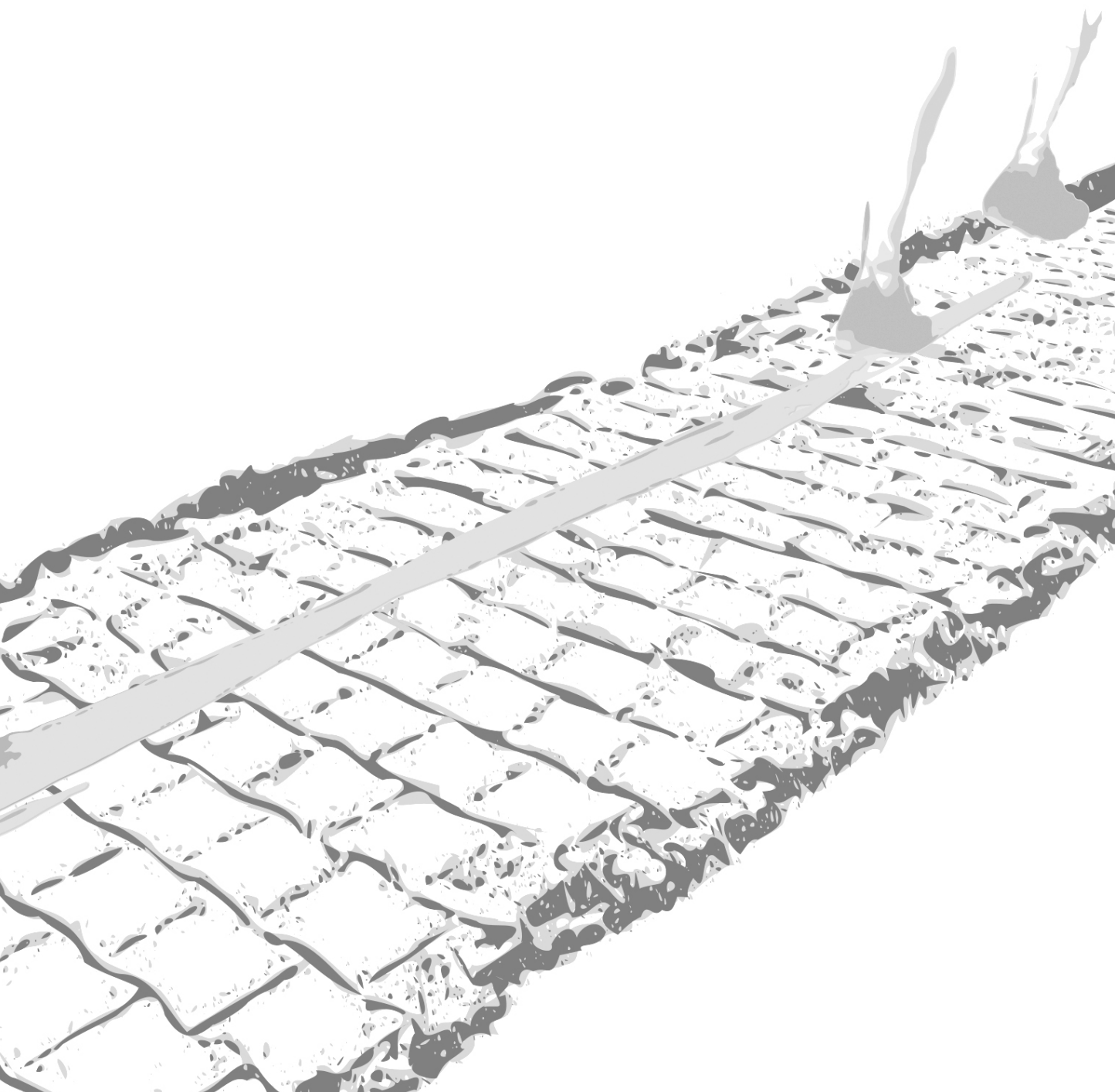

The metabolic syndrome is a multi-component condition that includes obesity hypertriglyceridemia and insulin resistance. The prevalence of the metabolic syndrome is rising world-wide and is associated with an increased risk for the development of cardiovascular diseases and type 2 diabetes. In the past decades it has been discovered that obese persons have slightly elevated markers of inflammation in their plasma. This low-grade chronic inflammation, also called metabolic inflammation, is hypothesized to function as the link between the various components of the metabolic syndrome. In this thesis, we have evaluated how alterations in triglyceride (TG) and fatty acid (FA) metabolism and inflammatory pathways interact in the development of obesity and insulin resistance, which are both primary risk factors for the development of type 2 diabetes.

Adipose tissue plays a central role in the development of the metabolic syndrome. Under healthy conditions, excess calories are stored in adipose tissue. When energy intake continues to exceed energy expenditure, the adipose tissue needs to expand in order to store these excess calories. When the capacity of the adipose tissue to expand is not yet reached, the excessive calories are mainly stored as fat. When the storage capacity of adipose tissue is reached, the excessive calories may be stored in non-adipose tissue (ectopic fat). This pathophysiological condition is associated with an increased risk for insulin resistance.

One of the functions of the scavenger receptor CD36 is to facilitate the entry of FA into a variety of cells, including adipocytes. In chapter 2 we have investigated the role of CD36 in preadipocyte recruitment and adipocyte functionality in gonadal, visceral and subcutaneous adipose tissue. For this purpose, we used CD36-deficient mice ($CD36^{-/-}$ mice) that were given a high fat diet (HFD). The $CD36^{-/-}$ mice showed diminished uptake of TG-rich particle derived FA in adipose tissue. As a consequence, gonadal, visceral and subcutaneous fat pads were smaller in these animals. A reduction in fat pad size can be caused by a reduction in size or a reduction in total number of adipocytes. We showed that adipocyte size was reduced in gonadal, visceral and subcutaneous fat pads of $CD36^{-/-}$ mice. In addition, a reduced total number of gondadal adipocytes was observed in $CD36^{-/-}$ mice. This reduction was caused by a decreased number of very small adipocytes (<50 μm). Our data suggest that CD36-deficiency reduces the capacity of preadipocytes to become adipocytes, since we measured a reduced number of very small adipocytes but an increased pool of preadipocytes in gonadal fat of $CD36^{-/-}$ mice. This deficiency in preadipocyte recruitment was not due to an intrinsic developmental defect, since in vitro differentiation experiments did not reveal a reduction in intra cellular lipid accumulation. Smaller adipocytes as observed in $CD36^{-/-}$ mice would be expected to have a decreased rate of lipolysis. Surprisingly, lipolysis was increased in adipocytes from $CD36^{-/-}$ mice. Altogether our results indicate that CD36 plays an important role in adipose tissue functionality both by regulating FA uptake and release. This in turn has an impact on the distribution of fat to adipose and non-adipose tissues. The reduced uptake of FA in adipose tissue was paralleled by an increased uptake of FA in the liver. We demonstrated that the fatty liver of $CD36^{-/-}$ mice was more insulin resistant.

Expansion of adipose tissue is often accompanied by infiltration of immune cells into the adipose tissue. Therefore, adipose tissue is thought to play a central role in the

onset of metabolic inflammation, although in other organs such as the liver and muscle inflammation in response to lipid accumulation can be observed as well. Immune cells are able to secrete cytokines that elicit a pro inflammatory response that is associated with the development of insulin resistance and hypertriglyceridemia. Inflammation, insulin resistance, and deregulation of TG/FA metabolism are part of a vicious cycle that drives the progression of diabetes and cardiovascular diseases.

Systemic inflammation induces an increase in plasma TG levels. Aspirin treatment in type 2 diabetes patients resulted in a decrease in plasma TG. In chapter 3 we have aimed to investigate the mechanism by which aspirin reduced hypertriglyceridemia. Therefore we fed human apolipoprotein CI (apoCI)-expressing mice (*APOC1*), a mouse model with elevated plasma TG levels, as well as normolipidemic wild-type (WT) mice a HFD and treated them with aspirin. Aspirin treatment reduced hepatic NF-κB activity in HFD-fed *APOC1* and WT mice and in addition, aspirin decreased plasma TG levels in hypertriglyceridemic *APOC1* mice. This TG-lowering effect could not be explained by enhanced VLDL-TG clearance, but aspirin selectively reduced hepatic VLDL-TG production in both *APOC1* and WT mice without affecting VLDL-apo B production. Aspirin did not alter hepatic expression of genes involved in FA oxidation, lipogenesis and VLDL production, but decreased the incorporation of plasma-derived FA by the liver into VLDL-TG, which was independent of hepatic expression of genes involved in FA uptake and transport. We concluded that aspirin improves hypertriglyceridemia by decreasing VLDL-TG production without affecting VLDL particle production. Our results suggest that inhibition of inflammatory pathways by aspirin could be an interesting target for the treatment of hyptertriglyceridemia.

In chapter 4 we have investigated the effects of a botanical component META060 on body weight development and insulin sensitivity. META060 has shown anti-inflammatory activity in vitro. Compared to WT mice fed a HFD, mice fed a HFD supplemented with META060 were protected against the development of diet-induced obesity. Moreover the mice that received META060 had improved glucose tolerance, indicating that this component has potential therapeutic value in the management of obesity and insulin resistance.

The adaptive immune system plays a clear role in metabolic inflammation. Increased amounts of specific pro inflammatory subtypes of T-lymphocytes and activated B-lymphocytes have been found in the adipose tissue of obese subjects. Furthermore, mice fed a HFD have a restricted T Cell Receptor profile. In addition, antibodies obtained from diet-induced obese mice are able to elicit adipose tissue inflammation and insulin resistance in B-lymphocyte deficient mice. Altogether this indicates that the adaptive immune system is important in metabolic inflammation and its associated pathologies.

Antibody molecules activate cellular responses that are important for inflammation by cross-linking their Fc portion with specific membrane receptors (FcR). In chapter 5 we have investigated whether functional FcR could be important in the development of diet-induced adipose tissue inflammation and diet-induced insulin resistance by subjecting FcR γ-chain$^{-/-}$ mice that miss the γ-chain that is needed for proper signal transduction and surface expression of FcR, to a HFD. Compared to WT mice, FcR γ-chain$^{-/-}$ mice had

reduced diet-induced obesity, diminished adipose tissue inflammation and less peripheral insulin resistance, indicating that functional FcR are likely to play a role in the development of metabolic inflammation.

Taken together, the studies described in this thesis contribute to the understanding that functionality of adipose tissue and metabolic inflammation are important factors in the development of diet-induced obesity and insulin resistance. We show that CD36 is important for proper adipocyte functioning, thereby reducing the risk of ectopic fat storage in the liver. We have identified that FcR antibody effector pathways may be involved in the development of obesity and insulin resistance, which suggest new diagnostic and therapeutic possibilities for managing the metabolic syndrome. Furthermore we found that anti-inflammatory agents reduce hypertriglyceridemia and insulin resistance.

NEDERLANDSE SAMENVATTING VOOR NIET-INGEWIJDEN

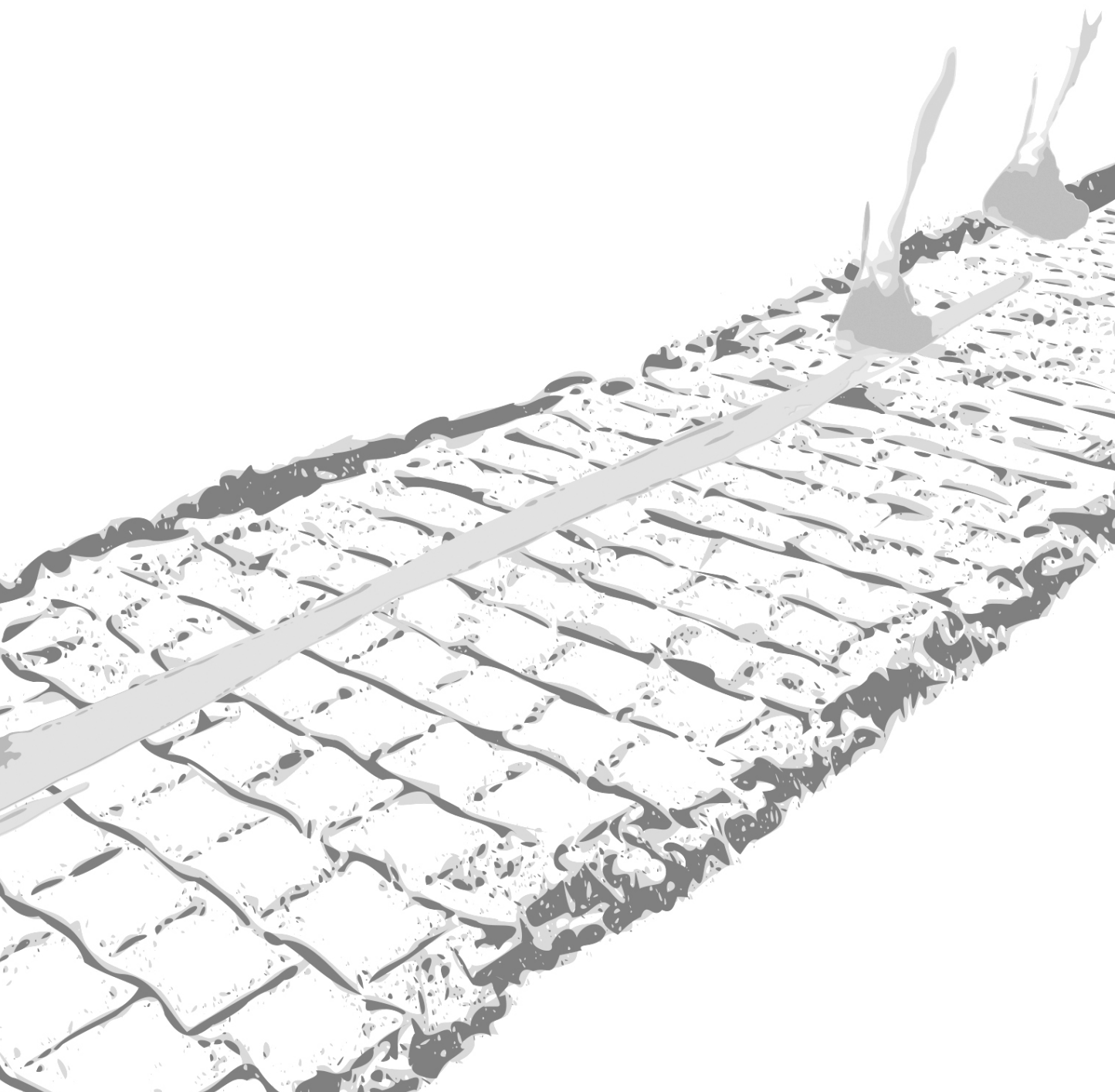

Het aantal mensen met het metabool syndroom neemt werelwijd al enkele tientallen jaren toe. Metabool syndroom is de aanduiding voor een verzameling van een verschillend aantal verstoringen in de stofwisseling, zoals hypertriglyceridemie (een verhoogd gehalte aan vet in het bloed) en insulineresistentie (een verminderde gevoeligheid voor insuline). Deze verstoringen in de stofwisseling leiden tot een verhoogd risico op het ontwikkelen van hart- en vaatziekten en type 2 diabetes. Er is sprake van het metabool syndroom wanneer 3 of meer van de volgende risicofactoren tegelijkertijd aanwezig zijn: veel vet in de buikstreek, een hoge bloeddruk, een verhoogd nuchter bloedsuikergehalte, een verhoogd gehalte aan vet in het bloed of een verlaagd HDL-cholesterol gehalte in het bloed. Zwaarlijvigheid, oftewel obesitas, is een belangrijke component in het metabool syndroom. Het steeds vaker voorkomen van overgewicht en obesitas leidt dan ook tot een toename van het metabool syndroom.

Om te bepalen of er sprake is van overgewicht of obesitas, wordt er gebruik gemaakt van de Body Mass Index (BMI). Deze wordt als volgt berekend: het lichaamsgewicht in kilogram, gedeeld door de lichaamslengte in meter in het kwadraat (kg/m2). Een BMI tussen 18,5 en 25 wordt beschouwd als gezond, een BMI van meer dan 25 wordt beschouwd als te zwaar (overgewicht) en een BMI van meer dan 30 wordt beschouwd als obesitas. Overmatige inname van calorieën ten opzicht van de hoeveelheid verbrandde calorieën is een van de belangrijkste oorzaken van obesitas, omdat deze extra calorieën voornamelijk als vet worden opgeslagen.

De belangrijkste vetten in ons dieet zijn triglyceriden (TG) en cholesterol. Omdat vetten slecht oplosbaar zijn in bloed, worden ze als lipoproteinen vervoerd door het lichaam. Deze lipoproteinen zijn wel oplosbaar in bloed en vervoeren het vet van en naar verschillende organen. Ons lichaam maakt verschillende lipoproteinen die variëren in samenstelling en dichtheid. Chylomicronen zijn lipoproteinen die vetten na een maaltijd vanuit de darm naar andere organen zoals hart, spier, vet en lever transporteren. Wanneer er een tijdje niet gegeten is, worden er door de lever Zeer Lage Dichtheid Lipoproteinen (engels: VLDL) geproduceerd om het lichaam van vetten te voorzien. Zowel chylomicronen als VLDL bevatten voornamelijk TG en daarom worden deze deeltjes ook wel TG-rijke lipoproteinen genoemd. De TG deeltjes zijn te groot om als zodaning door de organen te worden opgenomen. Daarom breekt het enzym lipoprotein lipase (LPL) in het bloed het grote TG deeltje af tot 3 vetzuren (FA) en glycerol. Dit proces wordt lipolyse genoemd. Op deze wijze wordt TG als vetzuur en glycerol opgenomen door andere organen zoals wit vetweefsel (voor opslag), spier en hart (voor leveren van energie) en bruin vetweefsel (voor warmteproductie). In het desbetreffende orgaan worden deze vetzuren verbrand voor energie of weer omgezet in TG voor opslag. 'Vrije' vetzuren zijn toxisch en vandaar dat deze eenmaal in de organen weer direct worden omgezet in TG.

Het wit vetweefsel speelt een centrale rol in de ontwikkeling van het metabool syndroom. Onder gezonde condities wordt een teveel aan calorieën voornamelijk opgeslagen als vet in het wit vetweefsel. Wanneer de energieinname langdurig het energieverbruik overschrijdt, moet het wit vetweefsel uitgebreid worden om de opslagcapaciteit te verhogen. Dit proces is echter gelimiteerd en wanneer de grenzen van dit proces zijn bereikt, zal vet ook worden opgeslagen in andere organen zoals spier en lever (dit wordt ectopic vet genoemd). Deze conditie verhoogt het risico op het krijgen van insulineresistentie.

CD36 is een eiwit dat zich bevindt aan de oppervlakte van cellen en helpt bij de opname van vetzuren in diverse organen, waaronder het witte vetweefsel. In hoofdstuk 2 hebben we de rol van CD36 in de cellen van het witte vetweefsel (adipocyten) onderzocht. We hebben hiervoor gebruik gemaakt van een muismodel dat geen CD36 heeft; de zogenaamde CD36-deficiënte (CD36-/-) muis. Zowel de CD36-deficiënte muizen als de controle muizen gaven we een vetrijk dieet, zodat deze muizen obesitas ontwikkelden. De CD36-deficiënte muis nam minder in gewicht toe dan de controle muis. Tevens was de opname van vetzuren uit TG-rijke deeltjes in het witte vetweefsel verminderd in deze muis en de witte vetweefsels waren dientengevolge kleiner in de CD36-deficiënte muis, in vergelijking met de controle muis. Kleiner vetweefsel kan worden veroorzaakt door kleinere vetcellen of door een verminderd aantal vetcellen. We zagen dat in gonadaal (rond de geslachtsorganen), visceraal (buikholte) en subcutaan (onderhuids) wit vetweefsel de vetcellen kleiner waren. In het gonadale vetweefsel zagen we tevens een verminderd aantal cellen, wat veroorzaakt werd door een vermindering in het aantal zeer kleine vetcellen (diameter < 50 µm). Onze bevindingen impliceren dat CD36-deficiëntie de capaciteit van preadipocyten (voorlopers van adipocyten) om adipocyten te worden beperkt, aangezien we een verminderd aantal zeer kleine vetcellen waarnamen, maar een verhoogde verzameling van preadipocyten. Deze vermeende verminderde capaciteit van preadipocyten wordt niet veroorzaakt door een inherent ontwikkelingsdefect van CD36-deficiënte muizen, want in vitro experimenten lieten geen vermindering zien in intracellulaire vetstapeling in preadipocyten. Meestal laten kleinere vetcellen, zoals waargenomen in de CD36-deficiënte muis, minder lipolyse zien. Wij namen echter een verhoogde lipolyse waar in de adipocyten van CD36-deficiënte muizen. Samenvattend laten onze resultaten zien dat CD36 een belangrijke rol speelt in de functionaliteit van wit vetweefsel door het reguleren van zowel vetzuuropname als vetzuurafgifte. Dit heeft impact op de verdeling van vet (TG) over vetweefsel en andere organen. We hebben namelijk ook gezien dat de verminderde vetzuuropname in vetweefsel gepaard gaat met een verhoogde opname van vetzuren in de lever. Dat dit gevolgen heeft voor de insulinegevoeligheid blijkt uit de waarneming dat CD36-deficiënte muizen meer insuline resistent zijn in de lever dan controle muizen die een vetrijk dieet hebben gekregen.

Uitbreiding van wit vetweefsel gaat vaak gepaard met infiltratie van immuun cellen in dit weefsel, wat resulteert in een milde ontsteking. Onder gezonde condities is dit van tijdelijke aard, maar gedurende chronisch energie overschot, kan deze milde ontsteking ook chronisch worden. Deze milde chronische ontsteking wordt ook wel metabole ontsteking genoemd, omdat verondersteld wordt dat deze ontsteking door een teveel aan voedingsstoffen wordt veroorzaakt. In obese mensen zijn stoffen die kenmerkend zijn voor ontsteking in licht verhoogde mate waargenomen in het bloedplasma. Deze milde systemische ontsteking in het lichaam is hoogstwaarschijnlijk het gevolg van metabole ontsteking in het vetweefsel en andere perifere organen zoals de lever. Metabole ontsteking lijkt een mogelijke oorzaak te zijn in de ontwikkeling van insulineresistentie. Uit eerder onderzoek kan worden afgeleid dat ontsteking, insulineresistentie en ontregeling van TG en FA metabolisme onderdeel zijn van een vicieuze cirkel die het risico op ontwikkeling van diabetes type 2 en hart- en vaatziekten verhoogd.

Systemische ontsteking veroorzaakt een stijging van het plasma TG niveau, wat ook wel hypertriglyceridemie wordt genoemd. Eerder onderzoek met type 2 diabetes patiënten heeft laten zien dat behandeling met aspirine leidt tot een verlaging van bloedplasma TG. In hoofdstuk 3 hebben we het mechanisme onderzocht dat leidt tot een verlaging van hypertriglyceridemie door aspirine. Hiervoor hebben we APOC1 muizen, die vanwege een genetische mutatie een verhoogd bloedplasma TG gehalte hebben en controle muizen met een normaal bloedplasma TG gehalte gebruikt. Beide groepen gaven we een vetrijk dieet, met of zonder toevoeging van aspirine in het drinkwater. Aspirine verlaagde de NF-κB activiteit (kenmerkend voor ontsteking) in de lever van APOC1 en controle muizen. Bovendien verlaagde aspirine de plasma TG niveaus van hypertriglyceridemische APOC1 muizen. Deze TG verlaging kon niet worden verklaard door een verhoogde klaring (of te wel opname) van VLDL-TG door perifere organen. Echter, aspirine verlaagde de VLDL-TG productie door de lever. Hierbij bleef de productie van apoB, het belangrijkste eiwit van VLDL onveranderd, wat aangeeft dat de productie van het aantal VLDL deeltjes hetzelfde is, maar dat elk VLDL deeltje minder TG bevat. Vervolgens hebben we onderzocht op welke manier aspirine de VLDL-TG productie door de lever verminderd. We zagen dat aspirine geen verandering veroorzaakte in expressie van genen betrokken bij vetzuur oxidatie, lipogenese (vorming van TG) of VLDL productie. We konden wel aantonen dat er minder vetzuren vanuit het plasma door de lever werden ingebouwd in VLDL-TG. Dit was onafhankelijk van expressie van genen in de lever betrokken bij vetzuur opname en transport. Op basis van deze gegevens hebben we geconcludeerd dat aspirine hypertriglyceridemie kan verlagen door de VLDL-TG productie door de lever te verminderen, zonder hierbij het aantal geproduceerde deeltjes te veranderen. Onze resultaten suggereren dat de remming van ontsteking door aspirine, een interessante therapie kan zijn voor de behandeling van hypertriglyceridemie.

In hoofdstuk 4 hebben we het effect van een plantaardig stof, genaamd META060, op gewichtsontwikkeling en insulinegevoeligheid onderzocht. In vitro is aangetoond dat META060 ontstekingsremmende effecten heeft. Om het effect van META060 te onderzoeken gebruikten we controle muizen die een normaal vetrijk dieet kregen of een vetrijk dieet aangevuld met META060. Onze resultaten lieten zien dat muizen die META060 kregen, beschermd waren tegen dieet-geïnduceerde obesitas. Bovendien was de glucose tolerantie van muizen die META060 kregen hoger, wat duidt op een verbeterde insulinegevoeligheid. Deze bevindingen wijzen erop dat META060 potentiële therapeutische waarde heeft in de behandeling van obesitas en insulineresistentie.

Wetenschappelijk onderzoek van de afgelopen jaren heeft duidelijk gemaakt dat het adaptieve immuun systeem een belangrijke rol speelt in het ontstaan van metabole ontsteking. Een toename van bepaalde ontstekingsbevorderende witte bloedcellen (T-lymphocyten en geactiveerde B-lymphocyten) in het vetweefsel van obese mensen duidt op de betrokkenheid van het adaptieve immuun systeem. Ook is er recent gevonden dat antilichamen gevormd door dieet-geïnduceerde obese muizen, na overdracht in muizen die zelf geen antilichamen aanmaken, insulineresistentie kunnen veroorzaken. Dit geeft aan dat de humorale kant (B-lymphocyten & antilichamen) van het adaptieve immuun systeem van belang is bij de ontwikkeling van het metabool syndroom.

In hoofdstuk 5 hebben we één van de mogelijke mechanismen onderzocht dat het effect van antilichamen op insulineresistentie zou kunnen verklaren. Antilichamen hebben een zogenaamd constant deel dat het Fc fragment wordt genoemd. Dit Fc fragment kan binden aan Fc receptoren die zich bevinden op cellen van het aangeboren immuun systeem zoals macrophagen, mest cellen en dendritische cellen. Waneer dit Fc fragment van een antilichaam bindt aan een Fc receptor (FcR) wordt er een reactie in de cellen van het aangeboren immuun systeem op gang gebracht die resulteert in inflammatoire processen. Wij hebben onderzocht of functionele FcR belangrijk zijn bij de ontwikkeling van dieet-geïnduceerde obesitas, ontsteking in het wit vetweefsel en insulineresistentie. Dit hebben we gedaan door muizen die deficiënt zijn voor de zogenaamde γ-chain van de FcR op een vetrijk dieet te plaatsen en deze muizen te vergelijken met controle muizen op een vetrijk dieet. De γ-chain is van belang voor juiste expressie van FcR. Ook zorgt de γ-chain ervoor dat de FcR signalen kan doorgeven. Muizen die de γ-chain missen hebben onder andere een verminderde antilichaam response. Wij zagen dat FcR γ-chain deficiënte muizen minder in gewicht toenamen op een vetrijk dieet. Ook was er sprake van een verminderde inflammatie van wit vetweefsel en in perifere organen was de insulineresistentie als gevolg van het vetrijke dieet minder. Deze resultaten impliceren dat functionele FcR een rol spelen bij de ontwikkeling van metabool syndroom.

Samengevat laten de studies in dit proefschrift zien dat het juist functioneren van wit vetweefsel en metabole ontsteking een belangrijke rol spelen in de ontwikkeling van obesitas en insulineresistentie. We laten zien dat CD36 belangrijk is voor het goed functioneren van adipocyten, waardoor het risico op ectopische vetafzetting in de lever kleiner wordt. Tevens tonen we aan dat functionele FcR betrokken kunnen zijn bij de ontwikkeling van obesitas, wit vetweefsel inflammatie en insulineresistentie, wat mogelijkheden biedt voor ontwikkeling van diagnostiek en nieuwe therapieën. Daarnaast laten we zien dat anti-inflammatoire stoffen hypertriglyceridemie en insuline resistentie kunnen verminderen.

LIST OF PUBLICATIONS

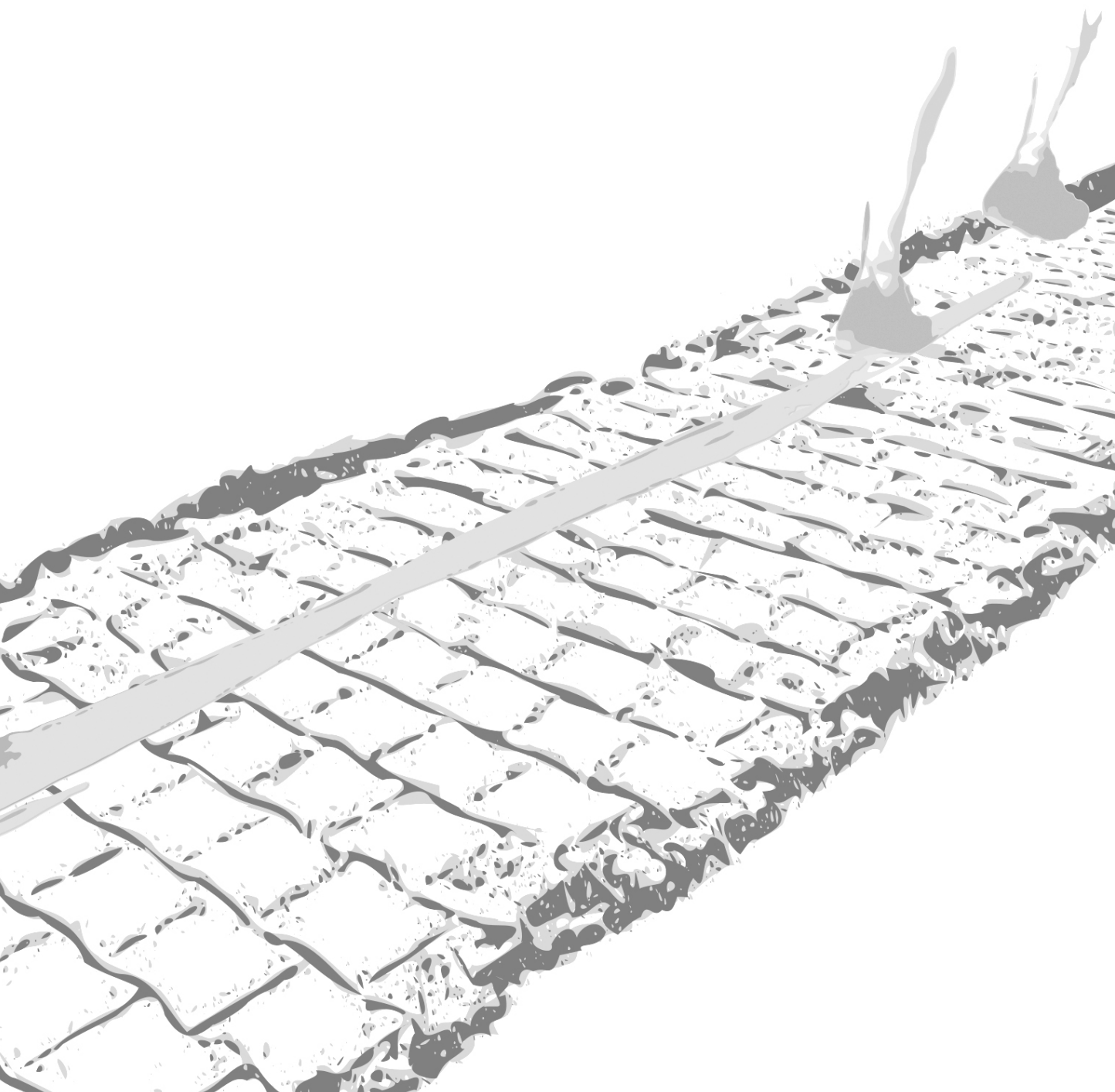

LIST OF PUBLICATIONS (FULL PAPERS):

Declercq J, Kumar A, Van Diepen JA, Vroegrijk IO, Gysemans C, Di Pietro C, Voshol PJ, Mathieu C, Ectors N, Van de Ven WJ, Verfaillie CM. Increased beta-cell mass by islet transplantation and PLAG1 overexpression causes hyperinsulinemic normoglycemia and hepatic insulin resistance in mice**. Diabetes, 2010** Aug;59(8):1957-65.

Vroegrijk IO, van Diepen JA, van den Berg S, Westbroek I, Keizer H, Gambelli L, Hontecillas R, Bassaganya-Riera J, Zondag GC, Romijn JA, Havekes LM, Voshol PJ. Pomegranate seed oil, a rich source of punicic acid, prevents diet-induced obesity and insulin resistance in mice. **Food Chem Toxicol, 2011** Jun;49(6):1426-30.

Stienstra R, van Diepen JA, Tack CJ, Zaki MH, van de Veerdonk FL, Perera D, Neale GA, Hooiveld GJ, Hijmans A, Vroegrijk I, van den Berg S, Romijn J, Rensen PC, Joosten LA, Netea MG, Kanneganti TD. Inflammasome is a central player in the induction of obesity and insulin resistance. **Proc Natl Acad Sci U S A, 2011** Sep 13;108(37):15324-9.

Steinbusch LK, Luiken JJ, Vlasblom R, Chabowski A, Hoebers NT, Coumans WA, Vroegrijk IO, Voshol PJ, Ouwens DM, Glatz JF, Diamant M. Absence of fatty acid transporter CD36 protects against Western-type diet-related cardiac dysfunction following pressure overload in mice. **Am J Physiol Endocrinol Metab, 2011** Oct;301(4):E618-27.

van Diepen JA, Vroegrijk IO, Berbée JF, Shoelson SE, Romijn JA, Havekes LM, Rensen PC, Voshol PJ. Aspirin reduces hypertriglyceridemia by lowering VLDL-triglyceride production in mice fed a high-fat diet**. Am J Physiol Endocrinol Metab., 2011** Dec;301(6):E1099-107.

Fonager J, Pasini EM, Braks JA, Klop O, Ramesar J, Remarque EJ, Vroegrijk IO, van Duinen SG, Thomas AW, Khan SM, Mann M, Kocken CH, Janse CJ, Franke-Fayard BM. Reduced CD36-dependent tissue sequestration of Plasmodium-infected erythrocytes is detrimental to malaria parasite growth in vivo. **J Exp Med, 2012** Jan 16;209(1):93-107.

Vroegrijk IO, van Diepen JA, van den Berg SA, Romijn JA, Havekes LM, van Dijk KW, Darland G, Konda V, Tripp ML, Bland JS, Voshol PJ. META060 protects against diet-induced obesity and insulin resistance in a high-fat-diet fed mouse. **Nutrition 2013,** Jan;29(1):276-83

van Diepen JA*, Stienstra R*, Vroegrijk IO, van den Berg SA, Salvatori D, Hooiveld GJ, Kersten S, Tack CJ, Netea MG, Smit JW, Joosten LA, Havekes LM, van Dijk KW, Rensen PC. Caspase-1 deficieny reduces intestinal and hepatic triglyceride-rich lipoprotein secretion. **J Lipid Res 2013** 2013 Feb;54(2):448-56 [* Both authors contributed equally]

Quintens R, Singh S, Lemaire K, de Bock K Granvik M, Schraenen A, Vroegrijk IO, Costa V, van Noten P, Lambrechts D, Lehnert S, van Lommel L, Thorrez L, de Faudeur G, Romijn JA, Shelton JM, Scorrano, Lijnen HR, Voshol PJ, Carmeliet Mammen PP, Schuit FC. Mice deficient in the respiratory chain gene Cox6a2 are protected against high-fat diet-induced obesity and insulin resistance. Accepted for publication in PloS One.

Vroegrijk IO, van Klinken JB, van Diepen JA, van den Berg SA, Febbraio M, Steinbusch LK, Glatz JF, Havekes LM, Voshol PJ, Rensen PC, van Dijk KW, van Harmelen V. CD36 is important for adipocyte recruitment and affects lipolysis. Accepted for publication in Obesity.

Vroegrijk IO, van den Berg SA, van Klinken JB, Havekes LM, Verbeek SJ, van Dijk KW, van Harmelen V. FcR γ-chain-/- are protected against diet-induced obesity and insulin resistance. In preparation.

CURRICULUM VITAE

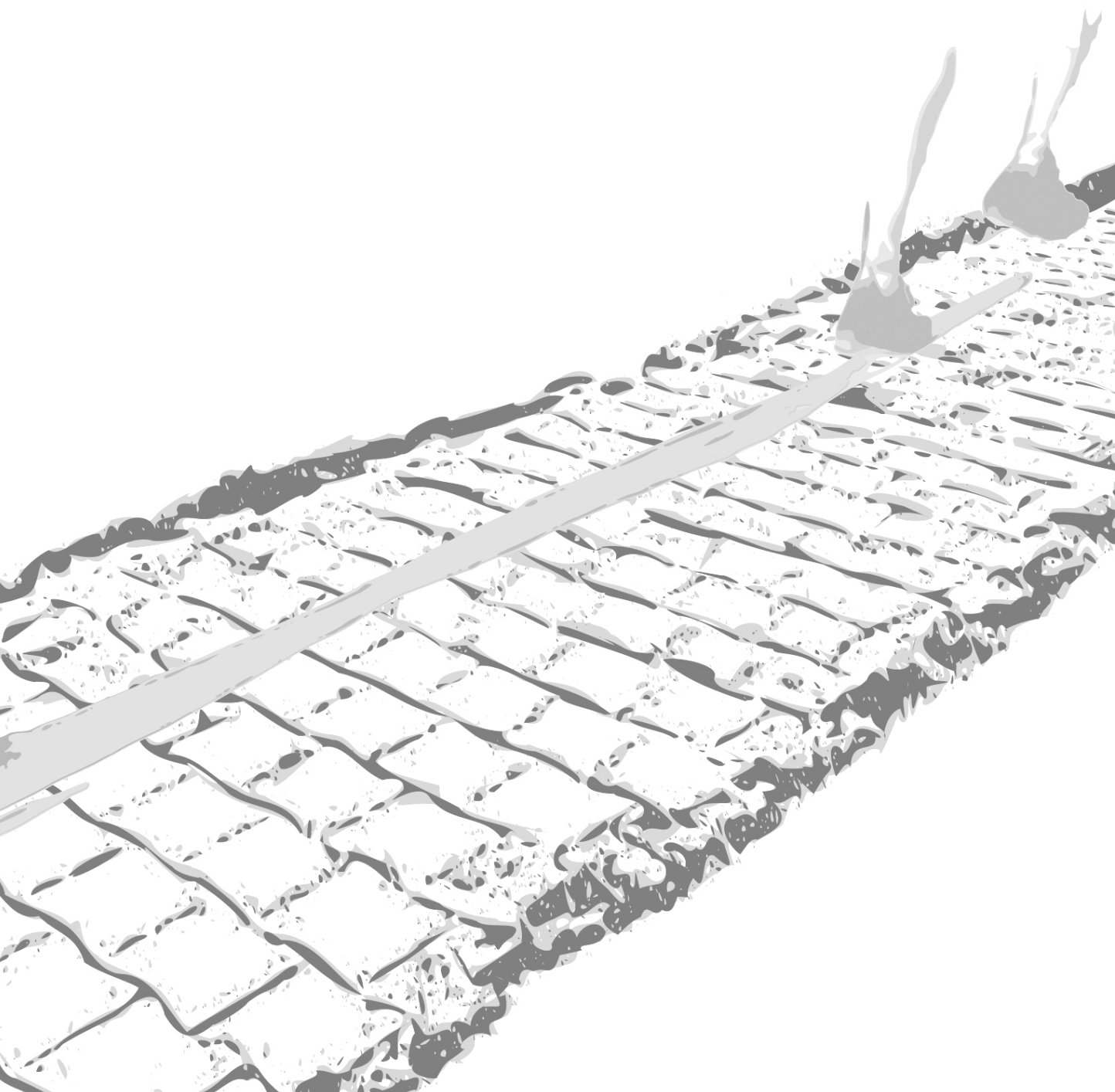

CURRICULUM VITAE

Irene Vroegrijk werd op 11 februari 1983 geboren te Roosendaal en Nispen. In 2001 behaalde zij haar VWO diploma aan het Markland College te Oudenbosch. Aansluitend startte zij in datzelfde jaar met de studie Voeding en Gezondheid aan de Wageningen Universiteit. Tijdens het collegejaar 2005-2006 was zij deel van het dagelijks bestuur van S.W.U. Thymos, de sportraad van Wageningen Universiteit. Haar afstudeeronderzoek voerde zij uit bij de groep Nutrition, Metabolism and Genomics van de afdeling Humane Voeding van de Wageningen Universiteit onder supervisie van Dr. L. Afman. Hiervoor onderzocht zij de effecten van calorische restrictie op expressie van verschillende genen in de lever van muizen. Na een stage aan de University of Guelph, Ontario, Canada bij de afdeling Human Health and Nutritional Sciences, behaalde zij in november 2007 haar Master diploma. In januari 2008 begon zij als promovenda met haar promotieonderzoek bij de afdeling Endocrinologie van het LUMC, onder supervisie van Prof. Dr. L.M. Havekes, Prof. Dr. J.A. Romijn, Prof. Dr. K. Willems van Dijk en Dr. P.J. Voshol. Het promotieonderzoek waarvan de resultaten zijn beschreven in dit proefschrift, werd afgerond in mei 2012. Sinds 1 juni 2012 werkt Irene als Regulatory Affairs Officer.